

**UNCLASSIFIED**

---

**AD 267 342**

*Reproduced  
by the*

**ARMED SERVICES TECHNICAL INFORMATION AGENCY  
ARLINGTON HALL STATION  
ARLINGTON 12, VIRGINIA**



---

**UNCLASSIFIED**

NOTICE: When government or other drawings, specifications or other data are used for any purpose other than in connection with a definitely related government procurement operation, the U. S. Government thereby incurs no responsibility, nor any obligation whatsoever; and the fact that the Government may have formulated, furnished, or in any way supplied the said drawings, specifications, or other data is not to be regarded by implication or otherwise as in any manner licensing the holder or any other person or corporation, or conveying any rights or permission to manufacture, use or sell any patented invention that may in any way be related thereto.

267 342

U. S. A R M Y  
TRANSPORTATION RESEARCH COMMAND  
FORT EUSTIS, VIRGINIA

TCREC TECHNICAL REPORT 61-104

WIND TUNNEL TESTS AND FURTHER ANALYSIS OF THE  
FLOATING WING FUEL TANKS FOR HELICOPTER RANGE EXTENSION

VOLUME 3

WING FLUTTER ANALYSIS  
45° SKEWED HINGE

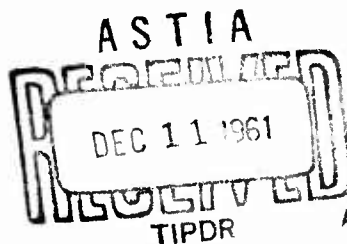
Project 9X38-09-006

Contract DA 44-177-TC-550

August 1961

prepared by :

VERTOL DIVISION  
THE BOEING COMPANY  
Morton, Pennsylvania



Project 9X38-09-006  
Contract DA44-177-TC-550  
August 1961

TCREC TECHNICAL REPORT 61-104

WIND TUNNEL TESTS AND FURTHER ANALYSIS OF THE  
FLOATING WING FUEL TANKS FOR HELICOPTER RANGE EXTENSION

VOLUME 3

WING FLUTTER ANALYSIS  
45° SKEWED HINGE

Report No. R-228

Prepared by:

VERTOL DIVISION  
THE BOEING COMPANY  
MORTON, PENNSYLVANIA

for  
U. S. ARMY TRANSPORTATION RESEARCH COMMAND  
FORT EUSTIS, VIRGINIA

HEADQUARTERS  
U. S. ARMY TRANSPORTATION RESEARCH COMMAND  
Fort Eustis, Virginia

FOREWORD

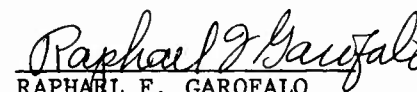
The U. S. Army, through the facilities of the U. S. Army Transportation Research Command, Fort Eustis, Virginia, has been studying various methods for extending the range of Army aircraft and, in particular, the range of the helicopter. One method being investigated, which indicates that ferry ranges of 2,000 miles or more are attainable, is one in which floating-wing fuel tanks are attached to a helicopter's fuselage through a hinge connection.

The report presented in the following pages is Volume 3 of a five-volume final report of the analysis and wind-tunnel investigation of the floating-wing system. Volume 3 presents the results of the wing flutter analysis of the floating wing at various fuel conditions. The conclusions contained herein are concurred in by this Command.

FOR THE COMMANDER:

APPROVED BY:

  
ROBERT D. POWELL, JR.  
USATRECOM Project Engineer

  
RAPHAEL F. GAROFALO  
CWO-4 USA  
Assistant Adjutant

## TABLE OF CONTENTS

ITEM	PAGE
FOREWORD . . . . .	ii
LIST OF ILLUSTRATIONS. . . . .	iv
NOMENCLATURE . . . . .	v
SUMMARY . . . . .	1
I INTRODUCTION . . . . .	2
II DESCRIPTION OF WING. . . . .	5
III METHOD OF ANALYSIS . . . . .	9
IV DISCUSSION OF RESULTS. . . . .	13
V CONCLUSIONS AND RECOMMENDATIONS. . . . .	27
VI REFERENCES . . . . .	28
APPENDICES:	
A. ANTI-SYMMETRIC FLUTTER ANALYSIS. . . . .	30
B. SYMMETRIC FLUTTER ANALYSIS . . . . .	41
C. NUMERICAL DATA . . . . .	53
DISTRIBUTION LIST . . . . .	71

# LIST OF ILLUSTRATIONS

FIGURE	DESCRIPTION	PAGE
1	Range Extension System, Floating Fuel Wing, H-21 . . . .	4
2	Wing Schematic Diagram . . . . .	6
3	Wing Properties. . . . .	7
4	Wing Natural Modes . . . . .	8
5	Anti-symmetric Flutter Determinant . . . . .	11
6	Symmetric Flutter Determinant. . . . .	12
7	Flutter Curves, 100% Fuel Condition. . . . .	18
8	Flutter Curves, 0% Fuel Condition. . . . .	19
9	Flutter Curves, Tip Cells Partial Fuel, Forward CG . . .	20
10	Flutter Curves, Tip Cells Partial Fuel, Aft CG . . . .	21
11	Flutter Curves, All Cells Partial Fuel, Forward CG . . .	22
12	Flutter Curves, All Cells Partial Fuel, Aft CG . . . .	23
13	Flutter Speed as a Function of Fuel, TN 4166 . . . . .	26

# NOMENCLATURE

$a$	Nondimensional distance from wing midchord to elastic axis, E.A.; $a = a'/b$
$a'$	Dimensional distance from wing midchord to E.A.; positive for aft E.A.
$b$	Semichord
$H_b$	Generalized coordinate
$\bar{I}_{wi}$	Pitching moment of inertia of wing element at Station $i$ about E.A.
$I_{fp}$	Fuselage moment of inertia in pitch about its C.G.
$\bar{M}_{wi}$	Mass of wing element at Station $i$
$M_{1eff}$	Effective wing mass for first mode
$M_{2eff}$	Effective wing mass for the second mode
$M_f$	Fuselage mass
$s$	Distance from aircraft C.G. to wing E.A.
$V$	Airspeed
$x_{wi}$	Distance from wing E.A. to wing element C.G. at Station $i$ , positive for C.G. aft of E.A.
$y_i$	Wing spanwise distance from the fuselage centerline to the elemental mass $\bar{M}_{wi}$
$\Delta y_i$	Bay width
$z_{bi}$	Vertical deflection at wing span Station $i$ ; positive down left wing - normal mode
$z$	Fuselage vertical coordinate, positive down
$\gamma$	Fuselage pitch deflection, positive nose up
$\bar{\sigma}_{wi}$	Static moment of wing element at Station $i$ about E.A.
$\Theta$	Fuselage roll, positive left wing down
$\phi_{bi}$	Wing torsional deflection at span Station $i$ ; positive nose up - left wing - normal mode
$\rho$	Air mass density



$\omega$  Flutter natural frequency  
 $\omega_{br}$  Wing natural frequency of  $r$  th mode,  $r$ : 1,2 etc.

Subscripts:

$f$  Denotes the fuselage  
 $i$  Denotes the wing spanwise Station  $i$ : 1,2,3  
 $w$  Denotes the wing  
 $1$  Denotes the first wing mode  
 $2$  Denotes the second wing mode

Other symbols are explained when used.

## SUMMARY

Anti-symmetric and symmetric flutter investigations are performed on the Range Extension floating wing for various fuel loading conditions and combinations of wing modes. The method employed in this analysis makes use of Theodorsen's oscillating aerodynamic loads for the generalized excitation. Mechanical equations of the system are obtained with Lagrange's method using several combinations of three wing modes, and two rigid fuselage modes as generalized coordinates. Solution of the flutter determinant is obtained by an IBM 650 computer program. Results of the flutter calculations are presented as plots of airspeed against wing modes frequency ratio, from which the flutter speed is determined by the intersection of the actual frequency ratio with the characteristic curve.

Results of the analysis indicate that the flutter characteristics of the delta hinge wing arrangement are unacceptable. The investigation shows that for both the 0% and 100% fuel configurations the flutter speeds are below the cruise speed of 80 knots. It is indicated that the low flutter critical speeds calculated here are closely associated with the aircraft roll-wing rigid body flap instability which has been determined to be an aircraft flight instability. The wing design is being revised to a straight hinge configuration in which the necessary aerodynamic wing spring is being furnished by a differential flap system. This change, which will eliminate the unusual flap-pitch coupling in the oscillatory airloads, should improve the flutter situation.

The effects of fuel slosh calculated herein can be evaluated on a relative basis. The slosh is approximately simulated by partial fuel conditions in which it is assumed that the fuel is sloshed fully forward or fully aft in the tanks so as to cause maximum shift of the chordwise C.G. position. Results show that the aft C.G. position obtained from partial fuel in all tanks lowers the basic flutter speed appreciably. This can be avoided by a fuel drainage schedule wherein one tank at a time is fully emptied, tending to eliminate the critical aft C.G. along the entire span.

To evaluate the final wing configuration from a flutter standpoint, it is recommended that a ground shake test be performed to substantiate the wing frequency estimates used in the analysis. Then flight flutter tests should be conducted starting with the empty wing configuration and continuing with successively larger fuel quantities until the full range of fuel variations is explored.

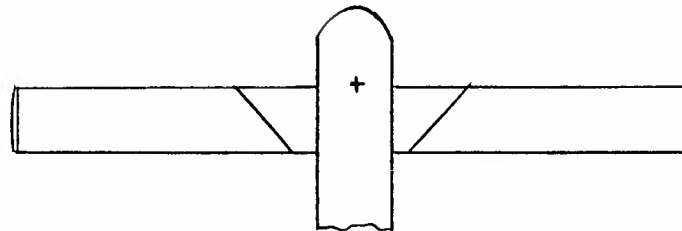
## I. INTRODUCTION

This flutter study is part of an analytical and wind tunnel study being conducted under the Reference 1 Transportation Research Command contract. The program is aimed at the development of a means for helicopter range extension through application of a floating fuel wing concept. Under an earlier contract, Reference 2, Vertol conducted an initial feasibility study of the floating wing concept. Results of this study are reported in Reference 3. The present analytical and wind tunnel investigation is under the Reference 1 contract and is based on a Vertol proposal, Reference 4. Phase I of the present contract, consisting of wind tunnel and mechanical instability studies, was reported in Reference 5 and 6. The present flutter analysis is a part of Phase II of the contract.

The range of present-day helicopters with normal fuel load is less than 400 nautical miles. Even with additional internal tanks, the helicopter range is less than 1100 miles. With floating wings, the range can be extended to as much as 2400 miles, corresponding to the longest over-water distance on the Pacific Ocean ferry route.

Each floating wing contains compartmented tankage connected by lines to the helicopter's main tank. The wing lift supports the fuel weight that it carries, and the helicopter acts as a tow to propel the wing forward. Wing attachment to the helicopter is through a hinge so as to eliminate the bending moments at the fuselage applied by conventional wings, thus avoiding the addition of extensive wing carry through structure to the helicopter.

The hinge line is not horizontal, but is skewed aft as shown.



As fuel is consumed and the wings become lighter, they tend to flap upward about the hinge. Because of the skewed orientation, the angle of attack at any chord line is reduced as the wings flap up, the lift is reduced, and the wing assumes a new mean position. Full span pilot controlled wing flaps are also provided, so that the trim attitude of the wing may be adjusted; these are also used as high lift devices during the running takeoff.

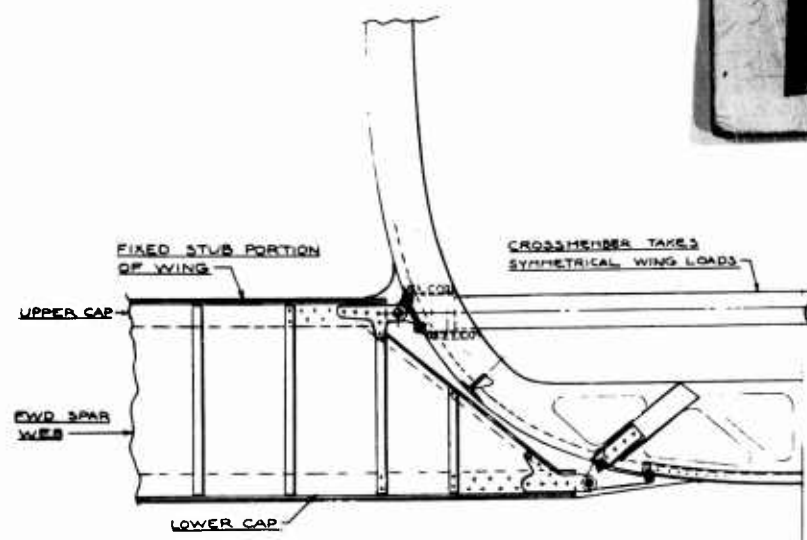
The analysis performed herein is intended to establish the flutter characteristics of the floating wing system. In normal flight, the surfaces of an aircraft are subject to almost continuous disturbances by random aerodynamic loads. Gusts and pilot course corrections, for example, put temporary loads on these surfaces. As with every elastic body, such loads cause deflections of the aircraft structure and, at each application of load, induce vibration in the body. Ordinarily, these vibrations are highly damped and rapidly disappear. However, under certain conditions involving the elastic, inertial and aerodynamic loads, the vibrations are not damped, but a divergent oscillation arises commonly known as flutter. In this event, after the initial disturbance, each successive vibration becomes of larger amplitude. These oscillations can be dangerously large and may lead to structural failure.

Aerodynamic forces on the wing can arise from oscillations in vertical translation and pitching at each wing span station, and the coordinates for the analysis have been selected for their contributions to such motions. The coordinated degrees of freedom were considered under two major categories: (1) symmetric, where vertical and pitch motion of the helicopter, rigid flap of the wing about its skewed hinge, and coupled flap bending-torsion were considered, and where all motions of the right wing were mirrored symmetrically by identical motion of the left wing, (2) anti-symmetric analysis where roll motion of the helicopter, rigid flap of the wing about its skewed hinge, and coupled flap bending torsion of the wing were considered, and where all motions of the right wing were accompanied by equal and opposite motions of the left wing. The pilot adjustable control flaps were not considered to be degrees of freedom because of the rather rigid electrical screw jack actuator between the wing and flap. In conventional wings where there are cable control systems from the flaps to the pilot, the flap pitch restraint is low, giving the flap a low natural frequency and making it an important degree of freedom.

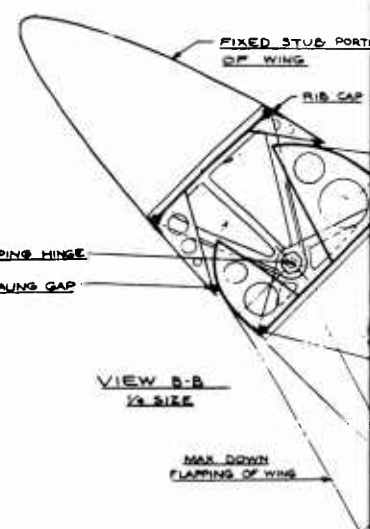
The flutter analysis of the floating wing arrangement is further complicated by the effect of sloshing fuel. An exact analytical method for including fuel motion in the flutter equation is not known, but several approximate solutions have been published which include the effective masses and inertias for the sloshing fuel. However, the most directly applicable method to the present wing flutter study approximates the sloshing fuel as a change in the chordwise center of gravity.

This report presents the flutter investigations conducted for the floating fuel wings. Section II describes the floating fuel wing and gives its natural modes under various fuel conditions. The flutter analysis methods are presented in Section III, together with detailed derivations in Appendix A and Appendix B for the anti-symmetric and symmetric analyses respectively. Section IV presents and discusses the flutter results and views the influence of fuel slosh, and the conclusions of the investigation are included in Section V. Numerical data including a typical computer sample are presented in Appendix C.

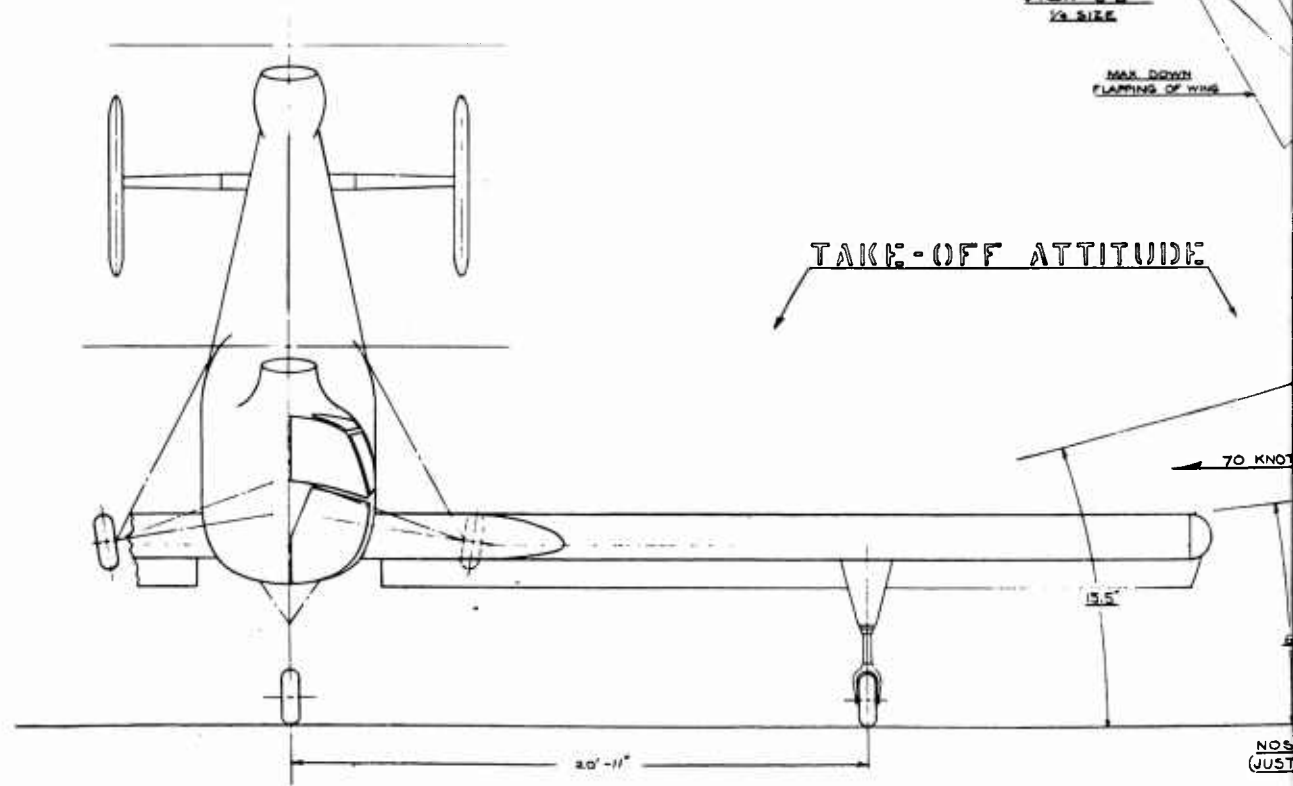
1



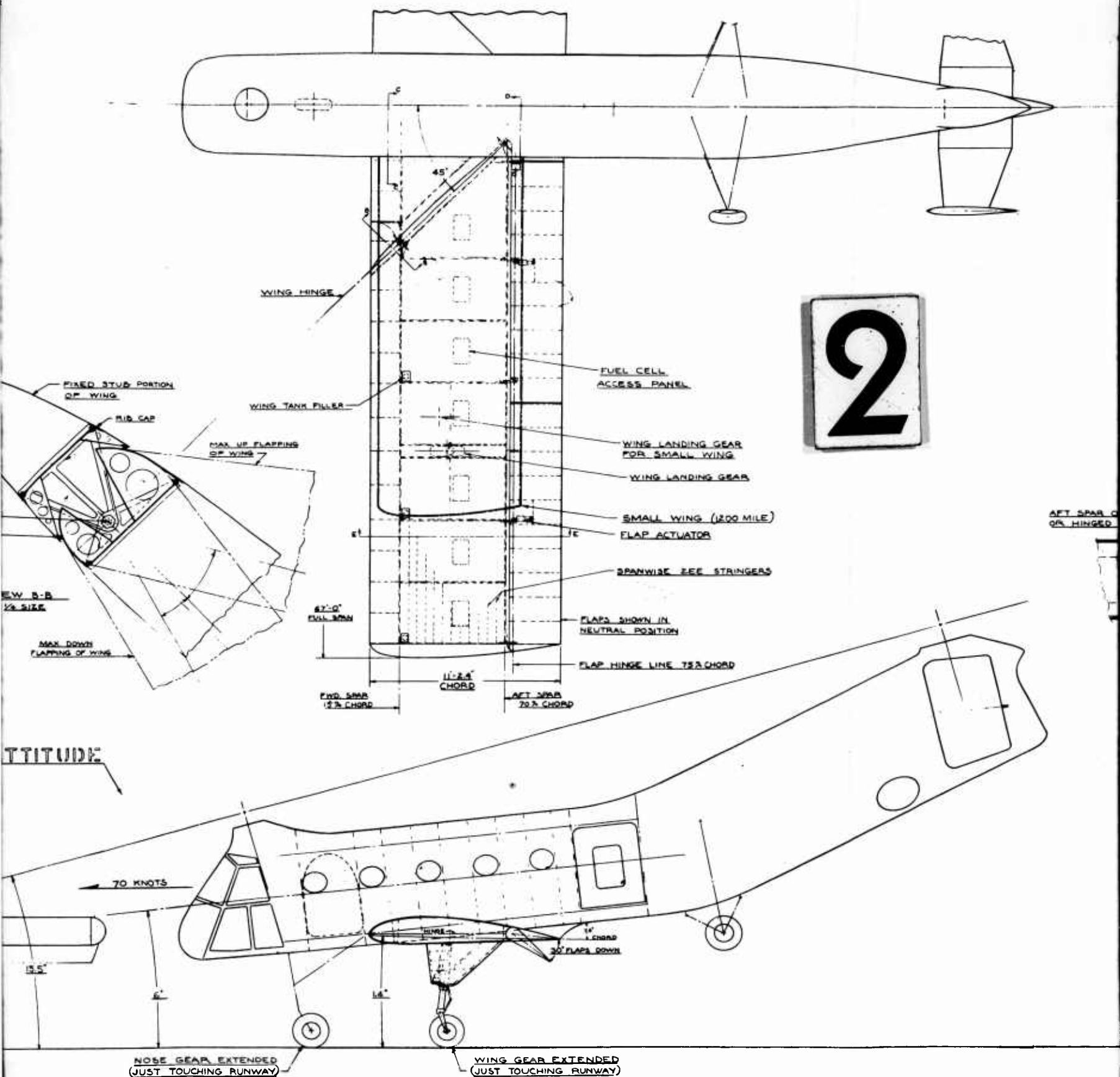
VIEW C-C  
1/2 SIZE



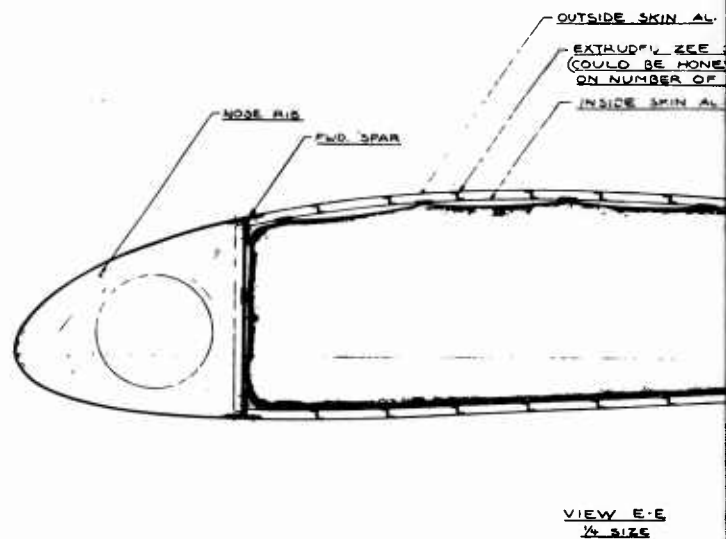
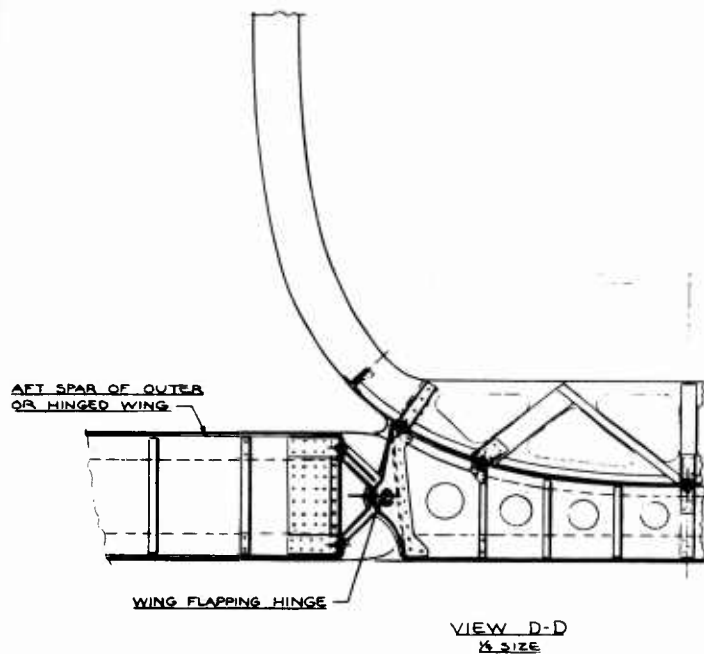
VIEW B-B  
1/2 SIZE



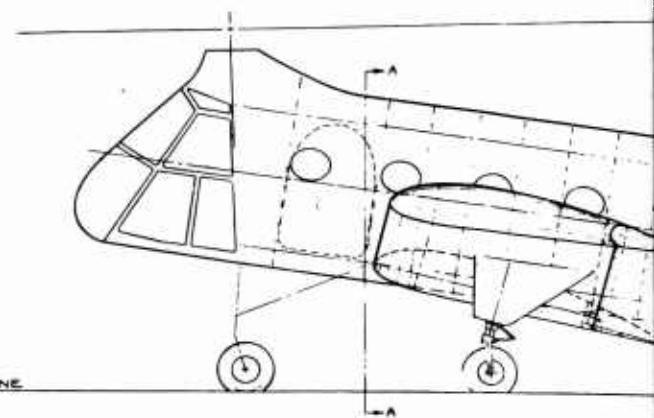
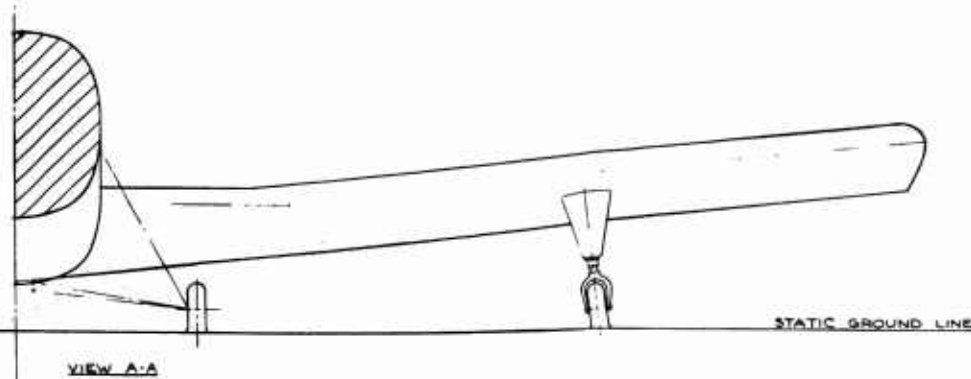
NOS  
(JUST



3



STATIC POSITION



# 4

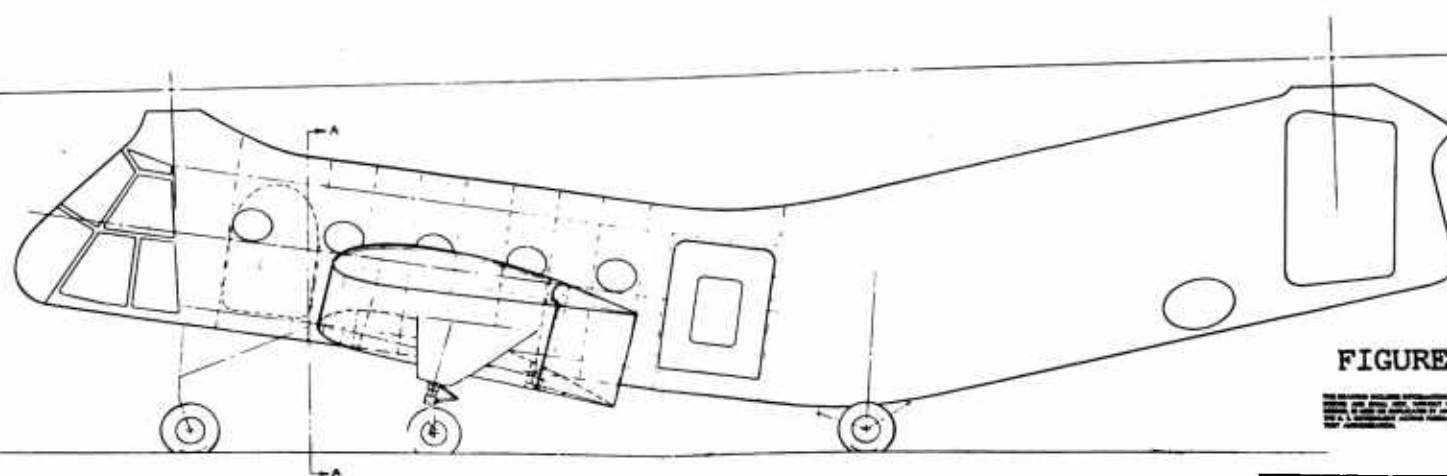
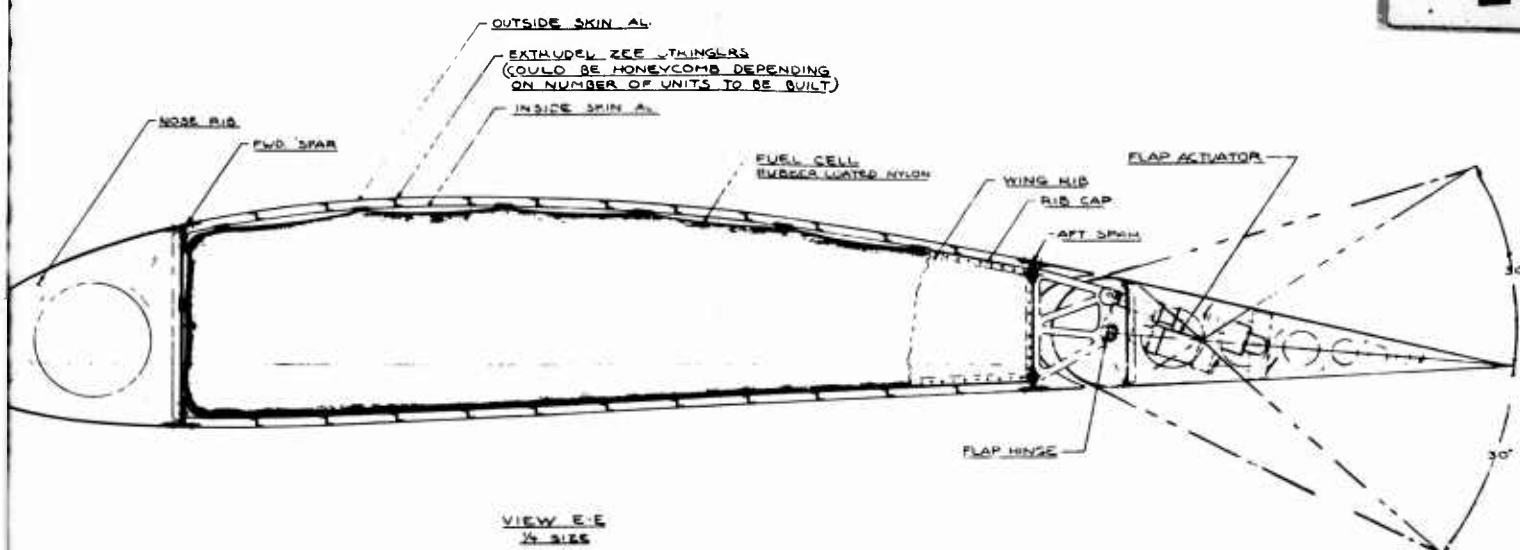


FIGURE 1

THIS DRAWING IS THE PROPERTY OF THE U.S. AIR FORCE AND IS NOT TO BE REPRODUCED OR TRANSMITTED IN ANY FORM OR BY ANY MEANS, ELECTRONIC OR MECHANICAL, INCLUDING PHOTOCOPYING, RECORDING, OR BY ANY INFORMATION STORAGE AND RETRIEVAL SYSTEM, WITHOUT PERMISSION IN WRITING FROM THE U.S. AIR FORCE.

DATE	10/1/61	BY	W. J. H. / J. H. H.
RANGE EXTENSION SYS		VERVOL	
FLOATING FUEL WING		H-21	
064101		064101	



## II. DESCRIPTION OF THE WING

Each of the wings is hinged freely about an axis set at a yaw angle of  $45^\circ$  with respect to the longitudinal axis of the helicopter. The hinge offset angle is such that a flap-up motion decreases the wing angle of attack, and a flap-down motion increases this angle, thus tending to keep the wing at a constant lift without the helicopter having to carry the wing weight. Figure 1 illustrates the helicopter-wing system as applied to an H-21.

The wing analyzed under this feasibility study has a 67 ft. total wing span and an 11.2 ft. chord. The flaps comprise 30% of the chord, and are pilot adjustable by electrically actuated jacks to provide control of the trim attitude. Each wing contains seven integral fuel tanks, with sets of tanks interconnected as shown in Figure 2. Each wing tank carries 166.7 gallons of fuel giving a total capacity for both wings of 2,343 gallons. Individual wings weigh 1000 lbs. empty, and 8000 lbs. fully fueled. The helicopter is operated with the cabin empty, but with its own fuel tanks full on take-off with 300 gallons, at a gross weight of 11,100 lbs. This is below the normal gross weight of 13,500 lbs. The helicopter-tank to engine-fuel system operates in the normal manner. The helicopter tank is maintained at about  $3/4$  full by a pumping system from the wing tanks throughout the flight. The present drainage schedule is for the tip tank pair to be emptied first, then the most inboard set of tanks, and finally the middle tank pair, so as to maintain the wing C.G. near the center of the span, and avoid loading the helicopter.

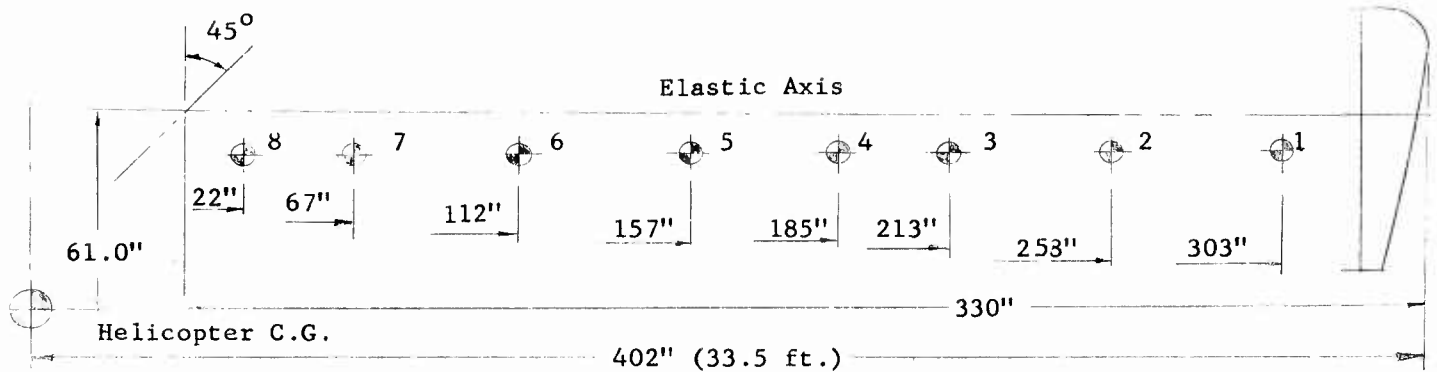
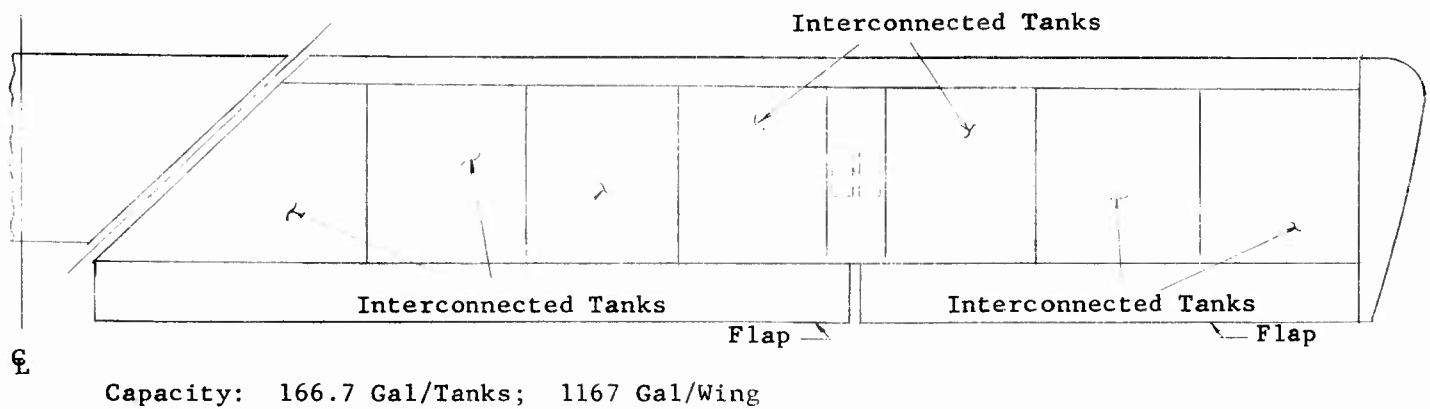
Based on preliminary structural and weight estimates, the elastic center shown in Figure 2 is at 40% chord, and the fully fueled C.G. is at 42.4% chord. Detailed mass, mass moment of inertia and stiffness distributions are shown in Figure 3. The pitching mass moments of inertia of the fuel are taken to be 45% of their rigid value. The percentage figure is taken from the flutter and slosh test investigation of Reference 19, Figure 56.

Cruise speed for maximum range of the aircraft is 80 knots, the maximum level flight speed is 90 knots based on power limitation, and the terminal dive speed is 103 knots. Stall speeds are 30 knots with wing empty and 70 knots with fully loaded wing.

Several natural modes of the wing considered in the flutter analyses are shown in Figure 4. First is the rigid body flapping mode of the wing about its hinge. The motion is restrained by an aerodynamic spring resulting from the change of angle of attack with flap. For 80 knots cruising speed, the natural frequency is 1.310 cps for the empty wing and 0.342 cps for the fully loaded wing. Note that because of the skewed hinge, each flapwise element of the wing exhibits both a vertical and a pitch motion in this rigid body flap mode. Wing bending natural modes, the first with flap bending predominant, the second with torsion predominant, are also shown in Figure 4. Other fuel loading conditions which vary the chordwise and spanwise C.G. locations are also given. The rigid body modes are calculated directly in Appendix C; the flexible modes are calculated by an associated matrix computer analysis with the numerical data given in Appendix C.

FIGURE 2

WING SCHEMATIC DIAGRAM



DISCRETE MASS LOCATIONS

<u>Individual Wing Weight</u>	<u>Helicopter Weight</u>	<u>Helicopter Wing System Weight</u>
0% Fuel, 1,000 lbs.	11,100 lbs.	13,100 lbs.
100% Fuel, 8,000 lbs.	11,100 lbs.	27,100 lbs.

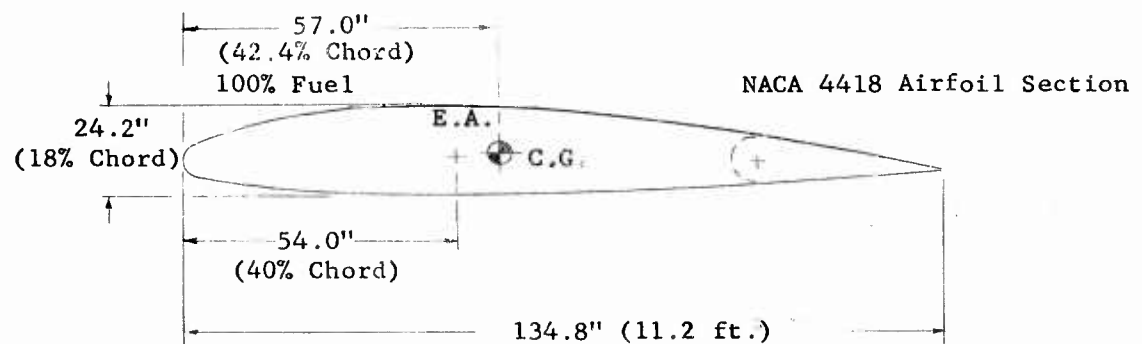
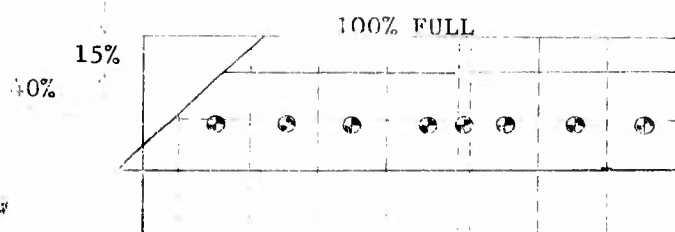
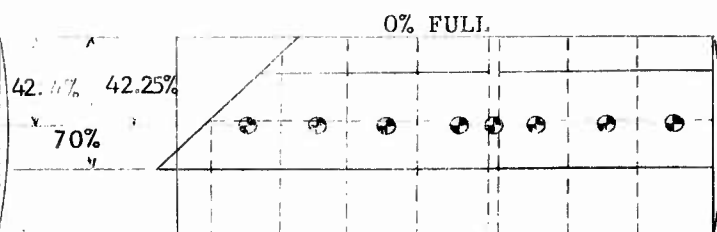


FIGURE 3  
WING PROPERTIES

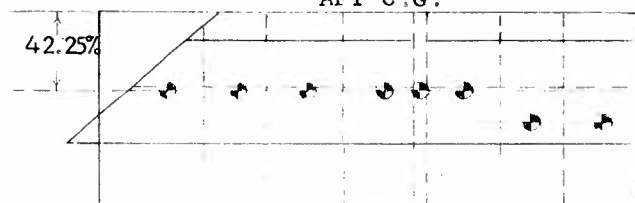


$EI \times 10^{-9}$	2.0	2.2	2.7	3.2	3.6	3.6	3.0	2.5
$GJ \times 10^{-9}$	5.4	5.4	5.4	5.4	5.4	5.4	5.4	5.4
MASS	2.9	2.9	2.9	2.9	.46	2.9	2.9	2.9
PITCH $\times 10^{-3}$	2.4	2.4	2.4	2.4	1	2.4	2.4	2.4
INERTIA								



$EI \times 10^{-9}$	2.0	2.2	2.7	3.2	3.6	3.6	3	2.5
$GJ \times 10^{-9}$	5.4	5.4	5.4	5.4	5.4	5.4	5.4	5.4
MASS	.36	.36	.36	.36	.46	.36	.36	.36
PITCH $\times 10^{-3}$	.3	.3	.3	.3	1.0	.3	.3	.3
INERTIA								

2 TIP TANKS 24.2% FULL  
AFT C.G.



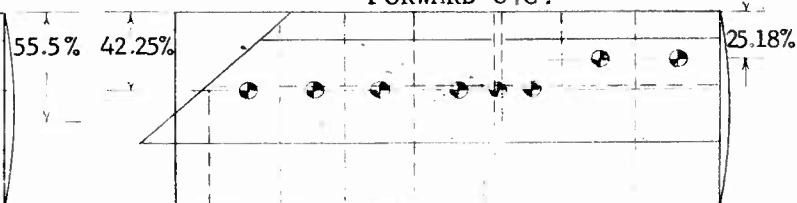
$EI \times 10^{-9}$	2.0	2.2	2.7	3.2	3.6	3.6	3.0	2.5
$GJ \times 10^{-9}$	5.4	5.4	5.4	5.4	5.4	5.4	5.4	5.4
MASS	2.9	2.9	2.9	2.9	.46	2.9	.97	.97
PITCH $\times 10^{-3}$	2.4	2.4	2.4	2.4	1.0	2.4	.8	.8
INERTIA								

24 2% FULL ALONG ENTIRE WING  
AFT C.G.



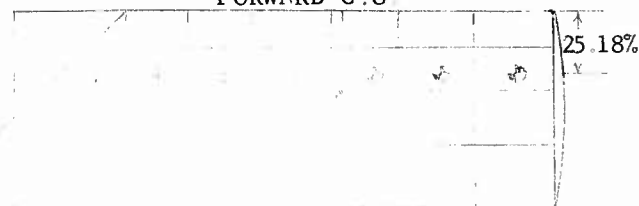
$EI \times 10^{-9}$	2.0	2.2	2.7	3.2	3.6	3.6	3.0	2.5
$GJ \times 10^{-9}$	5.4	5.4	5.4	5.4	5.4	5.4	5.4	5.4
MASS	.97	.97	.97	.97	.46	.97	.97	.97
PITCH $\times 10^{-3}$	.8	.8	.8	.8	1.0	.8	.8	.8
INERTIA								

2 TIP TANKS 25.8% FULL  
FORWARD C.G.



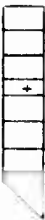

















$EI \times 10^{-9}$	2.0	2.2	2.7	3.2	3.6	3.6	3.0	2.5
$GJ \times 10^{-9}$	5.4	5.4	5.4	5.4	5.4	5.4	5.4	5.4
MASS	2.9	2.9	2.9	2.9	.46	2.9	1.0	1.0
PITCH $\times 10^{-3}$	2.4	2.4	2.4	2.4	1.0	2.4	.9	.9
INERTIA								

25.8% FULL ALONG ENTIRE WING  
FORWARD C.G.



$EI \times 10^{-9}$	2.0	2.2	2.7	3.2	3.6	3.6	3.0	2.5
$GJ \times 10^{-9}$	5.4	5.4	5.4	5.4	5.4	5.4	5.4	5.4
MASS	1.0	1.0	1.0	1.0	.46	1.0	1.0	1.0
PITCH $\times 10^{-3}$	.9	.9	.9	.9	1	.9	.9	.9
INERTIA								

## WING NATURAL MODES

Natural Frequency, CPS						
Fuel Loading						
Mode	Empty	Full	2 Tip Tanks 25.8% Fuel Fwd. C.G.	2 Tip Tanks 24.2% Fuel Aft C.G.	25.8% Fuel Along Span Max. Fwd C.G.	24.2% Fuel Along Span Max. Aft C.G.
Rigid Flap	1.310	0.342	0.509	0.518	0.572	0.581
	 Vert. Up 10.38 Nose Up	 4.08	 4.48	 5.30	 6.70	 6.45
First Coupled Flap Bending Torsion Mode	 Vert. Up 18.35 Nose Up	 7.48	 9.62	 8.23	 11.18	 12.78
Second Coupled Flap Bending Torsion Mode						

### III. METHOD OF ANALYSIS

The equations of motion for the anti-symmetric and symmetric analyses are determined from the kinetic and potential energies by the use of the Lagrange procedure in Appendices A and B. Oscillatory aerodynamic loads are introduced through the generalized force in each equation of motion using Theodorsen's two-dimensional, incompressible unsteady aerodynamics, Reference 7, with numerical values of these airloads taken from AF Report 4798, Reference 8. The equations of motion are then written in matrix form to obtain a flutter determinant. Symmetric and anti-symmetric determinants are presented in Figures 5 and 6; detail derivations are given in Appendices A and B.

It is noted that the flutter derivations presented in the appendices consider the calculated wing modes as normal modes of the combined fuselage-wing system. Consistent with this assumption, the products of the generalized coordinates between the fuselage and wing are zero by the orthogonality condition that exists between normal modes. However, wing mode calculations of the present analysis were performed without the fuselage properties. Therefore, the calculated wing modes are not normal modes of the system, thereby eliminating the assumed orthogonality condition. In compensating for this inconsistency, the flutter determinants shown in Figure 5 and 6 include the additional mass coupling terms between the fuselage and wing coordinates.

In general, each main diagonal element of a flutter determinant represents the mass and inertia effective in a degree of freedom, the spring restraint in the degree of freedom, and the oscillatory airloads produced by and acting in the degree of freedom. Each off-diagonal element represents the airload coupling existing between the degree of freedom of its determinant row position and the degree of freedom of its determinant column position.

The anti-symmetric flutter determinant is shown in Figure 5. The degrees of freedom are:

$\theta$  = fuselage roll

$H_{b1}$  = first coupled flap bending-torsion mode, wing

$H_{b2}$  = second coupled flap bending-torsion mode, wing

The first coordinate, fuselage roll, introduces mass terms and aerodynamic loads, but does not contain any spring terms because of the zero natural frequency of this mode. The two flexible modes are written generally, so as to accommodate any type of wing mode, whether it be flexible bending-torsion or rigid body on the wing hinge. Accommodation of three wing modes would have been more convenient in handling the present problem (rigid flap, first and second coupled flap bending torsion), but an available computer program with two wing modes made the latter more expedient. It is shown later that all three pairs of these modes were employed, so as to cover the flutter coupling possibilities.

The symmetric flutter determinant is shown in Figure 6. The degrees of freedom are:

$Z$  = fuselage vertical motion

$\delta$  = fuselage pitch

$H_{b1}$  = first coupled flap bending-torsion mode, wing

$H_{b2}$  = second coupled flap bending-torsion mode, wing

The first two coordinates introduce mass and aerodynamic terms but do not contain spring terms because of their zero natural frequencies. The two flexible modes are used in the same way as in the antisymmetric case.

Since it is assumed that the oscillations are harmonic, for example  $H_{b1} = \bar{H}_{b1} e^{i\omega t}$  and  $\ddot{H}_{b1} = -\omega^2 \bar{H}_{b1} e^{i\omega t}$ , the unknown flutter frequency  $\omega$  appears in every acceleration term. Each equation is divided through by  $\omega^2$ , causing the frequency to appear as a denominator of the fuselage effective spring constant  $M_{1eff} \omega_{b1}^2$  and  $M_{2eff} \omega_{b2}^2$ . This results in two ratios  $\omega_{b1}/\omega$  and  $\omega_{b2}/\omega$  in which the unknown flutter frequency appears.

An additional complexity exists, however, in the numerical evaluation of the airloads. The airloads are all functions of the Strouhall number  $V/b\omega$  where  $V$  = aircraft forward speed,  $2b$  = airfoil chord and  $\omega$  = flutter frequency. Since the flutter frequency is required in order to determine the airloads, but cannot be known until the flutter determinant is solved, it is seen that a trial and error solution is necessary.

A conventional method of solution avoids the trial and error procedure by artificially creating two unknowns:  $\lambda = (\omega_{b1}/\omega)^2$ , the squared ratio of the first coupled bending frequency to the flutter frequency, and  $\mathcal{F} = \omega_{b1}^2/\omega_{b2}^2$ , the squared ratio of the two modal frequencies. Since each element of the determinant is a complex number by virtue of the form in which the airloads are obtained, the determinant can be expanded and then separated into one real and one imaginary equation. These two equations can then be solved simultaneously for the two unknowns  $\lambda$  and  $\mathcal{F}$ .

Repetitions of this procedure are made for several airload sets corresponding to several values of the parameter  $V/b\omega$ . The  $\lambda$  and  $\mathcal{F}$  results, along with the corresponding  $V/b\omega$  number, are converted to an airspeed  $V$  and a ratio  $\omega_{b1}/\omega_{b2}$ . Finally a plot of  $V$  versus ratio  $\omega_{b1}/\omega_{b2}$  is made, composed of points for each  $V/b\omega$ . The intersection of the known  $\omega_{b1}/\omega_{b2}$  line with the plotted curve determines the flutter speed  $V$  of the aircraft. The slope of the curve at the intersection is a measure of the sensitivity of the flutter to the magnitude of the modal natural frequencies.



FIGURE 6







Q

$$*_{\mathbf{z}} = \sum_{i=1}^n (-\bar{M}_{w_i} z_{b_{i,2}} + \bar{\sigma}_{w_i} z_{b_{i,1}} + \bar{I}_{w_i} \phi_{b_{i,2}}) , \quad *_{\mathbf{z}} = \sum_{i=1}^n (-\bar{M}_{w_i} z_{b_{i,2}} + \bar{\sigma}_{w_i} z_{b_{i,1}} + \bar{I}_{w_i} \phi_{b_{i,2}}) ,$$



#### IV. DISCUSSION OF RESULTS

Results of the flutter analyses are summarized briefly in the table below, with the detailed flutter curves shown later.

CASE			FLUTTER, KNOTS					
100% Fuel  8000 lbs.	0% Fuel  1000 lbs.	2 Tip Cells 25.8% Fuel Fwd. C.G.  6650 lbs.	1. Rigid Mode 2. First Coupled Flap-Torsion		1. Rigid Mode 2. Second Coupled Flap-Torsion		1. First Coupled Flap-Torsion 2. Second Coupled Flap Torsion	
			Anti	Sym.	Anti	Sym.	Anti	Sym.
1			67	90				
2					65	160		
3							No	No
	4		130	90				
	5				120	180		
	6						No	No
		7	90	55				
		8			No	95		
		9					No	No
2 Tip Cells 24.2% Fuel Aft C.G.  6600 lbs.	All Cells 25.8% Fuel Max Fwd CG  2850 lbs.	All Cells 24.2% Fuel Max Aft C.G.  2690 lbs.						
10			55	48				
11					55	65		
12							No	No
	13		No	No				
	14				95	160		
	15						No	No
		16	35	55				
		17			45	35		
		18					No	No

The cases include full fuel, empty, tip cells partially full to produce maximum forward and aft C.G. in the tip cell, and partial fuel in all the cells so as to produce the maximum forward and aft C.G. for the whole wing. For each fuel configuration analyses have been performed for various modal combinations, rigid and first coupled flap bending-torsion, rigid and second coupled flap bending-torsion, first and second coupled flap bending-torsion modes. The table gives the critical flutter speed in knots for the anti-symmetric and symmetric analyses.

Cases 1, 2, 3 cover the fully fueled wing, and show a minimum flutter speed at 65 knots. With rigid flap and first flexible flap-torsion coupled, flutter appears at 67 knots for the anti-symmetric case and 90 knots for the symmetric case. Rigid flap with second bending torsion leaves the anti-symmetric critical at 65 knots, but increases the symmetric to 160 knots. Coupling the bending-torsion modes produces no flutter solution, so this case is stable.

Cases 4, 5 and 6 review the flutter results for 0% fuel with each wing at the 1000 lb structural weight. Again, as in the previous cases, the modes were paired, rigid-first flexible, rigid-second flexible and first flexible - second flexible, for the flutter investigations. Both combinations with rigid flap produce flutter speeds, whereas the flexible pair, as for the fully loaded wing, indicates no flutter speed. Flutter criticals here are generally higher than for the fully fueled wing, reflecting an approximately 2 to 1 frequency increase in the modes.

Since the 7000 lb fuel load is so large with respect to the 1000 lb structural weight, the problem of fuel slosh in the chordwise direction is investigated. While much work has been done in this field, no completely satisfactory representation appeared to be available. As an approximation of the slosh effect it is assumed that the major effect of the fuel slosh is to move the chordwise center of gravity to an extreme forward or aft position.

Cases 7, 8 and 9 assume that the pair of cells nearest the wing tip are drained until a partial fuel level is reached. This portion of the fuel is then considered to be sloshed forward so as to rigidly fill the forward portion of the tank, and results in a maximum forward C.G. travel. The fuel quantity for this condition is calculated in Appendix C to be 25.8% of the tip cell, normal fuel. Flutter analyses, using the same modal combinations show stability with the operating speed band for three of the six pairs; two cases show medium flutter speeds, and one case a low flutter speed. The rigid first flexible symmetric flutter speed calculated at 55 knots, is within the operating speed and less than the minimum for a fully loaded wing. Marginal flutter conditions exist for other modal combinations, namely rigid-second flexible symmetrical and rigid-first flexible anti-symmetrical with calculated speeds near 90 knots.

Similar cases, where the fuel is sloshed aft so as to rigidly fill the aft section of the outboard tanks, and move their C.G.'s to the most aft position are shown for identical modal pairs in cases 10, 11 and 12. Appendix C calculates the fuel quantity for this condition to be 24.2% of the maximum tip cell load. In this configuration, a low flutter speed exists in each modal pair that includes the rigid flap mode. Flutter speeds as low as 48 knots are calculated in this group of cases.

It is clear from the investigation of tip cell C.G. variations that the chordwise C.G. does influence the flutter speed, lowering it from 65 knots with full fuel to a minimum of 48 knots, a change of 17 knots. However, it is probable that any configuration change which would raise the flutter speeds of the fully loaded wing would also be effective for these partial fuel cases.

The last six cases presume a drastic slosh condition, where in cases 13, 14, and 15, every tank is partially loaded to 25.8% of capacity and the quantity is sloshed fully forward, and to 24.2% of capacity and this quantity is sloshed fully aft. The forward C.G. produces flutter in only two modal combinations, but the aft C.G. version produces low flutter speeds whenever the rigid mode is included. Forward C.G. flutter speeds appear at 95 and 160 knots when including the second flexible mode with rigid flap. With the adverse influence of the aft C.G., flutter speeds occur between 35 and 55 knots for the rigid-flexible mode pairs.

Since the cruise speed of the floating wing system is slated to be 80 knots, these flutter results are obviously unacceptable. It will be shown later that these low critical speeds are closely related to the general roll instability of the delta hinge arrangement. Some improvement could be obtained through inclusion of hydraulic dampers at the hinges, recommended previously for mechanical instability control. The latest design arrangement with a straight hinge parallel to the fuselage longitudinal axis and geared flaps to maintain the proper wing attitude, will probably not exhibit these undesirable flutter characteristics.

### Flutter Frequency Ratio Plots

The results of the flutter calculations are presented in more detail in Figure 7 through 11. As described under Section III, the analysis is conducted by varying the airloads over a range of the parameter  $V/bw$ , and solving for flutter speeds and modal frequency ratio as though the latter were unknowns. These results are plotted as flutter speed versus frequency ratio, and when the curves intersect actual modal frequency ratios, a real flutter speed is predicted. The frequency ratio plots are presented in the following figures:

<u>Figure</u>	<u>Fuel Condition</u>
7	100% Fuel
8	0% Fuel
9	Tip Cells Partial Fuel, Forward C.G.
10	Tip Cells Partial Fuel, Aft C.G.
11	All Cells Partial Fuel, Forward C.G.
12	All Cells Partial Fuel, Aft C.G.

As an example, results for the 100% fuel condition, Cases 1, 2, and 3 appear in Figure 7. Three modal combinations are presented, 1. Rigid Flap-First Coupled Mode, 2. Rigid Flap-Second Coupled Mode, 3. First Coupled Mode-Second Coupled Mode. The actual frequency ratios for these mode combinations are:

<u>Fuel</u>	<u>Rigid Flap</u>	<u>First Coupled Mode, CPS</u>	<u>Second Coupled Mode, CPS</u>
100%	0	4.08	7.48

$$\frac{\text{Rigid Flap}}{\text{First Coupled Mode}} = \frac{0}{4.08} = 0$$

$$\frac{\text{Rigid Flap}}{\text{Second Coupled Mode}} = \frac{0}{7.48} = 0$$

$$\frac{\text{First Coupled Mode}}{\text{Second Coupled Mode}} = \frac{4.08}{7.48} = 0.547$$

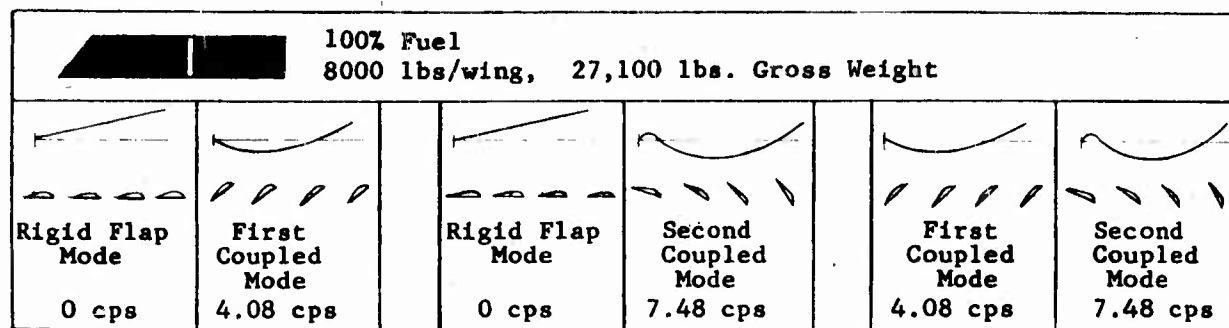
It is noted that the rigid body flap mode of the wing on its delta hinge is taken to be at zero frequency for the wing in a vacuum. The determinant solution contains airloads which provide the steady aerodynamic spring. That is, an up motion of the wing on its hinge reduces the angle of attack, reducing the steady lift and causing the wing to drop on its hinge. Similarly, a down motion of the wing increases the angle of attack and the lift and raises the wing back towards its neutral position. If the wing is analyzed in the presence of this type of air-spring alone, the flapping natural frequency is 0.16 CPS.

In the symmetric solution, the zero frequency ratio line intersects the stability boundary curve in both combinations with rigid flap showing a flutter speed of 90 and 160 knots.

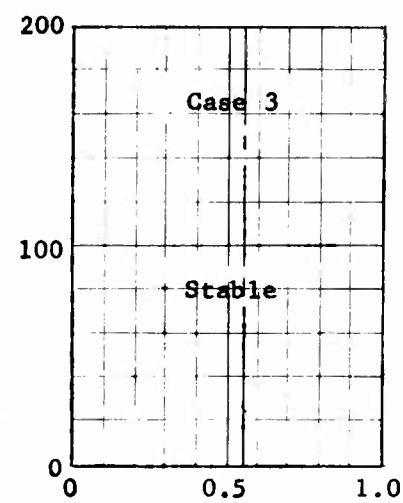
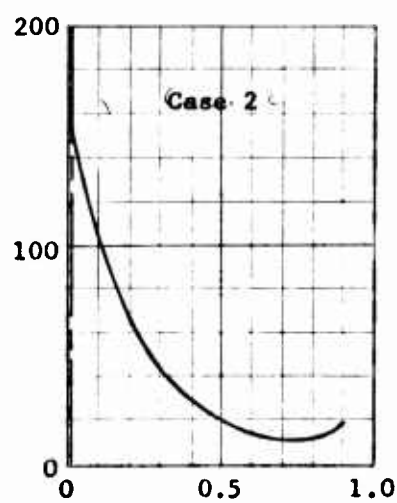
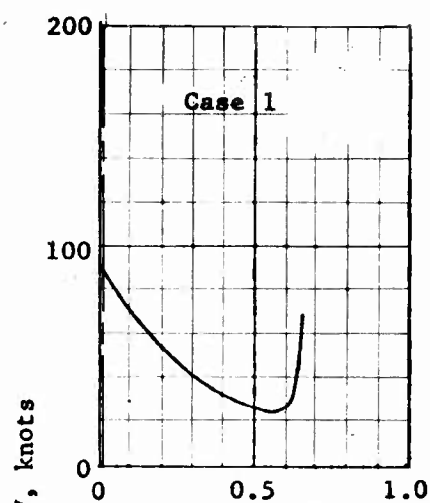
The symmetric solution composed of the first and second coupled modes produces no stability boundary curve within the normal range of  $V/bw$  values. Lower flutter speeds are obtained from the anti-symmetric solution having intersections which define flutter speeds at 67 and 65 knots. Again, no stability boundary curve is produced by the coupled mode combination. Since the  $V/bw$  points shown cover the range of practical interest, additional points required for defining the stability boundary curve in some cases were not calculated. Frequency ratio curves for the additional fuel conditions are presented using a similar format in Figures 8 through 12.

Figure 7

Flutter Curves, 100% Fuel Condition



SYMMETRIC



ANTI-SYMMETRIC

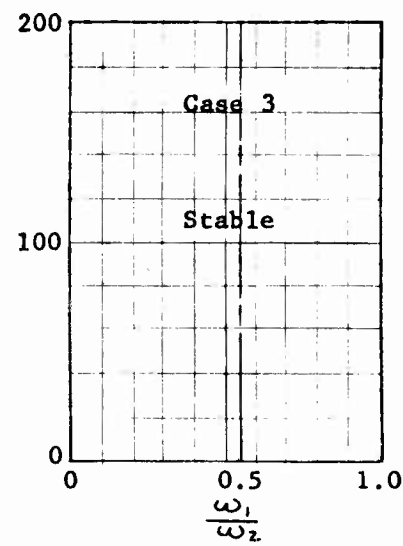
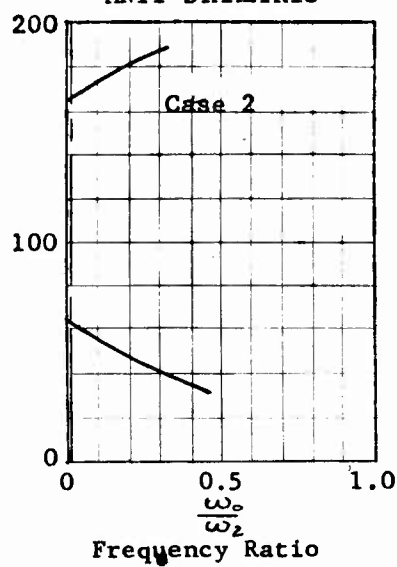
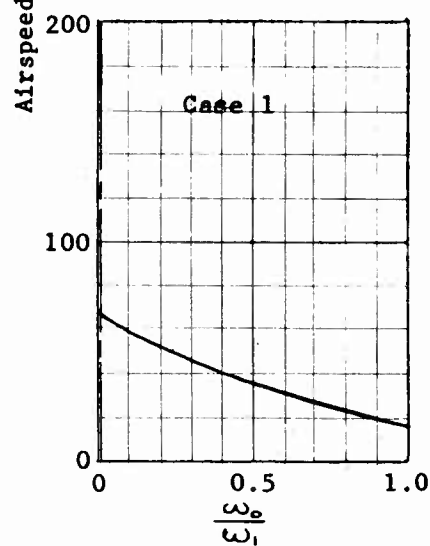
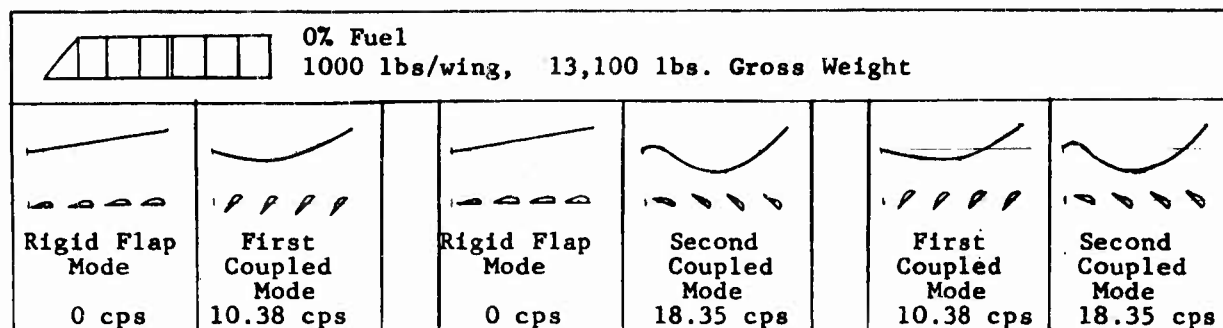


Figure 8

Flutter Curves, 0% Fuel Condition



SYMMETRIC

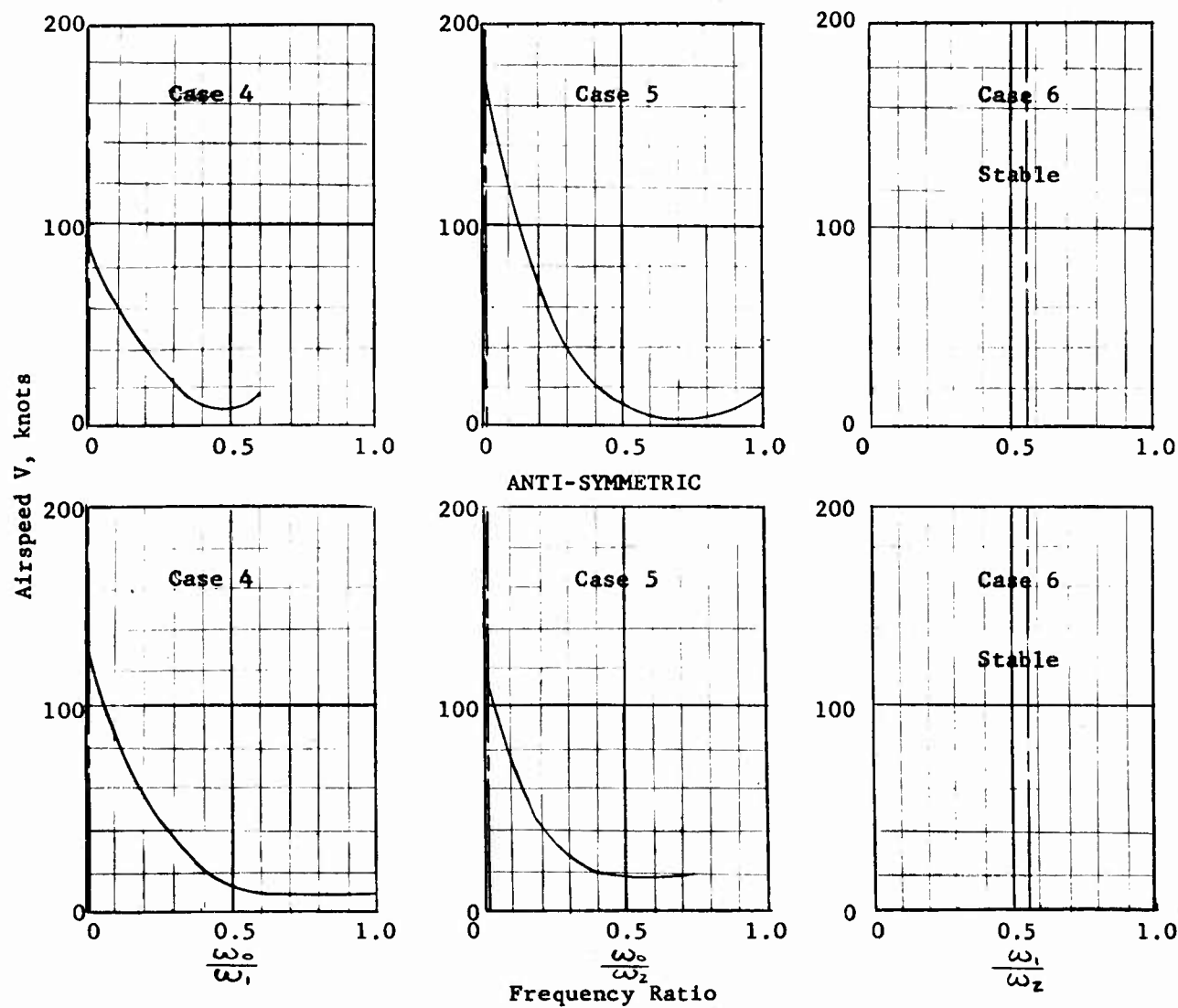


Figure 9

Flutter Curves, Tip Cells Partial Fuel, Forward C.G.

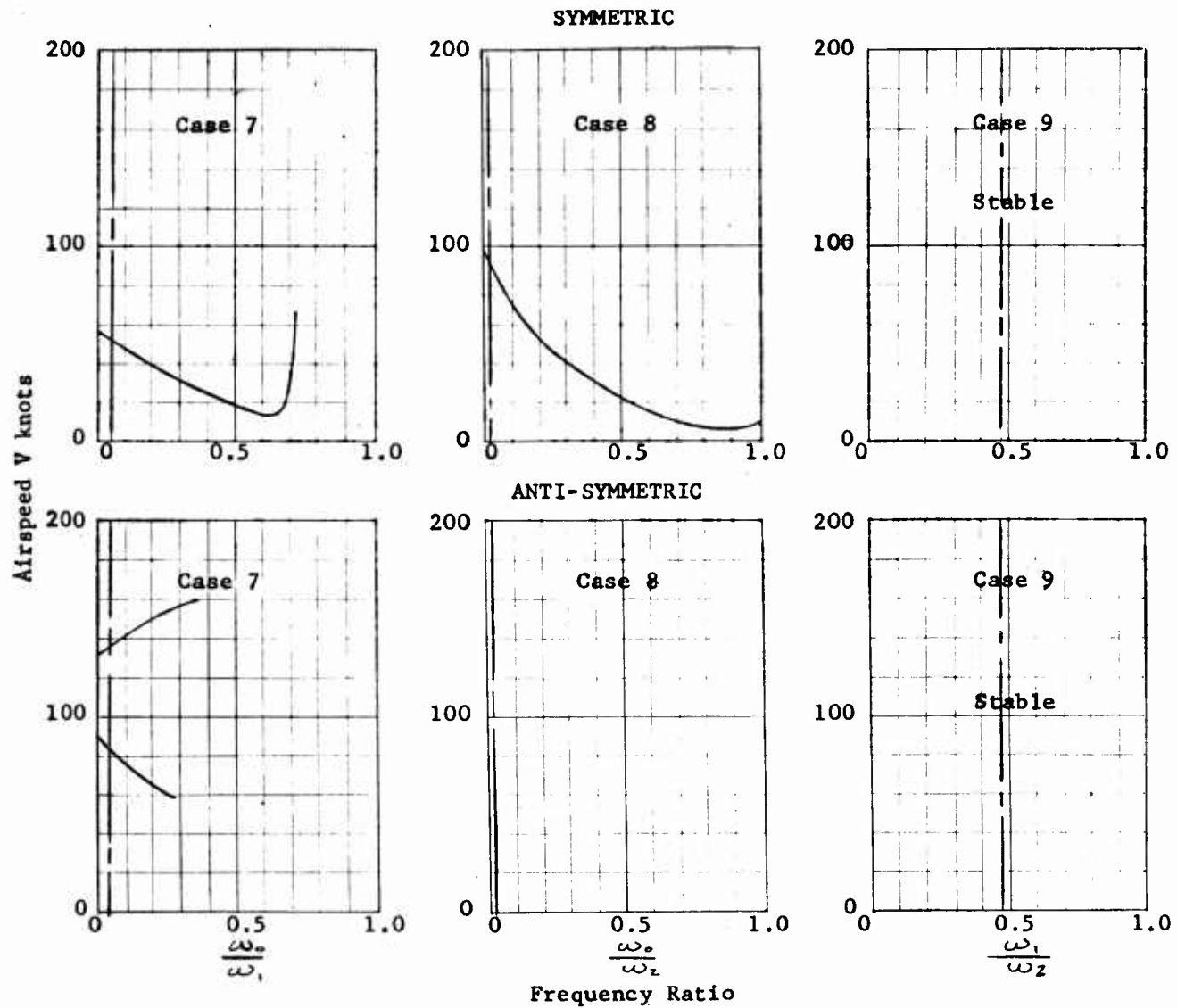
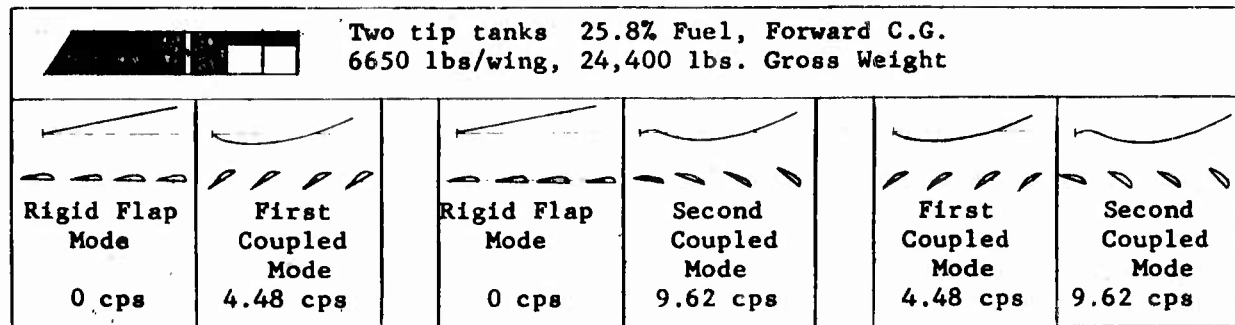




Figure 10

Flutter Curves, Tip Cells Partial Fuel, Aft C.G.

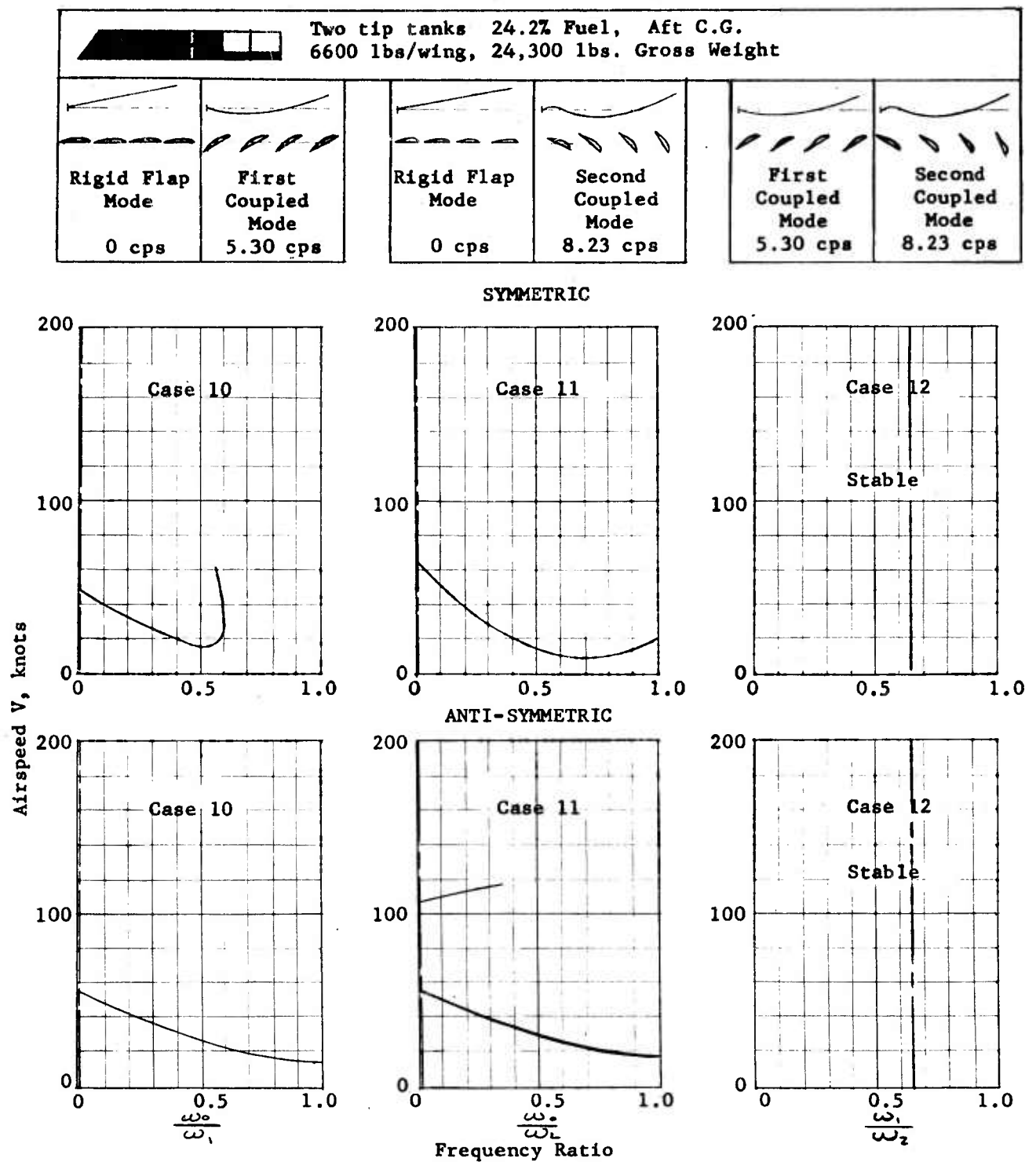
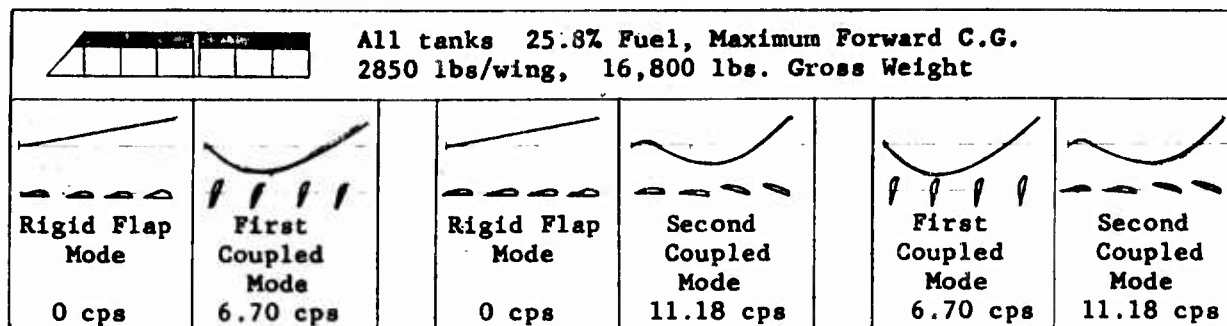


Figure 11

Flutter Curves, All Cells Partial Fuel, Forward C.G.



SYMMETRIC

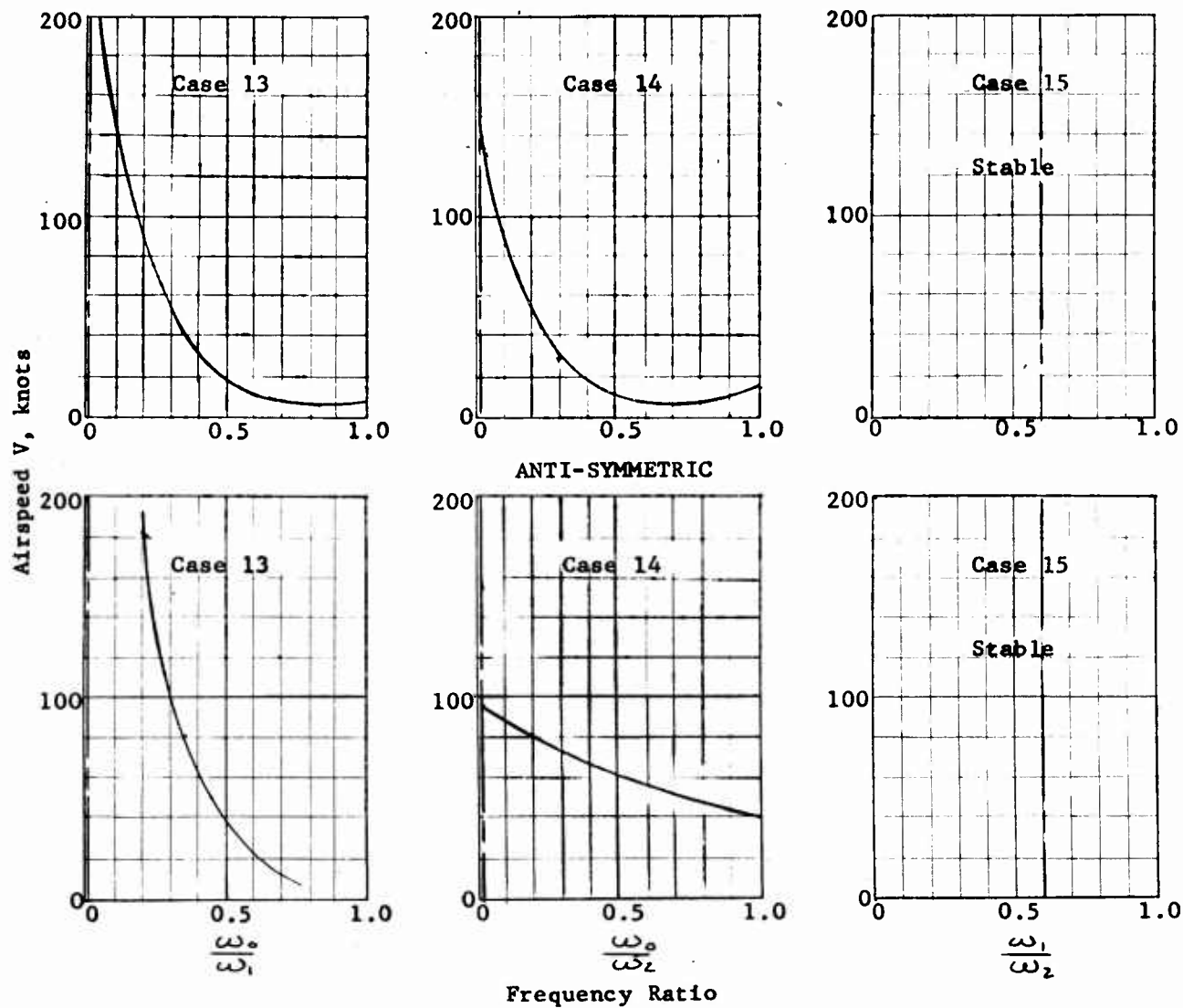
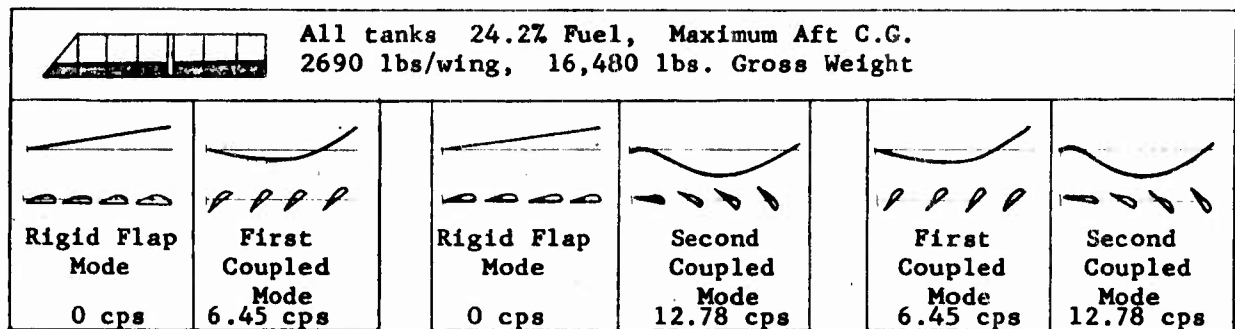
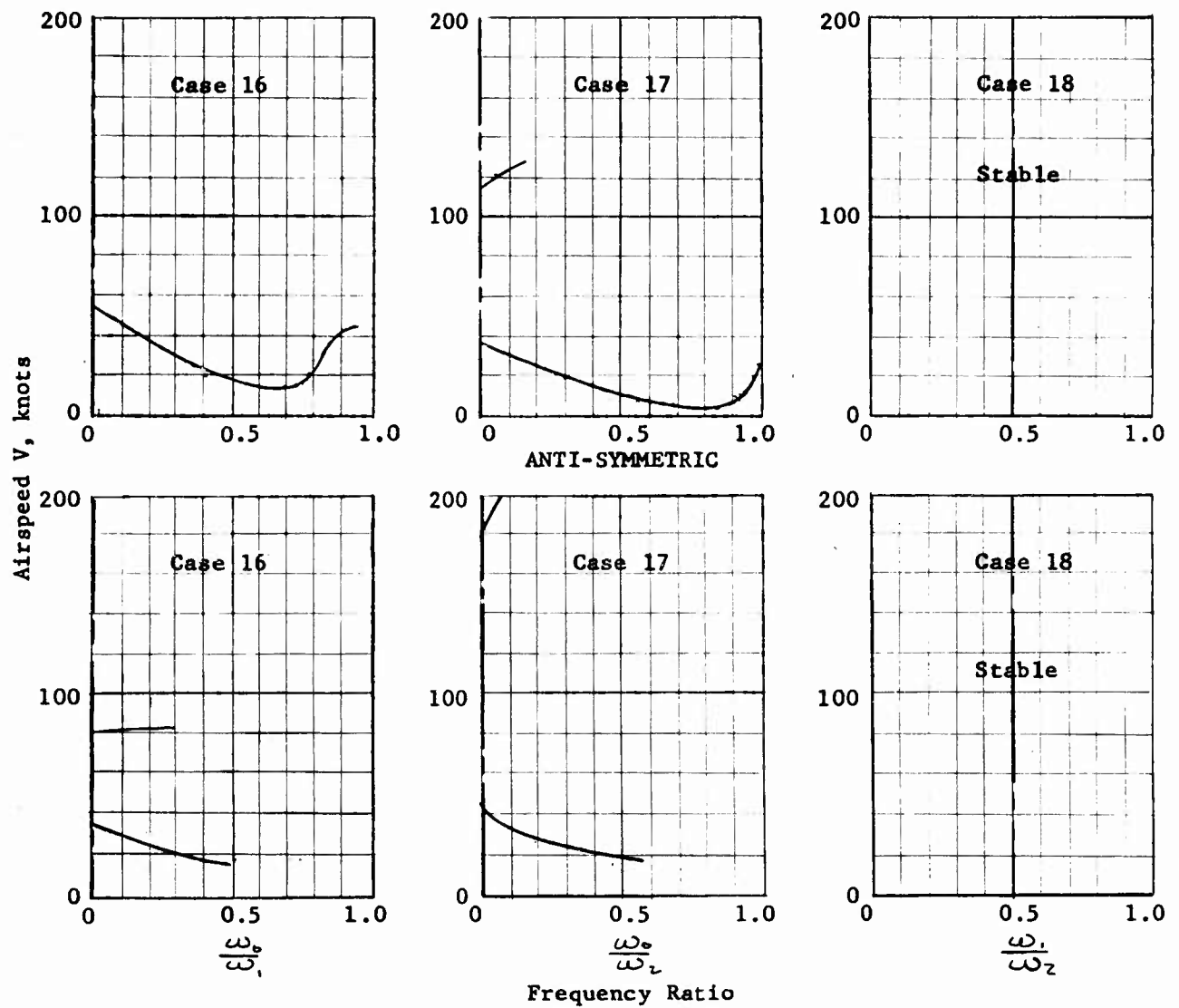


Figure 12

Flutter Curves, All Cells Partial Fuel, Aft C.G.



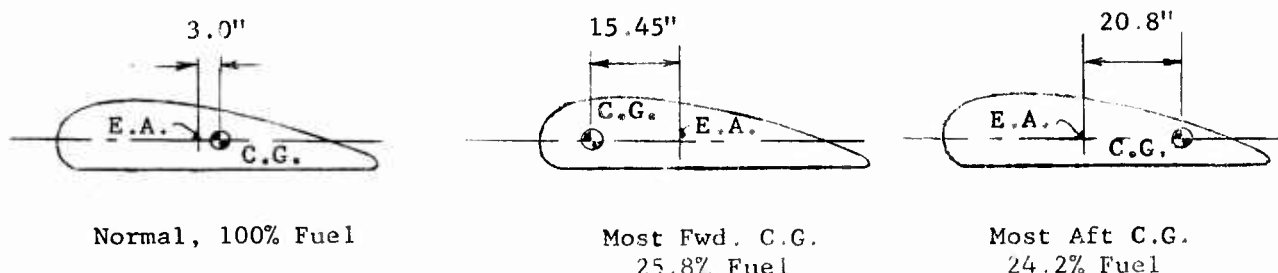
SYMMETRIC



### Flutter Literature on Fuel Slosh

In this investigation, the gross effect of fuel sloshing is approximately simulated by determining a most forward and most aft extreme C.G. position for a practical case. The maximum possible forward and aft C.G. condition are calculated in Appendix C, and result in the following conditions:

#### Partial Fuel Conditions



While the above method of C.G. shifting results in a reasonable solution for the fuelslosh problem with the present wing, the literature was reviewed for other work on the subject. Most investigations have been aimed at determining slosh frequencies and effective masses and inertias for the sloshing fuels, with most of the recent work directed at liquid fueled rocket applications.

One of the basic works on the subject is that of Lamb, Reference 11, who showed that for a rectangular container the slosh frequency is dependent on the length of the container and the liquid depth. If the present wing tank dimensions are used in the Lamb expression, assuming only chordwise sloshing the slosh frequency varies with fuel depth as follows:

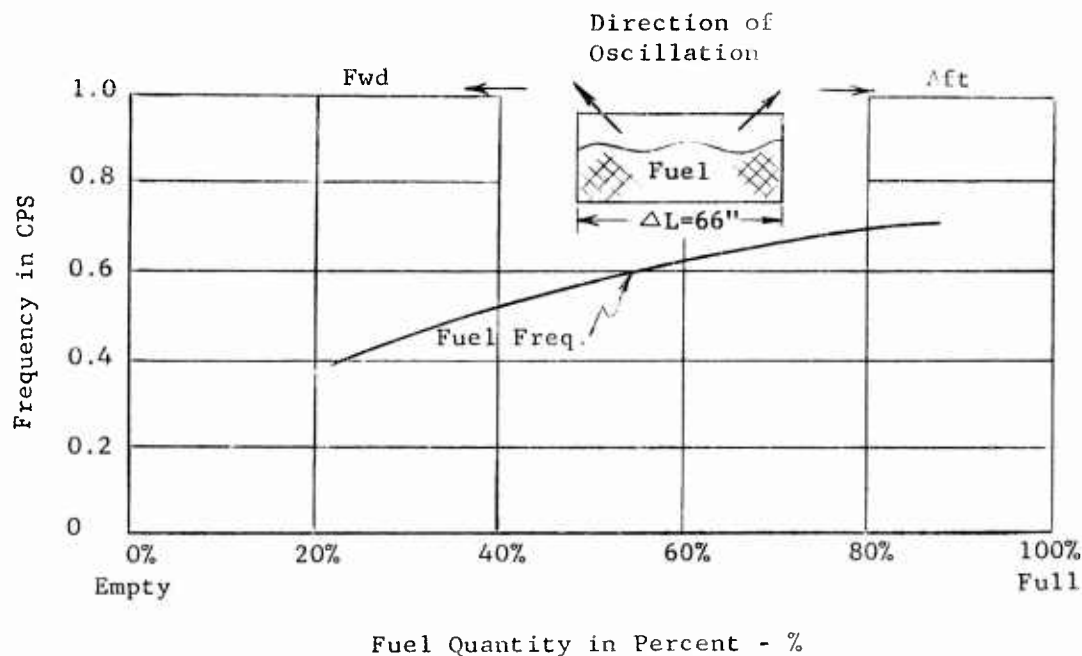
$$\omega = \frac{1}{2\pi} \sqrt{\frac{g}{n} \frac{\pi}{n} \frac{\tanh(\pi/n)}{\Delta L}}, \text{ CPS}$$

where  $g$ , acceleration due to gravity

$h$ , depth of fluid

$\Delta L$ , length of rectangular container

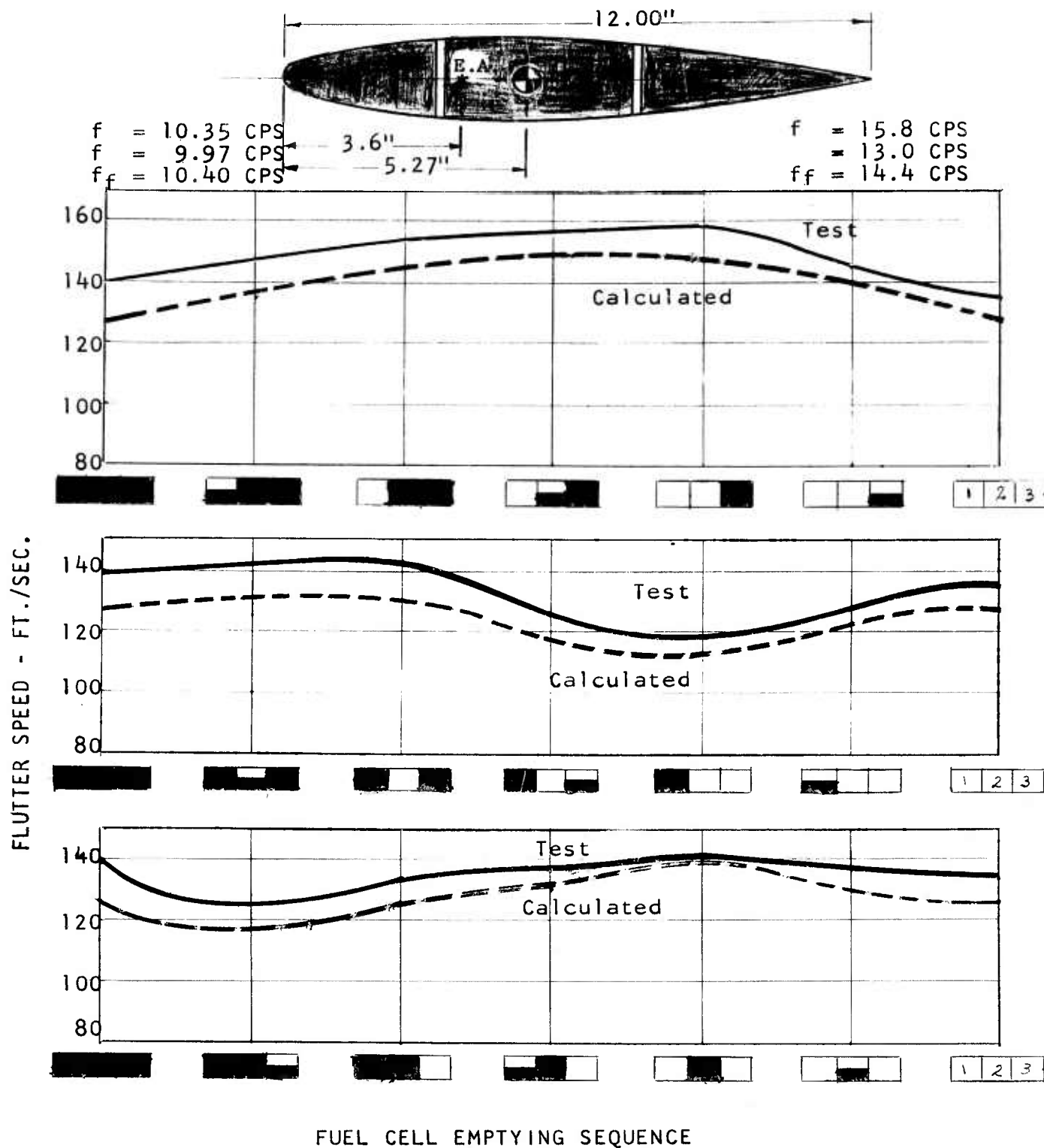
$n = \frac{\Delta L}{h}$ , length to height ratio



An exact analytical method for including fuel motion in the flutter equations is not known, but several approximate solutions have been published. Luskin and Lapin, Reference 12, attempted to include fuel sloshing in aircraft buffeting analyses by a linearization in the equations of motion. The fuel was represented by a simple spring mass system. Other works which estimate effective fuel properties are References 13 through 19; Reference 15 also contains an extensive bibliography of other works in the field.

The most directly applicable reference to the present wing flutter study is Reference 19. This is an experimental investigation of the effect of fuel sloshing in the translation-pitching flutter of a model wing. Experiments were performed on a model wing with internal fuel tanks restrained by springs to produce uncoupled vertical and pitching motions. There are three fuel cells arranged chordwise; i.e., one tank near the leading edge, the second at the midsection, and the third near the trailing edge. By variations of the emptying sequence, the effect of chordwise C.G. and percentage of fuel on the flutter speed of the model may be seen. A plot of the flutter speed versus percent fuel for three emptying sequences is shown in Figure 13.

FIGURE 13  
FLUTTER SPEED AS A FUNCTION OF FUEL  
MODEL (A) TEST RESULT OF PITCHING-TRANSMISSION FLUTTER FROM TN4166-12/57



## V. CONCLUSIONS AND RECOMMENDATIONS

The possibility of flutter on the H-21 Range Extension System wing with the delta hinge arrangement has been investigated over a range of fuel weight conditions. Calculations have been performed for symmetric and anti-symmetric conditions, and for combinations of the three lowest wing modes.

For the wing with 100% fuel load, flutter is predicted at 65 knots, within the operating speed range. As fuel is consumed the flutter speed increases to 90 knots with 0% fuel. Compared to a cruise speed of 80 knots, and a maximum speed of 90 knots, both the 0% and 100% fuel flutter speeds are unacceptable.

These low critical flutter speeds are closely related to the inflight static roll instability determined to be characteristic of the delta hinge configuration. The critical flutter modes involve considerable rigid body motion of the wing on its hinge at frequencies under 0.5 cps. A modified configuration currently under study eliminates the delta hinge, replacing it with a straight hinge and a differential flap arrangement on each wing. The latter provides an aerodynamic spring similar to the delta hinge which tends to keep the wing in its neutral position, but is designed so as to be statically and dynamically stable. This design change will considerably modify the unusual flap-pitch coupling in the oscillatory airloads, and should improve the flutter situation.

A number of partial fuel configurations were included in the flutter analysis of the delta hinge arrangement. These may be considered on a relative basis, and will point up the fueling conditions which can significantly affect the flutter speeds. The influence of fuel slosh is investigated by first presuming partial fuel in the tip tanks with the quantity sloshed fully forward or aft so as to produce maximum chordwise C.G. travel, and then behaving as a rigid mass in that position. The forward C.G. decreases the flutter speed to 55 knots, the aft C.G. decreases the flutter speed to 55 knots relative to a 100% fuel flutter speed of 65 knots. A more drastic sloshed condition is also considered in which partial fuel in all tanks is sloshed fully forward and fully aft. In this instance the forward C.G. raises the flutter speed to 95 knots and the aft C.G. lowers it to 35 knots. Partial fuel in all the tanks is thus a very undesirable situation. This can be avoided by first fully draining the tip tanks, then the inboard tanks, and finally the midspan tanks. This procedure also has the advantage of tending to maintain the spanwise C.G. near the spanwise center of lift so that loads on the fuselage of the helicopter are minimized.

To evaluate the final wing configuration from a flutter standpoint, the safest course to follow is a build up procedure in the initial flight testing. First, it is recommended that a ground shake test of the wings be performed on the ground with wings suspended in a manner simulating the airborne rigid body spring rate. This will evaluate the wing frequency estimates used in the analysis. Secondly, flight flutter testing should be conducted with sufficient strain gage and potentiometer instrumentation to define the wing motion, and a shaker should be used to excite the wing. Initial flights would be conducted with the wing empty, and the measured data examined after the flight for any sign of flutter instability. Successively larger fuel quantities would then be flown, and the data examined until the full range of fuel variations had been explored. As an alternate to shaker excitation, the air jet method of Reference 20 could be used for the inflight investigations.

## VI. REFERENCES

1. Army Contract DA-44-177-TC-550, "Wind Tunnel Tests and Further Study of the Floating Wing Fuel Tanks for Helicopter Range Extension."
2. Army Contract DA-44-177-TC-478, Transportation Research and Engineering Command Project No. 9-38-01-000 ST801, 1958.
3. C. B. Fay, "Feasibility Study of Helicopter Range Extension Using Floating Wing Fuel Tanks," Boeing-Vertol Report R-156, September 28, 1958, ASTIA No. AD203262.
4. "Proposal for Wind Tunnel Test and Further Study of the Floating Wing Fuel Tanks for Helicopter Range Extension," Boeing-Vertol Report PR-275, March, 1959.
5. C. Fay, R. Johnstone, "Wind Tunnel Tests and Further Analyses of the Floating Wing Fuel Tanks for Helicopter Range Extension, Volume 1, Helicopter Range Extension Wind Tunnel Study," Boeing-Vertol Report R-204.
6. V. Capurso, R. Ricks, R. Gabel, "Wind Tunnel Tests and Further Analyses of the Floating Wing Fuel Tanks for Helicopter Range Extension, Volume 2, Ground and Air Mechanical Instability," Boeing-Vertol Report R-197.
7. T. Theodorsen, "General Theory of Aerodynamic Instability and the Mechanism of Flutter," National Advisory Committee for Aeronautics, Report No. 496, April, 1935.
8. B. Smilg, L. Wasserman, "Application of Three-Dimensional Flutter Theory to Aircraft Structures," Air Force Technical Report 4798, July, 1942.
9. T. Theodorsen, I. E. Garrick, "Mechanism of Flutter, a Theoretical and Experimental Investigation of the Flutter Problem," National Advisory Committee for Aeronautics, Report No. 685, 1940.
10. R. L. Bisplinghoff, H. Ashley, R. L. Halfman, "Aeroelasticity," Addison-Wesley Publishing Co., Inc., Reading, Mass., 1955.
11. H. Lamb, "Hydrodynamics," 6th Edition, Dover Publications, New York, N. Y., 1945.
12. H. Luskin, E. Lapin, "An Analytical Approach to the Fuel Sloshing and Buffeting Problems of Aircraft," Journal of the Aeronautical Sciences, April, 1952.
13. K. F. Merten, B. H. Stephenson, "Some Dynamic Effects of Fuel Motion in Simplified Model Tip Tanks on Suddenly Excited Bending Oscillations," NACA TN 2789, September, 1952.

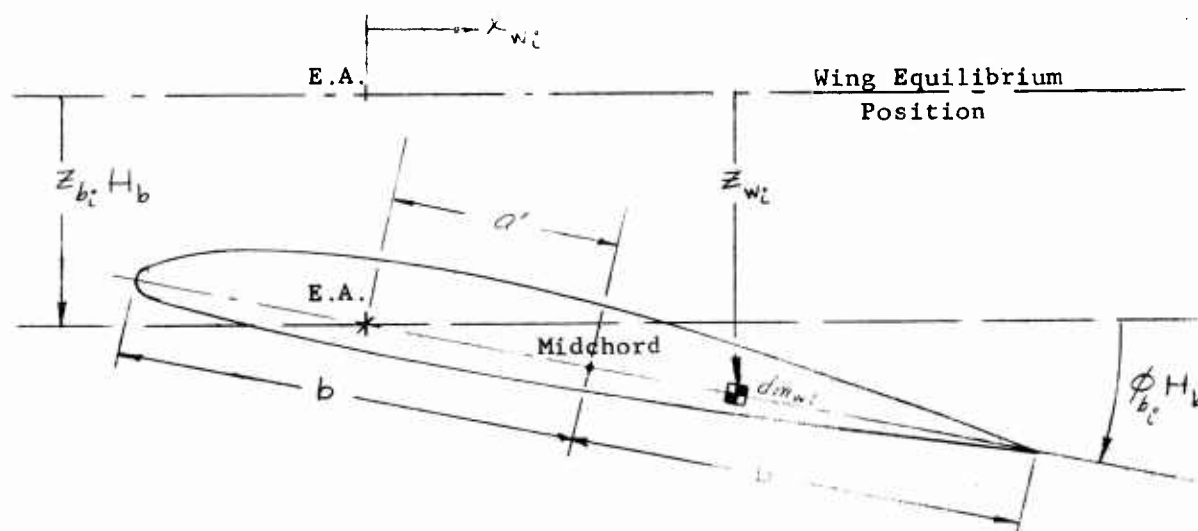
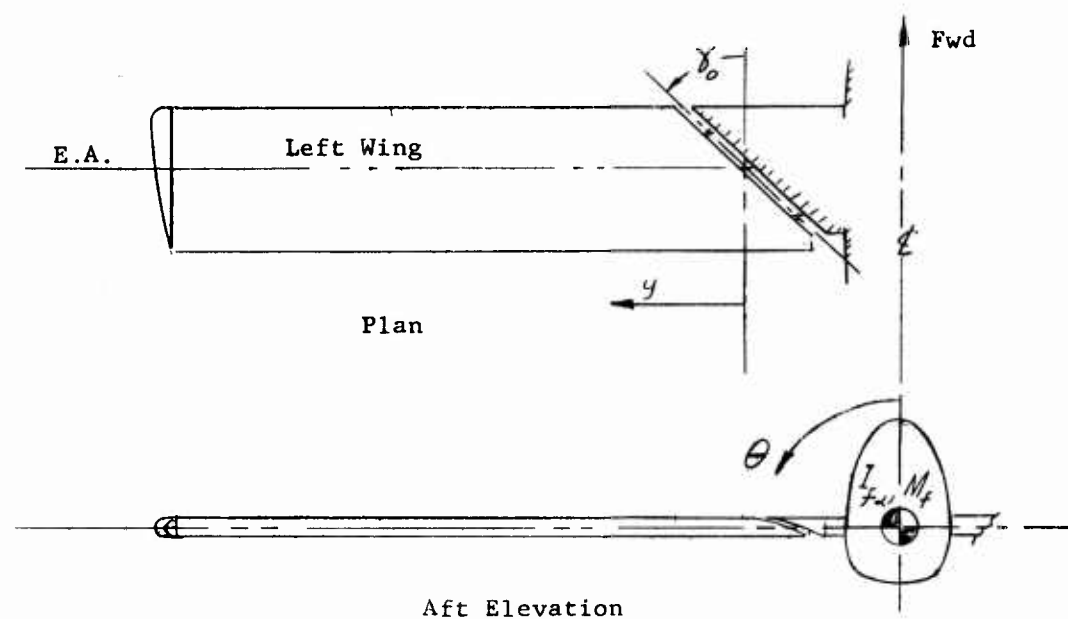


14. J. R. Reese, J. L. Sewall, "Effective Moment of Inertia of Fluid in Offset, Inclined, and Swept-Wing Tanks Undergoing Pitching Oscillations," NACA TN 3353, January, 1955.
15. J. W. Miles, "On the Sloshing of Liquid in a Flexible Tank," American Society of Mechanical Engineers, Paper No. 57-A-12, 1957.
16. B. Budiansky, "Sloshing of Liquids in Circular Canals and Spherical Tanks," Journal of the Aeronautical Sciences, March, 1960.
17. J. L. McCarthy, D. G. Stephens, "Investigation of the Natural Frequencies of Fluids in Spherical and Cylindrical Tanks," NASA TN D-252, May, 1960.
18. R. M. Cooper, "Dynamics of Liquids in Moving Containers," Journal of the American Rocket Society, August, 1960.
19. J. L. Sewall, "An Experimental and Theoretical Study of the Effect of Fuel on Pitching-Translation Flutter," NACA TN 4166, December, 1957.
20. M. B. Zisfein and B. B. D'Ewart, "A New Approach to Safe Flight Flutter Testing," AFOSR TN60-1027, September, 1960.

APPENDIX A

ANTI-SYMMETRIC FLUTTER ANALYSIS

# SCHEMATIC OF DEGREES OF FREEDOM FOR ANTI-SYMMETRIC FLUTTER ANALYSIS



Typical Wing Section  
Kinematics  
(Looking Inboard)

## System Kinematics

Wing vertical displacement at span station i,

$$Z_{wi} = y_i \theta + z_{b_i} H_{b_i} + z_{b_2i} H_{b_2} + x_{wi} \phi_{b_i} H_{b_i} + x_{wi} \phi_{b_2i} H_{b_2}$$

The velocity,

$$\dot{Z}_{wi} = y_i \dot{\theta} + z_{b_i} \dot{H}_{b_i} + z_{b_2i} \dot{H}_{b_2} + x_{wi} \phi_{b_i} \dot{H}_{b_i} + x_{wi} \phi_{b_2i} \dot{H}_{b_2}$$

and the square of the velocity,

$$\begin{aligned} \dot{Z}_{wi}^2 = & y_i^2 \dot{\theta}^2 + z_{b_i}^2 \dot{H}_{b_i}^2 + z_{b_2i}^2 \dot{H}_{b_2}^2 + x_{wi}^2 \phi_{b_i}^2 \dot{H}_{b_i}^2 + x_{wi}^2 \phi_{b_2i}^2 \dot{H}_{b_2}^2 \\ & + 2 y_i z_{b_i} \dot{\theta} \dot{H}_{b_i} + 2 y_i z_{b_2i} \dot{\theta} \dot{H}_{b_2} + 2 y_i x_{wi} \phi_{b_i} \dot{\theta} \dot{H}_{b_i} + 2 y_i x_{wi} \phi_{b_2i} \dot{\theta} \dot{H}_{b_2} \\ & + 2 z_{b_i} z_{b_2i} \dot{H}_{b_i} \dot{H}_{b_2} + 2 z_{b_i} x_{wi} \phi_{b_i} \dot{H}_{b_i}^2 + 2 z_{b_i} x_{wi} \phi_{b_2i} \dot{H}_{b_i} \dot{H}_{b_2} \\ & + 2 z_{b_2i} x_{wi} \phi_{b_i} \dot{H}_{b_i} \dot{H}_{b_2} + 2 z_{b_2i} x_{wi} \phi_{b_2i} \dot{H}_{b_2}^2 + 2 x_{wi}^2 \phi_{b_i} \phi_{b_2i} \dot{H}_{b_i} \dot{H}_{b_2} \end{aligned}$$

Factoring out the generalized coordinates,

$$\begin{aligned} \dot{Z}_{wi}^2 = & y_i^2 \dot{\theta}^2 + [z_{b_i}^2 + x_{wi}^2 \phi_{b_i}^2 + 2 z_{b_i} x_{wi} \phi_{b_i}] \dot{H}_{b_i}^2 \\ & + [z_{b_2i}^2 + x_{wi}^2 \phi_{b_2i}^2 + 2 z_{b_2i} x_{wi} \phi_{b_2i}] \dot{H}_{b_2}^2 \\ & + [2 y_i z_{b_i} + 2 y_i x_{wi} \phi_{b_i}] \dot{\theta} \dot{H}_{b_i} + [2 y_i z_{b_2i} + 2 y_i x_{wi} \phi_{b_2i}] \dot{\theta} \dot{H}_{b_2} \\ & + [2 z_{b_i} z_{b_2i} + 2 x_{wi} z_{b_i} \phi_{b_2i} + 2 x_{wi} z_{b_2i} \phi_{b_i} + 2 x_{wi}^2 \phi_{b_i} \phi_{b_2i}] \dot{H}_{b_i} \dot{H}_{b_2} \end{aligned}$$

The fuselage angular displacement and velocity are:

$\theta$  and  $\dot{\theta}$  respectively in roll.

## Energy Equations

### Kinetic Energy

$$\begin{aligned} T = & \frac{1}{2} \left[ \frac{1}{2} I_{xx} \right] \dot{\theta}^2 + \frac{1}{2} \int_{\text{WING ROOT}}^{\text{LEFT WING TIP}} \int_{\text{WING T.E.}}^{\text{WING L.E.}} \dot{Z}_w^2 dm_w dy \quad \text{or} \\ = & - \left[ \frac{1}{2} I_{xx} \right] \dot{\theta}^2 + \frac{1}{2} \sum_{L=1}^{\text{LEFT WING TIP}} \dot{Z}_{wi}^2 \bar{M}_{wi} \end{aligned}$$

where :

$$\begin{aligned} \bar{M}_{wi} &= \int_{\text{T.E.}}^{\text{L.E.}} dm_w dy \quad \text{mass of each wing spanwise segment acting at station i.} \\ dm_w &= \text{mass per unit chord per wing segment.} \end{aligned}$$

## Kinetic Energy (continued)

Substituting the expression for

$$T = \frac{1}{2} \left[ \frac{1}{2} I_{\alpha} \right] \dot{\theta}^2 + \frac{1}{2} \sum_{i=1}^{n \sim \text{LEFT WING TIP}} \overline{M}_{W_i} \left\{ y_i^2 \dot{\theta}^2 + \left[ z_{b_{1i}}^2 + x_{W_i}^2 \phi_{b_{1i}}^2 + 2 x_{W_i} z_{b_{1i}} \phi_{b_{1i}} \right] \dot{H}_{b_1}^2 \right. \\ \left. + \left[ z_{b_{2i}}^2 + x_{W_i}^2 \phi_{b_{2i}}^2 + 2 x_{W_i} z_{b_{2i}} \phi_{b_{2i}} \right] \dot{H}_{b_2}^2 + \left[ 2 y_i z_{b_{1i}} + 2 x_{W_i} y_i \phi_{b_{1i}} \right] \dot{\theta} \dot{H}_{b_1} \right. \\ \left. + \left[ 2 y_i z_{b_{2i}} + 2 x_{W_i} y_i \phi_{b_{2i}} \right] \dot{\theta} \dot{H}_{b_2} + \left[ 2 z_{b_{1i}} z_{b_{2i}} + 2 x_{W_i} z_{b_{1i}} \phi_{b_{2i}} + 2 x_{W_i} z_{b_{2i}} \phi_{b_{1i}} + 2 x_{W_i} \phi_{b_{1i}} \phi_{b_{2i}} \right] \dot{H}_{b_1} \dot{H}_{b_2} \right\}$$

Since  $\theta$ ,  $H_{b_1}$ , and  $H_{b_2}$  are normal modes, then by the principle of the orthogonality condition between normal modes, products of the normal coordinates are zero. Thus the coefficients of  $\dot{\theta} \dot{H}_{b_1}$ ,  $\dot{\theta} \dot{H}_{b_2}$  and  $\dot{H}_{b_1} \dot{H}_{b_2}$  are zero. Therefore the kinetic energy expression is reduced to

$$T = \frac{1}{2} \left[ \frac{1}{2} I_{\alpha} \right] + \frac{1}{2} \sum_{i=1}^{n \sim \text{WING TIP}} \overline{M}_{W_i} \left\{ y_i^2 \dot{\theta}^2 + \left[ z_{b_{1i}}^2 + x_{W_i}^2 \phi_{b_{1i}}^2 + 2 x_{W_i} z_{b_{1i}} \phi_{b_{1i}} \right] \dot{H}_{b_1}^2 \right. \\ \left. + \left[ z_{b_{2i}}^2 + x_{W_i}^2 \phi_{b_{2i}}^2 + 2 x_{W_i} z_{b_{2i}} \phi_{b_{2i}} \right] \dot{H}_{b_2}^2 \right\}.$$

Let:

$$A = \left[ \frac{1}{2} I_{\alpha} \right] + \sum_{i=1}^{n \sim \text{WING TIP}} \overline{M}_{W_i} y_i^2, \quad \frac{1}{2} \text{ coefficient of } \dot{\theta}^2$$

$$B = \sum_{i=1}^{n \sim \text{WING TIP}} \overline{M}_{W_i} \left[ z_{b_{1i}}^2 + x_{W_i}^2 \phi_{b_{1i}}^2 + 2 x_{W_i} z_{b_{1i}} \phi_{b_{1i}} \right], \quad \frac{1}{2} \text{ coefficient of } \dot{H}_{b_1}^2$$

$$C = \sum_{i=1}^{n \sim \text{WING TIP}} \overline{M}_{W_i} \left[ z_{b_{2i}}^2 + x_{W_i}^2 \phi_{b_{2i}}^2 + 2 x_{W_i} z_{b_{2i}} \phi_{b_{2i}} \right], \quad \frac{1}{2} \text{ coefficient of } \dot{H}_{b_2}^2$$

Then,

$$T = \frac{1}{2} \left[ A \dot{\theta}^2 + B \dot{H}_{b_1}^2 + C \dot{H}_{b_2}^2 \right].$$

## Potential Energy

$$V = \frac{1}{2} k_{b_1} H_{b_1}^2 + \frac{1}{2} k_{b_2} H_{b_2}^2$$

where :  $k_{b_1}$  and  $k_{b_2}$  are effective spring rates of the wing modes considered.

### Lagrange's Equation

The equations of motion are obtained by the following operation due to Lagrange.

$$\frac{d}{dt} \left[ \frac{\partial T}{\partial \dot{q}} \right] + \frac{\partial V}{\partial q} - \frac{\partial T}{\partial q} = F_q$$

where:  $q$  = a generalized coordinate

$F_q$  = generalized force in the  $q$  coordinate

Application of the above operation to the kinetic and potential energy expressions yields,

$$\frac{d}{dt} \left[ \frac{\partial T}{\partial \dot{\theta}} \right] = A \ddot{\theta}, \quad \frac{\partial V}{\partial \theta} = 0, \quad -\frac{\partial T}{\partial \theta} = 0$$

$$\frac{d}{dt} \left[ \frac{\partial T}{\partial \dot{H}_{b_1}} \right] = B \ddot{H}_{b_1}, \quad \frac{\partial V}{\partial H_{b_1}} = k_{b_1} H_{b_1}, \quad -\frac{\partial T}{\partial H_{b_1}} = 0$$

$$\frac{d}{dt} \left[ \frac{\partial T}{\partial \dot{H}_{b_2}} \right] = C \ddot{H}_{b_2}, \quad \frac{\partial V}{\partial H_{b_2}} = k_{b_2} H_{b_2}, \quad -\frac{\partial T}{\partial H_{b_2}} = 0$$

And the equations of motion are,

$$\begin{aligned} A \ddot{\theta} &= F_\theta \\ B \ddot{H}_{b_1} + k_{b_1} H_{b_1} &= F_{b_1} \\ C \ddot{H}_{b_2} + k_{b_2} H_{b_2} &= F_{b_2} \end{aligned}$$

The complete equations of motion require expressions for the generalized forces  $F_q$ . These are derived in the next section.

## Generalized Forces

The virtual work

$$W = \sum_{\text{ROOT}, i=1}^{n\text{-WING TIP}} M'_i \Delta y_i [\phi_{b_1 i} \delta H_{b_1} + \phi_{b_2 i} \delta H_{b_2}] + \sum_{i=1, \text{ROOT}}^{n\text{-WING TIP}} L_i \Delta y_i [z_{b_1 i} \delta H_{b_1} + z_{b_2 i} \delta H_{b_2} + y_i \delta \theta]$$

or

$$W = \sum_{i=1, \text{ROOT}}^{n\text{-WING TIP}} L_i \Delta y_i \delta \theta + \sum_{i=1, \text{ROOT}}^{n\text{-WING TIP}} (M'_i \phi_{b_1 i} + L_i z_{b_1 i}) \Delta y_i \delta H_{b_1} + \sum_{i=1, \text{ROOT}}^{n\text{-WING TIP}} (M'_i \phi_{b_2 i} + L_i z_{b_2 i}) \Delta y_i \delta H_{b_2}$$

and the generalized force expression is

$$F_g = \frac{\partial W}{\partial (\delta g)}$$

or:

Generalized  $\theta$  Force

$$F_\theta = \sum_{i=1, \text{ROOT}}^{n\text{-TIP}} L_i \Delta y_i$$

Generalized  $H_{b_1}$  Force

$$F_{b_1} = \sum_{i=1, \text{ROOT}}^{n\text{-TIP}} (M'_i \phi_{b_1 i} \Delta y_i + L_i z_{b_1 i} \Delta y_i)$$

Generalized  $H_{b_2}$  Force

$$F_{b_2} = \sum_{i=1, \text{ROOT}}^{n\text{-TIP}} (M'_i \phi_{b_2 i} \Delta y_i + L_i z_{b_2 i} \Delta y_i)$$

where:

$L_i =$  lift at elastic axis per unit span, positive down

$M'_i =$  moment at elastic axis per unit span, positive nose-up

# Generalized Forces as Oscillatory Aerodynamic Loads

From AF Rep 4798 pages 33 and 34,

$$L = \pi \rho b^3 \omega^2 \left\{ \frac{h}{b} [L_h] + \alpha [L_\alpha - L_h(\frac{1}{2} + a)] \right\}$$

$$M' = \pi \rho b^4 \omega^2 \left\{ \frac{h}{b} [M_h - L_h(\frac{1}{2} + a)] + \alpha [M_\alpha - L_\alpha(\frac{1}{2} + a) - M_h(\frac{1}{2} + a) + L_h(\frac{1}{2} + a)^2] \right\}$$

where:

$L$  = oscillatory aerodynamic lift acting on the wing per unit span.

$M'$  = oscillatory aerodynamic moment acting on the wing about its elastic axis per unit span.

$\alpha$  = torsional displacement about the elastic axis of the entire wing, positive for increasing angle of attack.

$h$  = vertical bending displacement of wing, positive down.

$a$  = location of the wing elastic axis measured from the wing mid-chord, as a fraction of the semi-chord, positive aft of mid-chord.

$b$  = wing semi-chord.

$\omega$  = flutter frequency.

$\rho$  = air mass density.

$L_h, L_\alpha, M_h$  and  $M_\alpha$  are complex aerodynamic coefficients tabulated in AF Rept. No. 4798 for various values of the  $V/b\omega$ , where  $V$  = forward speed of aircraft.

Rewriting these oscillatory aerodynamic forces using the notation of the present analysis, the lift per unit span becomes,

$$L_i = \pi \rho b^3 \omega^2 \left\{ \frac{\bar{z}_{b1i} H_{b1} + \bar{z}_{b2i} H_{b2} + y_i \theta}{b} [L_h] + (\phi_{b1i} H_{b1} + \phi_{b2i} H_{b2}) [L_\alpha - L_h(\frac{1}{2} + a)] \right\}.$$

and the aerodynamic moment about the wing elastic axis per unit span becomes,

$$M'_i = \pi \rho b^4 \omega^2 \left\{ \frac{\bar{z}_{b1i} H_{b1} + \bar{z}_{b2i} H_{b2} + y_i \theta}{b} [M_h - L_h(\frac{1}{2} + a)] + (\phi_{b1i} H_{b1} + \phi_{b2i} H_{b2}) [M_\alpha - L_\alpha(\frac{1}{2} + a) - M_h(\frac{1}{2} + a) + L_h(\frac{1}{2} + a)^2] \right\}$$



# Complete Equations of Motion

Substituting the oscillatory aerodynamic coefficients into the generalized force expressions, then the equations of motion become,

θ Equation

$$\left[ \frac{1}{2} I_{f\alpha} + \sum_{i=1, \text{ROOT}}^{n-\text{WING TIP}} \bar{M}_{W_i} y_i^2 \right] \ddot{\theta} = \pi \rho b^3 \omega^2 \sum_{i=1}^n \left[ \frac{z_{b1i} H_{b1} + z_{b2i} H_{b2} + y_i \theta}{b} \{L_h\} \right. \\ \left. + (\phi_{b1i} H_{b1} + \phi_{b2i} H_{b2}) \{L_\alpha - L_h(\frac{1}{2} + a)\} \right] y_i \Delta y_i$$

H<sub>b1</sub> Equation

$$\sum_{i=1}^n \bar{M}_{W_i} [z_{b1i}^2 + \chi_{W_i}^2 \phi_{b1i}^2 + 2 \chi_{W_i} z_{b1i} \phi_{b1i}] \ddot{H}_{b1} + \bar{K}_{b1} H_{b1} = \\ \pi \rho b^4 \omega^2 \sum_{i=1}^n \left[ \phi_{b1i} \left\{ \frac{z_{b1i} H_{b1} + z_{b2i} H_{b2} + y_i \theta}{b} [M_h - L_h(\frac{1}{2} + a)] \right. \right. \\ \left. \left. + (\phi_{b1i} H_{b1} + \phi_{b2i} H_{b2}) [M_\alpha - L_\alpha(\frac{1}{2} + a) - M_h(\frac{1}{2} + a) + L_h(\frac{1}{2} + a)^2] \right\} \right. \\ \left. + z_{b1i} \left\{ \frac{z_{b1i} H_{b1} + z_{b2i} H_{b2} + y_i \theta}{b^2} [L_h] \right. \right. \\ \left. \left. + (\phi_{b1i} H_{b1} + \phi_{b2i} H_{b2}) [L_\alpha - L_h(\frac{1}{2} + a)] \right\} \right] \Delta y_i$$

H<sub>b2</sub> Equation

$$\sum_{i=1}^n \bar{M}_{W_i} [z_{b2i}^2 + \chi_{W_i}^2 \phi_{b2i}^2 + 2 \chi_{W_i} z_{b2i} \phi_{b2i}] \ddot{H}_{b2} + \bar{K}_{b2} H_{b2} = \\ \pi \rho b^4 \omega^2 \sum_{i=1}^n \left[ \phi_{b2i} \left\{ \frac{z_{b1i} H_{b1} + z_{b2i} H_{b2} + y_i \theta}{b} [M_h - L_h(\frac{1}{2} + a)] \right. \right. \\ \left. \left. + (\phi_{b1i} H_{b1} + \phi_{b2i} H_{b2}) [M_\alpha - L_\alpha(\frac{1}{2} + a) - M_h(\frac{1}{2} + a) + L_h(\frac{1}{2} + a)^2] \right\} \right. \\ \left. + z_{b2i} \left\{ \frac{z_{b1i} H_{b1} + z_{b2i} H_{b2} + y_i \theta}{b^2} [L_h] \right. \right. \\ \left. \left. + (\phi_{b1i} H_{b1} + \phi_{b2i} H_{b2}) [L_\alpha - L_h(\frac{1}{2} + a)] \right\} \right] \Delta y_i$$

Collecting the coefficients of the generalized coordinates and assuming a harmonic solution of the form:

$$q = \bar{q} e^{i\omega t}$$

such that:

$$\ddot{q} = -\omega^2 \bar{q} e^{i\omega t} = -\omega^2 q,$$

then upon substitution, the flutter equations may be written in Matrix form as shown in Figure 4

where:

$$k_{b_1} = \omega_{b_1}^2 M_{1EFF}$$

$$k_{b_2} = \omega_{b_2}^2 M_{2EFF}$$

$$\omega_{b_1} = \text{natural frequency of the first wing normal mode in rad/sec.}$$

$$\omega_{b_2} = \text{natural frequency of the second wing normal mode in rad/sec.}$$

$$M_{1EFF} = \sum_{i=1}^n \{ \bar{M}_{w_i} \bar{z}_{b_1 i}^2 + \bar{I}_{w_i} \phi_{b_1 i}^2 + 2 \bar{J}_{w_i} \bar{z}_{b_1 i} \phi_{b_1 i} \}$$

$$M_{2EFF} = \sum_{i=1}^n \{ \bar{M}_{w_i} \bar{z}_{b_2 i}^2 + \bar{I}_{w_i} \phi_{b_2 i}^2 + 2 \bar{J}_{w_i} \bar{z}_{b_2 i} \phi_{b_2 i} \}$$

$$\bar{J}_{w_i} = \bar{M}_{w_i} \chi_{w_i}$$

$$\bar{I}_{w_i} = \bar{M}_{w_i} \chi_{w_i}^2$$

### Solution of the Antisymmetric Flutter Matrix

For a solution to exist the determinant of the flutter matrix coefficients must be zero. Since the coefficients are complex, expansion of the determinant results in two equations with real coefficients, and only one unknown, the flutter frequency  $\omega$ . This means that one equation is extraneous. To circumvent this, assume another variable, which, in this analysis is the ratio of the frequencies of the two wing modes. The two equations may then be solved simultaneously for two unknowns. Repeated solutions of the flutter determinant in this manner must be performed for various values of the reduced frequency  $V/b\omega$ . The solutions of the equations may then be converted to a plot of the forward velocity,  $V$ , against the corresponding frequency ratio, from which the flutter speed may be obtained by the intersection of the actual frequency ratio with the curve.

The steps for the solution of the flutter determinant are as follows. Let Roman Numerals represent the coefficients of the determinant (remembering that these are complex).

$$\begin{vmatrix} \text{II} & \text{III} & \text{IV} \\ \text{VI} & \text{VII} - M_{1EFF} \left( \frac{\omega_{b1}}{\omega} \right)^2 & \text{VIII} \\ \text{X} & \text{XI} & \text{XII} - M_{2EFF} \left( \frac{\omega_{b2}}{\omega} \right)^2 \end{vmatrix} = 0$$

Now, divide the second row by  $M_{1EFF}$  and the third row by  $M_{2EFF}$ , and represent the resulting terms by  $A, B, C, \dots$ , which are still complex. Then making the following substitutions,

$$\lambda = \left( \frac{\omega_{b1}}{\omega} \right)^2 \quad \text{and} \quad \xi = \left( \frac{\omega_{b2}}{\omega_{b1}} \right)^2$$

the determinant becomes

$$\begin{vmatrix} A & B & C \\ D & E - \lambda & F \\ G\xi & H\xi & K\xi - \lambda \end{vmatrix} = 0$$

Solution of this complex determinant for  $\lambda$  and  $\xi$  is programmed (Program No. 1120) on the IBM 650 computer, and the output is as follows.

Antisymmetric Flutter Program - Output Format (Program No. 1120)

AR	BR	CR
AI	BI	CI
DR	ER	FR
DI	EI	FI
GR	HR	KR
GI	HI	KI
M	N	P
V <sub>knots</sub>	Zeta	Lambda

where, A, B ..... K = coefficients of the reduced determinant.  
 Subscript R denotes the real part;  
 subscript I denotes the imaginary part.

M, N, P = coefficients (real) of the equation in  $\lambda$ , e.i.,

$$\lambda^2 M + \lambda N + P = 0$$

V<sub>knots</sub> = forward speed in knots;

$$V = \frac{V}{b\omega} \frac{b\omega_b}{\sqrt{\lambda}} \times \text{Conversion factor to knots.}$$

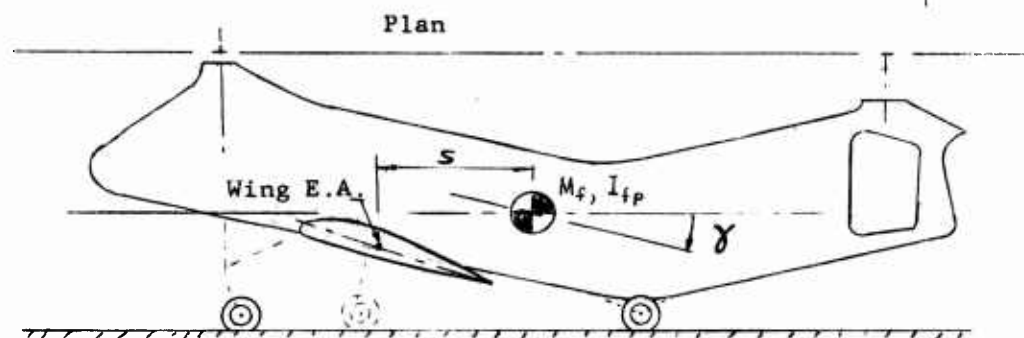
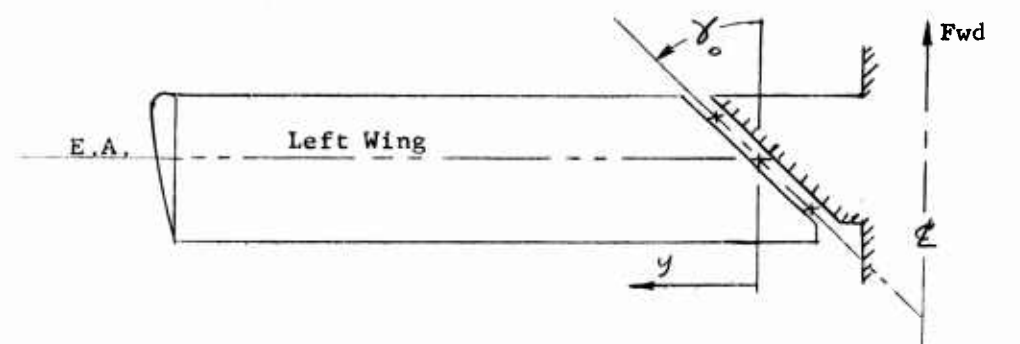
$$\text{Zeta} = \zeta$$

$$\text{Lambda} = \lambda$$

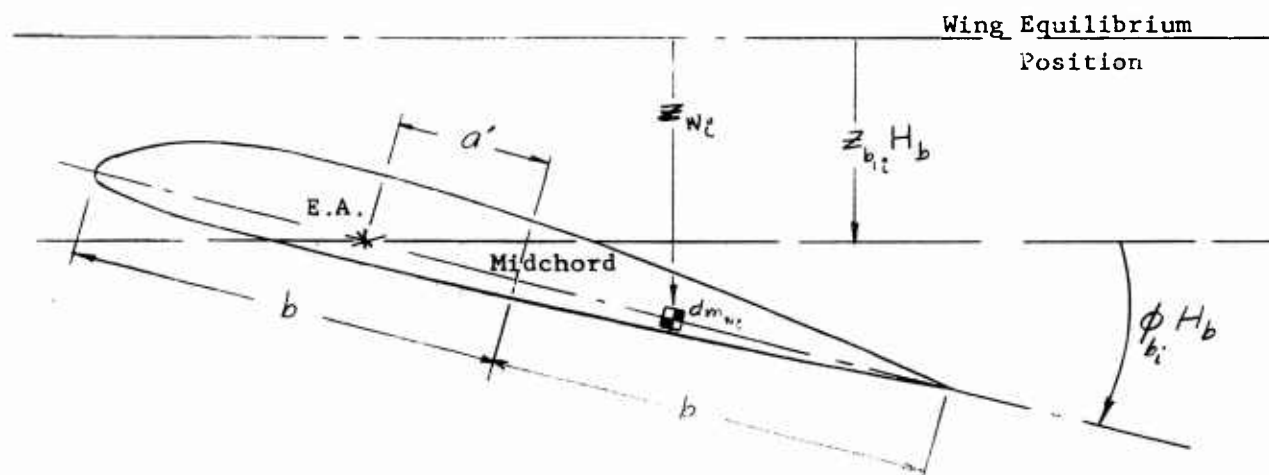
APPENDIX B

SYMMETRIC FLUTTER ANALYSIS

# SCHEMATIC OF DEGREES OF FREEDOM FOR SYMMETRIC FLUTTER ANALYSIS



Side Elevation (Left)



Typical Wing Section  
Kinematics  
(Looking Inboard, Left Wing)

### Symmetric Mode

#### System Kinematics

The wing vertical displacement at Station 1,

$$z_{w1} = z - s\gamma + z_{b1i} H_{b1} + z_{b2i} H_{b2} + x_{w1} \phi_{b1i} H_{b1} + x_{w1} \phi_{b2i} H_{b2}$$

The fuselage C.G. displacements:

Vertical,

$$z_f = z$$

Angular,

$$\gamma_f = \gamma$$

and the velocities are:

$$\dot{z}_{w1} = \dot{z} - s\dot{\gamma} + \dot{z}_{b1i} \dot{H}_{b1} + \dot{z}_{b2i} \dot{H}_{b2} + x_{w1} \phi_{b1i} \dot{H}_{b1} + x_{w1} \phi_{b2i} \dot{H}_{b2}$$

$$\dot{z}_f = \dot{z}$$

$$\dot{\gamma}_f = \dot{\gamma}$$

The squares of the velocities:

$$\dot{z}_f^2 = \dot{z}^2$$

$$\dot{\gamma}_f^2 = \dot{\gamma}^2$$

$$\begin{aligned} \dot{z}_{w1}^2 = & \dot{z}^2 + s^2 \dot{\gamma}^2 + \dot{z}_{b1i}^2 \dot{H}_{b1}^2 + \dot{z}_{b2i}^2 \dot{H}_{b2}^2 + x_{w1}^2 \phi_{b1i}^2 \dot{H}_{b1}^2 + x_{w1}^2 \phi_{b2i}^2 \dot{H}_{b2}^2 \\ & - 2s \dot{z} \dot{\gamma} + 2 \dot{z}_{b1i} \dot{z} \dot{H}_{b1} + 2 \dot{z}_{b2i} \dot{z} \dot{H}_{b2} + 2 x_{w1} \phi_{b1i} \dot{z} \dot{H}_{b1} + 2 x_{w1} \phi_{b2i} \dot{z} \dot{H}_{b2} \\ & - 2s \dot{z}_{b1i} \dot{\gamma} \dot{H}_{b1} - 2s \dot{z}_{b2i} \dot{\gamma} \dot{H}_{b2} - 2 x_{w1} s \phi_{b1i} \dot{\gamma} \dot{H}_{b1} - 2s x_{w1} \phi_{b2i} \dot{\gamma} \dot{H}_{b2} \\ & + 2 \dot{z}_{b1i} \dot{z}_{b2i} \dot{H}_{b1} \dot{H}_{b2} + 2 x_{w1} \dot{z}_{b1i} \phi_{b1i} \dot{H}_{b1}^2 + 2 x_{w1} \dot{z}_{b1i} \phi_{b2i} \dot{H}_{b1} \dot{H}_{b2} \\ & + 2 \dot{z}_{b2i} \phi_{b1i} \dot{H}_{b1} \dot{H}_{b2} + 2 x_{w1} \dot{z}_{b2i} \phi_{b2i} \dot{H}_{b2}^2 + 2 x_{w1}^2 \phi_{b1i} \phi_{b2i} \dot{H}_{b1} \dot{H}_{b2} \end{aligned}$$

Since,  $z$ ,  $\gamma$ ,  $H_{b1}$  and  $H_{b2}$  are normal modes, then by the principle of orthogonality, coefficients of the products of the generalized coordinates must be zero. Applying this principal on the last equation yields,

$$\begin{aligned} \dot{z}_{w1}^2 = & \dot{z}^2 + s^2 \dot{\gamma}^2 + [\dot{z}_{b1i}^2 + x_{w1}^2 \phi_{b1i}^2 + 2 x_{w1} \dot{z}_{b1i} \phi_{b1i}] \dot{H}_{b1}^2 \\ & + [\dot{z}_{b2i}^2 + x_{w1}^2 \phi_{b2i}^2 + 2 x_{w1} \dot{z}_{b2i} \phi_{b2i}] \dot{H}_{b2}^2 \end{aligned}$$

## Symmetric Modes

### Energy Equations

#### Kinetic energy

$$T = \frac{1}{2} \left[ \frac{1}{2} M_f \right] \dot{z}_f^2 + \frac{1}{2} \left[ \frac{1}{2} I_{fp} \right] \dot{\gamma}_f^2 + \int_{\text{LEFT WING ROOT}}^{\text{LEFT WING TIP}} \int_{\text{WING T.E.}}^{\text{WING L.E.}} \dot{z}_w^2 dy dm_w \quad \text{or}$$

$$T = \frac{1}{2} \left[ \frac{1}{2} M_f \right] \dot{z}_f^2 + \frac{1}{2} \left[ \frac{1}{2} I_{fp} \right] \dot{\gamma}_f^2 + \sum_{i=1, \text{ LEFT WING ROOT}}^{\eta, \text{ LEFT WING TIP}} \dot{z}_{wi}^2 \bar{M}_{wi}$$

where:  $\bar{M}_{wi} = \int_{T.E.}^{L.E.} dm_w dy$ , mass of each wing spanwise segment acting at Station  $i$

$dm_w$  = mass per unit chord per wing segment

Substituting the expressions for the kinetic energy becomes,

$$T = \frac{1}{2} \left[ \frac{1}{2} M_f \right] \dot{z}_f^2 + \frac{1}{2} \left[ \frac{1}{2} I_{fp} \right] \dot{\gamma}_f^2 + \sum_{i=1, \text{ ROOT}}^{\eta, \text{ TIP}} \left[ \bar{M}_{wi} \dot{z}^2 + S^2 \bar{M}_{wi} \dot{\gamma}^2 + \left\{ \bar{M}_{wi} \dot{z}_{bi}^2 + \bar{I}_{wi} \dot{\phi}_{bi}^2 + 2 \bar{\sigma}_{wi} \dot{z}_{bi} \dot{\phi}_{bi} \right\} \dot{H}_{bi}^2 + \left\{ \bar{M}_{wi} \dot{z}_{b2i}^2 + \bar{I}_{wi} \dot{\phi}_{b2i}^2 + 2 \bar{\sigma}_{wi} \dot{z}_{b2i} \dot{\phi}_{b2i} \right\} \dot{H}_{b2i}^2 \right]$$

where:  $\bar{I}_{wi} = x_{wi}^2 \bar{M}_{wi} = \int_{T.E.}^{L.E.} x_{wi}^2 dm_w dy$

$$\bar{\sigma}_{wi} = x_{wi} \bar{M}_{wi} = \int_{T.E.}^{L.E.} x_{wi} dm_w dy$$

Collecting coefficients of the generalized coordinates gives,

$$\begin{aligned} A &= \frac{1}{2} M_f + \sum_{i=1, \text{ ROOT}}^{\eta, \text{ TIP}} \bar{M}_{wi} && \frac{1}{2} \text{ coeff. of } \dot{z}^2 \\ B &= \sum_{i=1, \text{ ROOT}}^{\eta, \text{ TIP}} \left\{ \bar{M}_{wi} \dot{z}_{bi}^2 + \bar{I}_{wi} \dot{\phi}_{bi}^2 + 2 \bar{\sigma}_{wi} \dot{z}_{bi} \dot{\phi}_{bi} \right\} && \frac{1}{2} \text{ coeff. of } \dot{H}_{bi}^2 \\ C &= \sum_{i=1, \text{ ROOT}}^{\eta, \text{ TIP}} \left\{ \bar{M}_{wi} \dot{z}_{b2i}^2 + \bar{I}_{wi} \dot{\phi}_{b2i}^2 + 2 \bar{\sigma}_{wi} \dot{z}_{b2i} \dot{\phi}_{b2i} \right\} && \frac{1}{2} \text{ coeff. of } \dot{H}_{b2i}^2 \\ D &= \frac{1}{2} \bar{I}_{fp} + \sum_{i=1, \text{ ROOT}}^{\eta, \text{ TIP}} \bar{M}_{wi} S^2 && \frac{1}{2} \text{ coeff. of } \dot{\gamma}^2 \end{aligned}$$



### Symmetric Modes

#### Kinetic Energy (continued)

The kinetic energy may be rewritten thus,

$$T = \frac{1}{2} \{ A \dot{z}^2 + B \dot{H}_{b_1}^2 + C \dot{H}_{b_2}^2 + D \dot{\theta}^2 \}$$

#### Potential Energy

$$V = \frac{1}{2} k_{b_1} H_{b_1}^2 + \frac{1}{2} k_{b_2} H_{b_2}^2$$

where:  $k_{b_1}, k_{b_2}$  = effective spring constant of each wing mode.

#### Lagrange's Equation

The mechanical equations of motion are obtained by the following operation (due to Lagrange) on the kinetic and potential energy expressions.

$$\frac{d}{dt} \left[ \frac{\partial T}{\partial \dot{q}} \right] + \frac{\partial V}{\partial q} - \frac{\partial T}{\partial q} = F_q$$

where:  $q$  = generalized coordinate

$F_q$  = generalized force in the coordinate  $q$

These result in mechanical equations of motion with the same number as there are generalized coordinates.

Substitution of the kinetic and potential energy expressions into the differential operation above yields the following equations of motion.

### Symmetric Modes

#### Lagrange's Equation (continued)

Equations of action,

$$A \ddot{z} = F_z$$

$$D \ddot{\gamma} = F_\gamma$$

$$B \ddot{H}_{b_1} + K_{b_1} H_{b_1} = F_{b_1}$$

$$C \ddot{H}_{b_2} + K_{b_2} H_{b_2} = F_{b_2}$$

### Generalized Forces

To complete the equations of motion, the generalized forces must be found. These may be obtained from the virtual work. Thus,

$$F_q = \frac{\partial W}{\partial \delta q}$$

where:  $W$  = virtual work

$F_q$  and  $q$  are as defined above.

$\delta q$  = increment of  $q$

The virtual work is,

$$W = \sum_{i=1, \text{ROOT}}^{N, \text{TIP}} \left[ M_i' \Delta y_i \{ \phi_{b_1 i} \delta H_{b_1} + \phi_{b_2 i} \delta H_{b_2} + \delta \gamma \} \right. \\ \left. + L_i \Delta y_i \{ z_{b_1 i} \delta H_{b_1} + z_{b_2 i} \delta H_{b_2} + \delta z - s \delta \gamma \} \right]$$

and the generalized forces are then

$$F_z = \sum_{i=1, \text{ROOT}}^{N, \text{TIP}} L_i \Delta y_i \quad \text{Generalized } z \text{ force}$$

$$F_\gamma = \sum_{i=1, \text{ROOT}}^{N, \text{TIP}} \{ M_i' \Delta y_i - s L_i \Delta y_i \} \quad \text{Generalized } \gamma \text{ force}$$

$$F_{b_1} = \sum_{i=1, \text{ROOT}}^{N, \text{TIP}} \{ M_i' \phi_{b_1 i} \Delta y_i + L_i z_{b_1 i} \Delta y_i \} \quad \text{Generalized } H_{b_1} \text{ force}$$

$$F_{b_2} = \sum_{i=1, \text{ROOT}}^{N, \text{TIP}} \{ M_i' \phi_{b_2 i} \Delta y_i + L_i z_{b_2 i} \Delta y_i \} \quad \text{Generalized } H_{b_2} \text{ force}$$

### Symmetric Modes

#### Generalized Forces (continued)

where:

$L_i$  = lift at elastic axis per unit span, positive down

$M'_i$  = moment about elastic axis per unit span, positive nose-up.

Using AF Report No. 4798, the generalized forces may be rewritten as oscillatory aerodynamic loads.

#### Generalized Forces as Oscillatory Aerodynamic Loads

From Reference (8) pages 33 and 34,

$$L = \pi \rho b^3 \omega^2 \left\{ \frac{h}{b} [L_h] + \alpha [L_\alpha - L_h \left( \frac{1}{2} + a \right)] \right\}$$

$$M' = \pi \rho b^4 \omega^2 \left\{ \frac{h}{b} [M_h - L_h \left( \frac{1}{2} + a \right)] + \alpha [M_\alpha - L_\alpha \left( \frac{1}{2} + a \right) - M_h \left( \frac{1}{2} + a \right) + L_h \left( \frac{1}{2} + a \right)^2] \right\}$$

where:

$L$  = oscillatory aerodynamic lift acting on the wing per unit span

$M'$  = oscillatory aerodynamic moment acting on the wing about its elastic axis per unit span

$\alpha$  = torsional displacement about the elastic axis of the entire wing, positive for increasing angle of attack

$h$  = vertical bending displacement of wing, positive down

$a$  = location of the wing elastic axis measured from the wing mid-chord, as a fraction of the semi-chord, positive aft of mid-chord

$b$  = wing semi-chord

$\omega$  = flutter frequency

$\rho$  = air mass density

$L_h, L_\alpha, M_h$  and  $M_\alpha$  are complex aerodynamic coefficients tabulated in AF Rept. No. 4798 for various values of the  $V/b\omega$ , where  $V$  = forward speed of aircraft.

## Symmetric Modes

### Generalized Forces as Oscillatory Aerodynamic Loads (continued)

Rewriting these oscillatory aerodynamic forces using the notation of the present analysis, the lift per unit span becomes,

$$L_i = \pi \rho b^3 \omega^2 \left\{ \frac{z - s\gamma + z_{b_{1i}} H_{b_1} + z_{b_{2i}} H_{b_2}}{b} [L_h] + (\gamma + \phi_{b_{1i}} H_{b_1} + \phi_{b_{2i}} H_{b_2}) [L_\alpha - L_h (\frac{1}{2} + a)] \right\}$$

and the aerodynamic moment about the wing elastic axis per unit span is,

$$M_i = \pi \rho b^4 \omega^2 \left\{ \frac{z - s\gamma + z_{b_{1i}} H_{b_1} + z_{b_{2i}} H_{b_2}}{b} [M_h - L_h (\frac{1}{2} + a)] \right. \\ \left. + (\gamma + \phi_{b_{1i}} H_{b_1} + \phi_{b_{2i}} H_{b_2}) [M_\alpha - L_\alpha (\frac{1}{2} + a) - M_h (\frac{1}{2} + a) + L_h (\frac{1}{2} + a)^2] \right\}$$

### Complete Equations of Motion

Substituting the expressions for the generalized forces in the equations of motion and writing out A, B, C and D in full, the complete equations of motion are obtained. Thus,

z Equation

$$\left[ \frac{1}{2} M_f + \sum_{i=1, \text{ROOT}}^{n_1 \text{ TIP}} M_{W_i} \right] \ddot{z} = \sum_{i=1, \text{ROOT}}^{n_1 \text{ TIP}} \pi \rho b^3 \omega^2 \left\{ \frac{z - s\gamma + z_{b_{1i}} H_{b_1} + z_{b_{2i}} H_{b_2}}{b} [L_h] \right. \\ \left. + (\gamma + \phi_{b_{1i}} H_{b_1} + \phi_{b_{2i}} H_{b_2}) [L_\alpha - L_h (\frac{1}{2} + a)] \right\} \Delta y_i$$

γ Equation

$$\left[ \frac{1}{2} I_f + \sum_{i=1, \text{ROOT}}^{n_1 \text{ TIP}} M_{W_i} S^2 \right] \ddot{\gamma} = \\ \sum_{i=1, \text{ROOT}}^{n_1 \text{ TIP}} \pi \rho b^4 \omega^2 \left\{ \frac{z - s\gamma + z_{b_{1i}} H_{b_1} + z_{b_{2i}} H_{b_2}}{b} [M_h - L_h (\frac{1}{2} + a)] \right. \\ \left. + (\gamma + \phi_{b_{1i}} H_{b_1} + \phi_{b_{2i}} H_{b_2}) [M_\alpha - L_\alpha (\frac{1}{2} + a) - M_h (\frac{1}{2} + a) + L_h (\frac{1}{2} + a)^2] \right\} \Delta y_i \\ - s \sum_{i=1, \text{ROOT}}^{n_1 \text{ TIP}} \pi \rho b^3 \omega^2 \left\{ \frac{z - s\gamma + z_{b_{1i}} H_{b_1} + z_{b_{2i}} H_{b_2}}{b} [L_h] \right. \\ \left. + (\gamma + \phi_{b_{1i}} H_{b_1} + \phi_{b_{2i}} H_{b_2}) [L_\alpha - L_h (\frac{1}{2} + a)] \right\} \Delta y_i$$

## Symmetric Modes

### Complete Equations of Motion (continued)

$H_{b1}$  Equation

$$\sum_{i=1, \text{ROOT}}^{n_1 \text{ TIP}} \{ \bar{M}_{w_i} \bar{z}_{b1i}^2 + \bar{I}_{w_i} \phi_{b1i}^2 + 2 \bar{\sigma}_{w_i} \bar{z}_{b1i} \phi_{b1i} \} H_{b1}^{\circ\circ} + K_{b1} H_{b1} =$$

$$\sum_{i=1, \text{ROOT}}^{n_1 \text{ TIP}} \pi \rho b^4 \omega^2 \phi_{b1i} \left\{ \frac{\bar{z} - S\delta + \bar{z}_{b1i} H_{b1} + \bar{z}_{b2i} H_{b2}}{b} [M_h - L_h (\frac{1}{2} + a)] \right. \\ \left. + (\delta + \phi_{b1i} H_{b1} + \phi_{b2i} H_{b2}) [M_\alpha - L_\alpha (\frac{1}{2} + a) - M_h (\frac{1}{2} + a) + L_h (\frac{1}{2} + a)^2] \right\} \Delta y_i$$

$H_{b2}$  Equation

$$\sum_{i=1, \text{ROOT}}^{n_1 \text{ TIP}} \{ \bar{M}_{w_i} \bar{z}_{b2i}^2 + \bar{I}_{w_i} \phi_{b2i}^2 + 2 \bar{\sigma}_{w_i} \bar{z}_{b2i} \phi_{b2i} \} H_{b2}^{\circ\circ} + K_{b2} H_{b2} =$$

$$\sum_{i=1, \text{ROOT}}^{n_1 \text{ TIP}} \pi \rho b^4 \omega^2 \phi_{b2i} \left\{ \frac{\bar{z} - S\delta + \bar{z}_{b1i} H_{b1} + \bar{z}_{b2i} H_{b2}}{b} [M_h - L_h (\frac{1}{2} + a)] \right. \\ \left. + (\delta + \phi_{b1i} H_{b1} + \phi_{b2i} H_{b2}) [M_\alpha - L_\alpha (\frac{1}{2} + a) - M_h (\frac{1}{2} + a) + L_h (\frac{1}{2} + a)^2] \right\} \Delta y_i$$

Collecting the coefficients of the generalized coordinates and assuming harmonic solution of the form

$$q = \bar{q} e^{i\omega t} \quad \text{so that}$$

$$\ddot{q} = -\omega^2 \bar{q} e^{i\omega t} = -\omega^2 q$$

then upon substitution, the equations of motion or flutter equations may be written in matrix form as in Figure 5;

where:

$$\omega_{b1}^2 M_{1EFF} = K_{b1}$$

$$\omega_{b2}^2 M_{2EFF} = K_{b2}$$

$\omega_{b1}$  = natural frequency of the first wing normal mode

$\omega_{b2}$  = natural frequency of the second wing normal mode

$$M_{1EFF} = \sum_{i=1, \text{ROOT}}^{n_1 \text{ TIP}} \{ \bar{M}_{w_i} \bar{z}_{b1i}^2 + \bar{I}_{w_i} \phi_{b1i}^2 + 2 \bar{\sigma}_{w_i} \bar{z}_{b1i} \phi_{b1i} \}$$

$$M_{2EFF} = \sum_{i=1, \text{ROOT}}^{n_1 \text{ TIP}} \{ \bar{M}_{w_i} \bar{z}_{b2i}^2 + \bar{I}_{w_i} \phi_{b2i}^2 + 2 \bar{\sigma}_{w_i} \bar{z}_{b2i} \phi_{b2i} \}$$

## Symmetric Modes

### Solution of the Symmetric Flutter

The solution of the Symmetric Flutter determinant is identical to the solution of the Antisymmetric Case with one exception: instead of a 3 x 3 determinant, the Symmetric Flutter determinant is a 4 x 4. This must be reduced to a 3 x 3 and may then be solved in a manner identical to the Antisymmetric Solution. This reduction of the 4 x 4 to a 3 x 3 determinant is done as follows.

Represent the elements of the determinant by Roman Numerals.

$$\begin{vmatrix}
 \text{II} & \text{III} & \text{IV} & \text{V} \\
 \text{VI} & \text{VII} & \text{VIII} & \text{IX} \\
 \text{X} & \text{XI} & \text{XII} - M_{\text{EFF}} \left( \frac{\omega_{b_1}}{\omega} \right)^2 & \text{XIII} \\
 \text{XIV} & \text{XV} & \text{XVI} & \text{XVII} - M_{\text{EFF}} \left( \frac{\omega_{b_2}}{\omega} \right)^2
 \end{vmatrix} = 0$$

Divide each element of each column by the first (top) element of the column. This reduces the first row elements to unity.

$$\begin{vmatrix}
 / & / & / & / \\
 \frac{\text{VI}}{\text{II}} & \frac{\text{VII}}{\text{III}} & \frac{\text{VIII}}{\text{IV}} & \frac{\text{IX}}{\text{V}} \\
 \frac{\text{X}}{\text{II}} & \frac{\text{XI}}{\text{III}} & \frac{\text{XII}}{\text{IV}} - \frac{M_{\text{EFF}}}{\text{IV}} \left( \frac{\omega_{b_1}}{\omega} \right)^2 & \frac{\text{XIII}}{\text{V}} \\
 \frac{\text{XIV}}{\text{II}} & \frac{\text{XV}}{\text{III}} & \frac{\text{XVI}}{\text{IV}} & \frac{\text{XVII}}{\text{V}} - \frac{M_{\text{EFF}}}{\text{V}} \left( \frac{\omega_{b_2}}{\omega} \right)^2
 \end{vmatrix} = 0$$

## Symmetric Modes

### Solution of the Symmetric Flutter Determinant (continued)

Subtracting the first column from the other three columns reduces the first row elements to zero, except the first, which is still unity. Therefore, by Cramer's rule the 4 x 4 determinant reduces to the minor of the first-row-column element, 1.

$$\begin{vmatrix} \frac{\text{VII}}{\text{III}} - \frac{\text{VI}}{\text{II}} & \frac{\text{VIII}}{\text{IV}} - \frac{\text{VI}}{\text{II}} & \frac{\text{IX}}{\text{V}} - \frac{\text{VI}}{\text{II}} \\ \frac{\text{XI}}{\text{III}} - \frac{\text{X}}{\text{II}} & \frac{\text{XII}}{\text{IV}} - \frac{\text{X}}{\text{II}} - \frac{M_{EFF}}{\text{IV}} \left( \frac{\omega_{b1}}{\omega} \right)^2 & \frac{\text{XIII}}{\text{V}} - \frac{\text{X}}{\text{II}} \\ \frac{\text{XV}}{\text{III}} - \frac{\text{XIV}}{\text{II}} & \frac{\text{XVI}}{\text{IV}} - \frac{\text{XIV}}{\text{II}} & \frac{\text{XVII}}{\text{V}} - \frac{\text{XIV}}{\text{II}} - \frac{M_{2EFF}}{\text{V}} \left( \frac{\omega_{b1}}{\omega} \right)^2 \end{vmatrix} = 0$$

The above determinant has a form identical to the Antisymmetric case; hence its solution also. To put the reduced matrix into its final form, divide the second column by the coefficient of  $(\omega_{b1}/\omega)^2$  and the third column by the coefficient of  $(\omega_{b2}/\omega)^2$ . Also make the following substitution:

$$\left( \frac{\omega_{b1}}{\omega} \right)^2 = \lambda \quad \text{and} \quad \left( \frac{\omega_{b2}}{\omega} \right)^2 = \xi \quad \text{so that} \quad \left( \frac{\omega_{b2}}{\omega} \right)^2 = \frac{\lambda}{\xi}$$

After further multiplying the third row by  $\xi$ , the determinant finally becomes

## Symmetric Modes

### Solution of the Symmetric Flutter Determinant (continued)

$$\begin{vmatrix} \frac{\text{VII}}{\text{III}} - \frac{\text{VI}}{\text{II}} & \frac{1}{M_{1EFF}} \left[ \frac{\text{VIII}}{\text{III}} - \frac{\text{VI} \times \text{IV}}{\text{II}} \right] & \frac{1}{M_{2EFF}} \left[ \frac{\text{IX}}{\text{III}} - \frac{\text{VI} \text{ V}}{\text{II}} \right] \\ \frac{\text{XI}}{\text{III}} - \frac{\text{X}}{\text{II}} & \frac{1}{M_{1EFF}} \left[ \frac{\text{XII}}{\text{III}} - \frac{\text{X} \times \text{IV}}{\text{II}} \right] - \lambda & \frac{1}{M_{2EFF}} \left[ \frac{\text{XIII}}{\text{III}} - \frac{\text{X} \text{ V}}{\text{II}} \right] \\ \left[ \frac{\text{XV}}{\text{III}} - \frac{\text{XIV}}{\text{II}} \right] \wp & \frac{1}{M_{1EFF}} \left[ \frac{\text{XVI}}{\text{III}} - \frac{\text{XIV} \times \text{IV}}{\text{II}} \right] \wp & \frac{1}{M_{2EFF}} \left[ \frac{\text{XVII}}{\text{III}} - \frac{\text{XIV} \text{ V}}{\text{II}} \right] \wp - \lambda \end{vmatrix} = 0$$

This may also be written in an abbreviated form by representing the elements by capital letters. It should be noted that the elements of the determinant are complex.

$$\begin{vmatrix} A & B & C \\ D & E - \lambda & F \\ G \wp & H \wp & K \wp - \lambda \end{vmatrix} = 0$$

The solution of the Symmetric Flutter determinant consists of (1) reduction of a 4 x 4 determinant to a 3 x 3 and (2) simultaneous solution of the two equations resulting from the expansion of the reduced determinant for the pseudo unknown frequency ratio  $\wp$  and  $\lambda$ , is programmed on the IBM 650 computer. The program is designated No. 1178. The output format is the same as in the Antisymmetric case, which was shown previously.



APPENDIX C

NUMERICAL DATA

TABLE I

H-21 RANGE EXTENSION HELICOPTER, BASIC NUMERICAL DATA

<u>Symbols</u>	<u>Dimensions</u>	<u>Value</u>	<u>Description</u>
$\rho$	lb-sec <sup>2</sup> /in <sup>4</sup>	$0.1147 \times 10^{-6}$	Air mass density @ sea level
$a'$	in	-13.4	Wing midchord to E.A. positive aft of midchord
$a$	-	.199	$a'/b$
$b$	in	67.4	Wing semichord
$V$	ft/sec	135.0	Forward speed of aircraft
$S$	in	61.0	Aircraft C.G. aft of wing E.A.
$M/2$	lb-sec <sup>2</sup> /in	14.4	Half of fuselage mass
$I_{f_\alpha}/2$	lb-in-sec <sup>2</sup>	30,000	Half of fuselage moment of inertia in roll
$I_{f_p}/2$	lb-in-sec <sup>2</sup>	404,000	Half of fuselage moment of inertia in pitch
$\gamma_o$	deg.	45.0	Wing hinge offset angle
$K_{w\alpha}$	in-lb/rad	$3.09 \times 10^6$	Wing aero. spring rate at 80 knots (135 FPS)

# DETERMINATION OF FLEXIBLE AND RIGID WING MODES

The frequencies and corresponding wing flexible mode shapes are calculated using the method of associated matrices programmed in the IBM 650 Computer. For the mode shape calculations, the wing is represented as a series of discrete lumped masses interconnected by massless elastic members which have both bending and torsional rigidity. Boundary conditions are for those of a pinned-free beam and the resulting modes are coupled bending and torsion which are also normal wing modes. The first flexible mode is predominantly flap bending and the second mode is usually torsion predominant. Inputs are prepared in the sample input sheet labeled Table (II).

Due to the wing hinge, a rigid mode of the wing exists during forward flight, and which consists in flapwise rotation about the hinge. Determination of the wing rigid mode is made with the aid of projective geometry.

Referring to the figure in the next page which shows the deflected wing as solid lines and the equilibrium position by dotted lines, the following are obtained:

For small wing flapwise deflections,

$$d_3 c_3 \neq \bar{d}_3 \bar{c}_3 = \bar{d}_1 \bar{c}_1$$

but

$$\bar{d}_1 \bar{c}_1 = a_1 o_1 \tan \gamma_o$$

Also:

$$c_3 c_3' = c_2 c_2' = c_2 b_2 \sin \alpha_w = c_2 b_2 \sin \alpha_w = \bar{c}_1 b_1 \sin \alpha_w \cos \gamma_o$$

and

$$d_3 d_3' = d_2 d_2' = d_2 a_2' \sin \alpha_w = \bar{d}_1 a_1 \sin \alpha_w \cos \gamma_o$$

Now

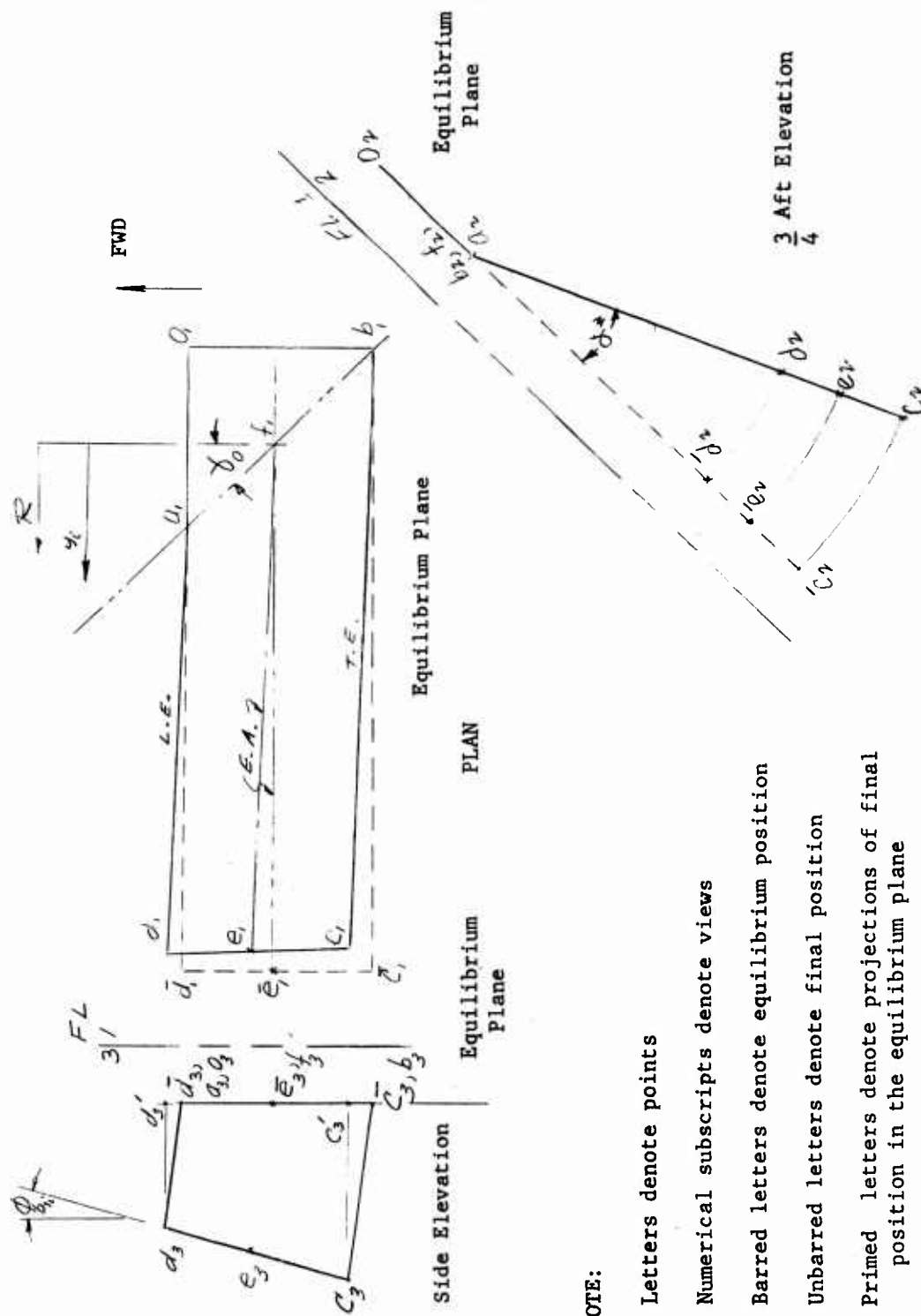
$$\sin \phi_{bli} = \frac{c_3 c_3' - d_3 d_3'}{d_3 c_3}, \text{ or after substitution}$$

$$\sin \phi_{bli} = \frac{(\bar{c}_1 b_1 - \bar{d}_1 a_1)}{a_1 o_1 \tan \gamma_o} \sin \alpha_w \cos \gamma_o$$

$$= \frac{a_1 o_1 \sin \alpha_w \sin \gamma_o}{a_1 o_1}$$

$$\sin \phi_{bli} = \sin \alpha_w \sin \gamma_o$$

# RIGID WING FLAP GEOMETRY



## NOTE:

Letters denote points

Numerical subscripts denote views

Barred letters denote equilibrium position

Unbarred letters denote final position

Primed letters denote projections of final position in the equilibrium plane

and since angles are small

$$\phi_{bli} = \alpha_w \sin \gamma_o$$

The vertical deflections are

$$z_{bli} = \frac{y_i \cos \gamma_o}{R \cos \gamma_o} z_{b_1 \text{ Tip}} = \frac{y_i}{R} z_{b_1 \text{ Tip}}$$

Where R is the length of the elastic axis from wing tip to the hinge. For a unit tip deflection,

$$z_{bli} = \frac{y_i}{R}$$

Also, since

$$z_{bi \text{ tip}} = 1 = R (\cos \gamma_o) \alpha_w$$

then:

$$\alpha_w = \frac{1}{R \cos \gamma_o}$$

to that

$$\frac{z_{bli}}{R} = \frac{\tan \gamma_o}{R}, \text{ constant along the span.}$$

Now for:

$$R = 303" \quad \gamma_o = 45^\circ$$

$$z_{bli} = y_i (.0033)$$

$$\phi_{bli} = .0033 \text{ Rad.}, \text{ constant along the span}$$

INPUT FORM-GENERAL MATRIX COMPUTER PROGRAM-MODIFIED FOR WING MODES

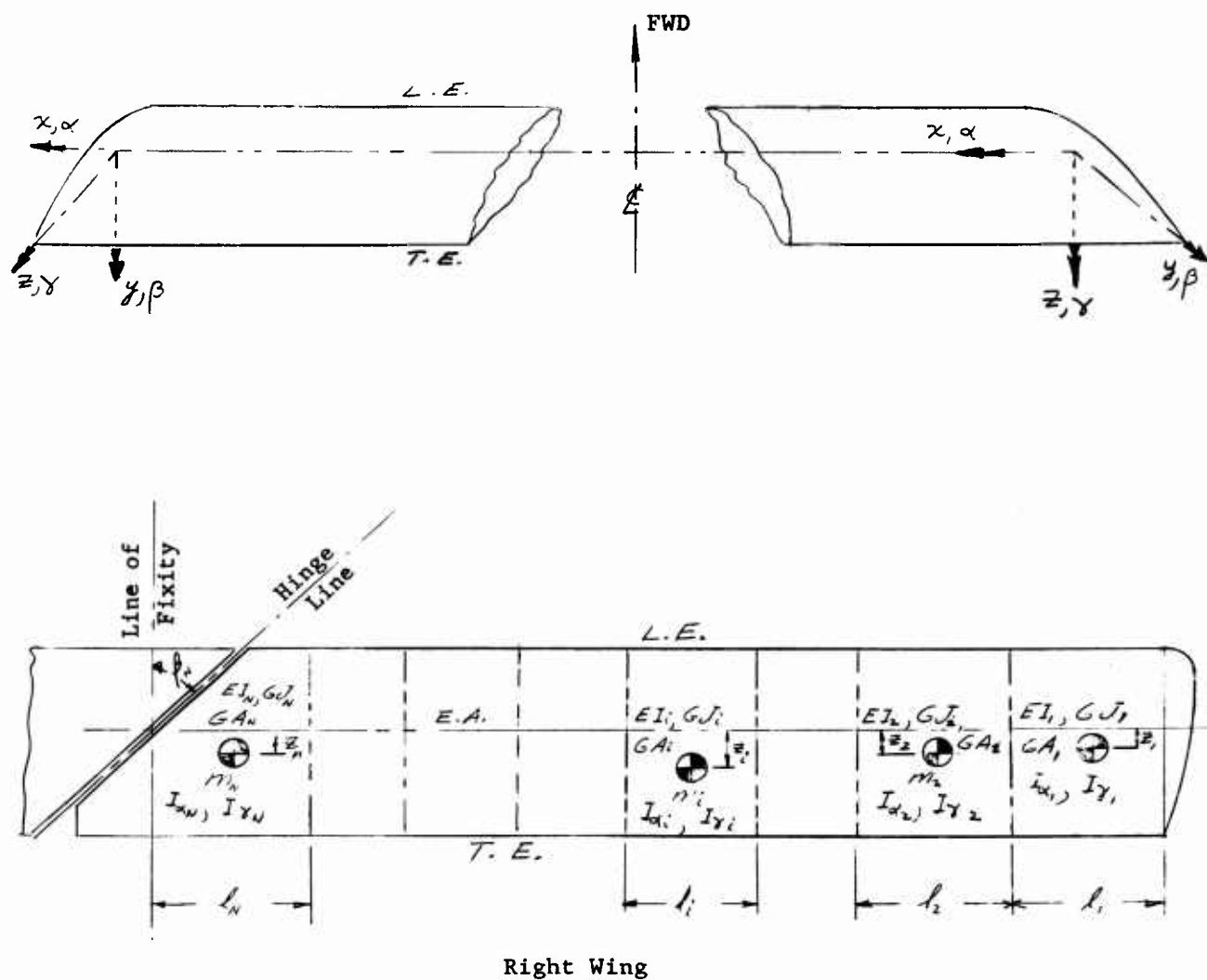
58

TABLE II (Continued)  
 BASIC NUMERICAL DATA (Continuation)  
 SECTION ELASTIC PROPERTIES OF THE WING

Station	$\Delta y$ - in.	$y_c$ - in.	EI - lb-in <sup>2</sup>	GJ - lb-in <sup>2</sup>	GA - lbs
Tip 1	45	303	2.50x10 <sup>9</sup>	5.38x10 <sup>9</sup>	1.506x10 <sup>5</sup>
2	45	258			
3	28	213			
4	28	185			
5	45	157			
6	45	112			
7	45	67			
Root 8	22	22			

### Schematic Diagram of the Wing for Mode-Shape Calculation

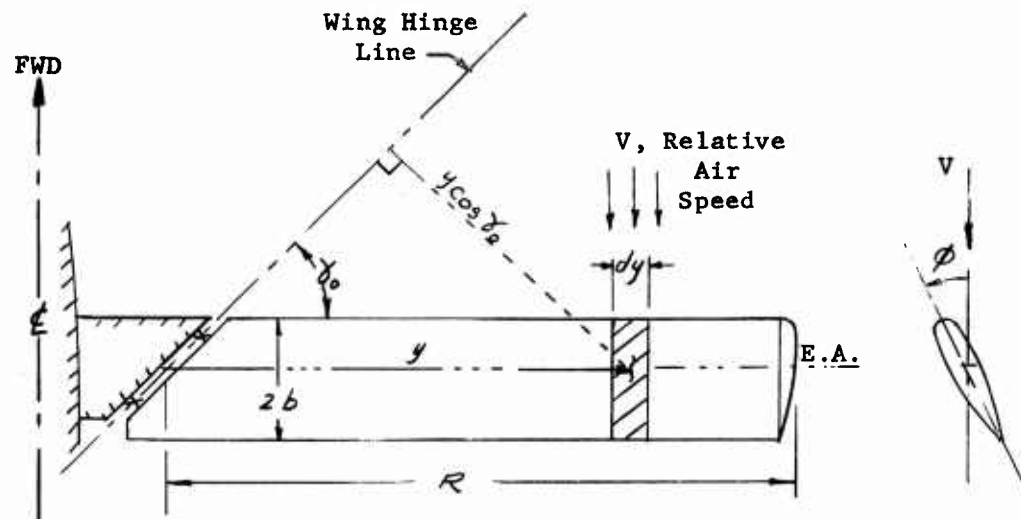
The derivation and inputs for the mode-shape calculation were previously obtained using symbols different from the Flutter nomenclature. In the sketch below the mode-shape calculation symbols are shown, including the sign convention.





### Wing Rigid Flap Frequency

When the aircraft is airborne, the wing can execute rigid flapping about the hinge at a certain frequency. The spring rate is due to aerodynamic loads on the wing. To determine this spring rate, consider the following:



Then from the "strip" theory, the steady flapping moment about the wing hinge axis is,

$$M_{\alpha_w} = \int_0^R \frac{1}{2} \rho a_\infty (2b) V^2 \phi y \cos \gamma_0 dy$$

from the calculation of the rigid mode shape,

$$\phi = \alpha_w \sin \gamma_0 \quad - \text{substituting this above, and simplifying,}$$

$$M_{\alpha_w} = a_\infty \rho b V^2 \alpha_w \sin \gamma_0 \cos \gamma_0 \int_0^R y dy \quad - \text{upon integration}$$

$$M_{\alpha_w} = \frac{1}{4} a_\infty \rho b V^2 \alpha_w R^2 \sin 2\gamma_0$$

This may also be rewritten as:

$$M_{\alpha_w} = K_{\alpha_w} \alpha_w \quad \text{where}$$

$K_{\alpha_w}$  = the effective aerodynamic spring. (This has been calculated in Reference (6) at sea level and 80 knots to be:  
 $K_{\alpha_w} = 3.09 \times 10^6$  in-lb/rad.)

Therefore,

$$= \frac{1}{4} a_0 \rho b V^2 R^2 \sin 2\gamma_0 .$$

The wing flap inertia is,

$$\sum_{ROOT}^{TIP} M_{wi} y_i^2 \cos^2 \gamma_0$$

and so the wing natural rigid flap frequency is,

$$\omega_{b_i} = \sqrt{\frac{K_{\alpha W}}{\text{Wing Flap Inertia}}} = \sqrt{\frac{\frac{1}{4} a_0 \rho b V^2 R^2 \sin 2\gamma_0}{\sum_{ROOT}^{TIP} M_{wi} y_i^2 \cos^2 \gamma_0}} \text{ Rad/sec}$$

and for  $\gamma = 45.0^\circ$

$$\omega_{b_i} = \sqrt{\frac{\frac{1}{2} a_0 \rho b V^2 R^2}{\sum_{ROOT}^{TIP} M_{wi} y_i^2}} \text{ Rad/sec}$$

# DETERMINATION OF MAXIMUM CHORDWISE DISPLACEMENT OF WING C.G. DUE TO CHANGE IN FUEL LEVEL

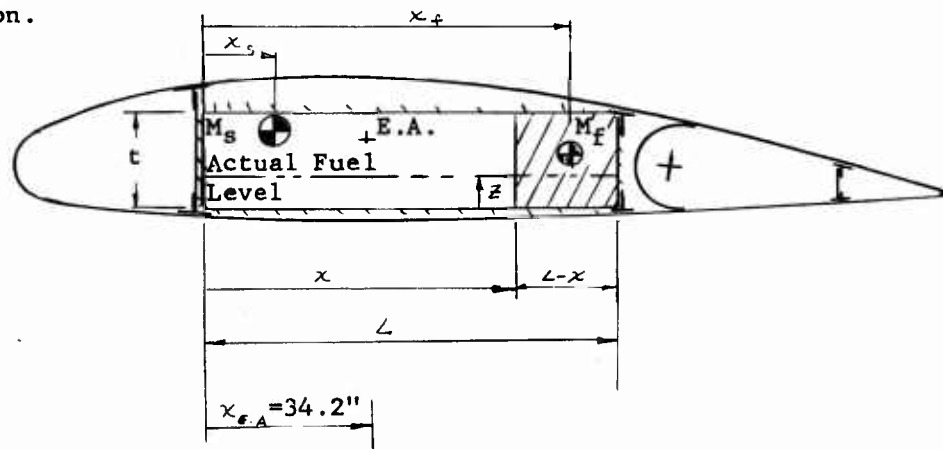
## Aft - Displacement

The H-21 Range Extension Wing has six fuel cells arranged along each semi-span. The procedure for transferring the wing fuel to the main tank is as follows:

- (1) The first two fuel cells nearest the wing tip are simultaneously transferred to the main tank.
- (2) When the first two cells are empty, the most inboard two cells are emptied. Then the midspan tanks are emptied last.

To determine the percentage fuel remaining in a cell that yields maximum displacement of the wing section C.G. in the chordwise direction, assume that any fuel in the cell which has a normally horizontal free surface occupies the rear end of the cell. In this condition the fuel would have a vertical free surface.

Considering the wing to be horizontal and the cell cross section to be rectangular, the following sketch shows the geometry of the wing-fuel cell combination.



Where:  $M_s$  = Mass of Unit Length of Wing Structure

$M_f$  = Mass of Fuel per Unit Length (spanwise)

Aft

From the Sketch, the Fuel Mass is

$$M_f = zL\delta = t(L-x)\delta$$

Where,  $\delta$  = Fuel Mass per unit area

From which,

$$x = L(1 - \frac{z}{t})$$

Also, it is easily shown that

$$x_f = L(1 - \frac{z}{2t})$$

The C.G. of the entire section then becomes,

$$\bar{x} = \frac{M_s x_s + M_f x_f}{M_s + M_f} \text{ or after substituting } M_f \text{ and } x_f \text{ and simplifying,}$$

$$\bar{x} = \frac{M_s x_s + \frac{zL^2}{2}\delta \{2 - \frac{z}{2t}\}}{M_s + zL\delta}$$

will be a maximum or a minimum when  $d\bar{x}/dz = 0$ ;

$$= \frac{(M_s + zL\delta)\{L^2\delta - zL^2/t\} - \{M_s x_s + zL^2\delta - z^2L^2\delta/2t\}L\delta}{(M_s + zL\delta)^2} = 0$$

Considering only the numerator and solving for  $z$ , the following is obtained.

$$z = \frac{1}{L} \left( \frac{M_s}{\delta} \right) \left[ -1 \pm \sqrt{1 + \frac{2t(L-x_s)}{M_s/\delta}} \right]$$

And the percentage of fuel remaining is

$$\frac{z}{t} \times 100$$

It must be noted that only positive values of  $z$  is valid.

Positive  $z$  is obviously a maximum.

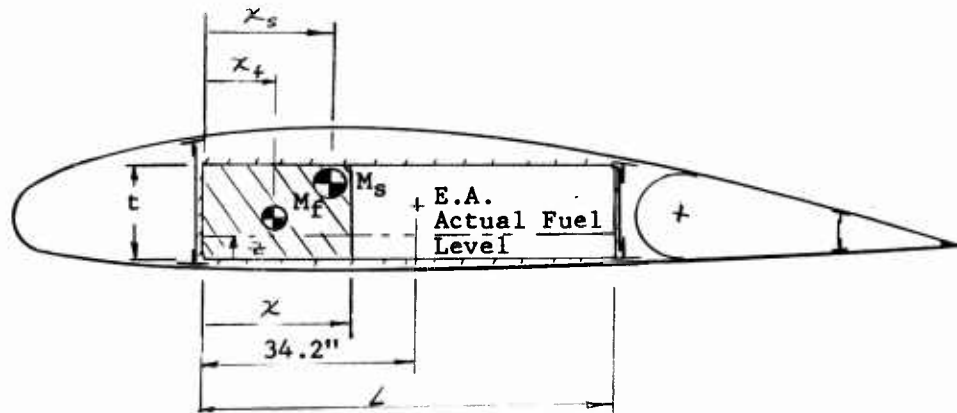
Substituting this into the expression for  $\bar{x}$  gives the wing section maximum chordwise C.G. travel Aft.

The distance of the wing C.G. from the E.A. is therefore:

$$\bar{x}_{E.A.C.G.} = \bar{x} - 34.2$$

### Forward Displacement

To determine the maximum chordwise wing section C.G. displacement, we proceed in a similar manner. This time, assume the fuel to occupy forward end of the cell thus:



Similarly, then

$$M_f = zL\delta = t\chi\delta$$

Which yields

$$\chi = \frac{z}{t}L$$

And

$$\chi_f = \frac{\chi}{2} = \frac{z}{2t}L$$

The C.G. of the entire section is then,

$$\bar{\chi} = \frac{\chi_s M_s + (zL\delta)\left(\frac{zL}{2t}\right)}{M_s + zL\delta}$$

Differentiating with respect to  $z$  for maximum-minimum and equating to zero, we have

$$\frac{d\bar{\chi}}{dz} = \frac{(M_s + zL\delta)\left(\frac{z^2L\delta}{t}\right) - (\chi_s M_s + \frac{z^2L^2\delta}{2t})L\delta}{(M_s + zL\delta)^2} = 0$$

### Forward

Considering only the numerator and solving for  $\bar{z}$ , the following is obtained:

$$\bar{z} = \frac{1}{L} \left( \frac{M_s}{\delta} \right) \left[ -1 \pm \sqrt{1 + \frac{2\bar{x}_s t}{M_s/\delta}} \right]$$

Again only a positive value is valid.

This positive  $\bar{z}$  is a minimum.

Substituting into the expression for  $\bar{x}$  yields the minimum C.G. chordwise displacement, and this distance with respect to the elastic axis is:

$$\bar{x}_{\text{C.G.-E.A.}} = \bar{x} - 34.2$$

### Calculation of Maximum C.G. Displacements

Substituting the following parameters into the previous equations yield the percent fuel and its C.G. location for maximum aft and forward displacement.

$$t = 18.42''$$

$$M_s = .844 \text{ lb-sec}^2/\text{in}$$

$$\delta = 5.04 \text{ \#/in}^2$$

$$L = 72.6''$$

$$X_s = 38.2 \text{ in}$$

#### Most Aft C.G.

$$\frac{\bar{z}}{t} \times 100 = 24.2\%$$

$$\bar{x}_{\text{C.G.-E.A.}} = 20.8'' \text{ aft of E.A.}$$

#### Most Forward C.G.

$$\frac{\bar{z}}{t} \times 100 = 25.8\%$$

$$\bar{x}_{\text{C.G.-E.A.}} = -15.45'' \text{ (or } 15.45'' \text{ forward of E.A.)}$$

TABLE III

COMPLEX AERODYNAMIC COEFFICIENTS - INPUTS  
FOR PROGRAM NO.1120 AND 1178  
COMMON TO ANTISYMMETRICAL AND SYMMETRICAL FLUTTER  
SAMPLE INPUT SHEET

Loc.	Item	Value	Loc.	Item	Value
0900	V/bw	7.00			
0910	L <sub>hR</sub>	-1.58250	0911	L <sub>hI</sub>	-10.9150
0912	L <sub>aR</sub>	080.8500	0913	L <sub>aI</sub>	.41500
0914	M <sub>hR</sub>	.5000		M <sub>hI</sub>	0
0916	M <sub>aR</sub>	.37500		M <sub>aI</sub>	-7.000

Loc.	Item	Value	Loc.	Item	Value
0900	V/bw	8.00			
0910	L <sub>hR</sub>	-1.89750	0911	L <sub>hI</sub>	-12.7650
0912	L <sub>aR</sub>	-106.5500	0913	L <sub>aI</sub>	2.5350
0914	M <sub>hR</sub>	.5000	0915	M <sub>hI</sub>	0
0916	M <sub>aR</sub>	.37500	0917	M <sub>aI</sub>	-8.000

Loc.	Item	Value	Loc.	Item	Value
0900	V/bw	8.33			
0910	L <sub>hR</sub>	-2.0020	0911	L <sub>hI</sub>	-13.4385
0912	L <sub>aR</sub>	-114.4920	0913	L <sub>aI</sub>	3.2420
0914	M <sub>hR</sub>	0.50000	0915	M <sub>hI</sub>	0
0916	M <sub>aR</sub>	.37500	0917	M <sub>aI</sub>	-8.3333

Loc.	Item	Value	Loc.	Item	Value
0900	V/bw	9.00			
0910	L <sub>hR</sub>	-2.1796	0911	L <sub>hI</sub>	-14.7191
0912	L <sub>aR</sub>	-136.434	0913	L <sub>aI</sub>	5.0732
0914	M <sub>hR</sub>	.5000	0915	M <sub>hI</sub>	0
0916	M <sub>aR</sub>	.37500	0917	M <sub>aI</sub>	-9.000

Loc.	Item	Value	Loc.	Item	Value
0900	V/bw	9.5			
0910	L <sub>hR</sub>	-2.3128	0911	L <sub>hI</sub>	-15.6796
0912	L <sub>aR</sub>	-152.890	0913	L <sub>aI</sub>	6.4466
0914	M <sub>hR</sub>	.5000	0915	M <sub>hI</sub>	0
0916	M <sub>aR</sub>	.37500	0917	M <sub>aI</sub>	-9.5000

Loc.	Item	Value	Loc.	Item	Value
0900	V/bw	10.0			
0910	L <sub>hR</sub>	-2.4460	0911	L <sub>hI</sub>	-16.6400
0912	L <sub>aR</sub>	-169.346	0913	L <sub>aI</sub>	7.8200
0914	M <sub>hR</sub>	.5000	0915	M <sub>hI</sub>	0
0916	M <sub>aR</sub>	.37500	0917	M <sub>aI</sub>	-10.000

Loc.	Item	Value	Loc.	Item	Value
0900	V/bw	16.67			
0910	L <sub>hR</sub>	-3.7530	0911	L <sub>hI</sub>	-29.7333
0912	L <sub>aR</sub>	-499.853	0913	L <sub>aI</sub>	32.8222
0914	M <sub>hR</sub>	0.5000	0915	M <sub>hI</sub>	0
0916	M <sub>aR</sub>	.37500	0917	M <sub>aI</sub>	-16.6667

Loc.	Item	Value	Loc.	Item	Value
0900	V/bw	20.0			
0910	L <sub>hR</sub>	-4.30	0911	L <sub>hI</sub>	-36.35
0912	L <sub>aR</sub>	-685.0	0913	L <sub>aI</sub>	48.15
0914	M <sub>hR</sub>	.50	0915	M <sub>hI</sub>	0
0916	M <sub>aR</sub>	.3750	0917	M <sub>aI</sub>	-20.0

TABLE IV  
ANTISYMMETRIC FLUTTER ANALYSIS  
Rigid and First Flap Bending Mode

Case

Mechanical Inputs

Program No. 1120

100% Full - H-21 Range Extension Wing #1

LOC.	ITEM	VALUE	LOC.	ITEM	VALUE	LOC.	ITEM	VALUE	LOC.	ITEM	VALUE
0900	$V/bw$	A11	0902	$\omega_{b2}$	25.63	0904	$I_{xx}/2$	30,000.0	0906	$\rho$	$11468 \times 10^{-6}$
0901	$\omega_{b1}$	1.0	0903	$M_{x2}/2$	14.40	0905	$\{ \frac{1}{2} + a \}$	0.300	0907	$b$	67.4
									0908	$s$	61.0
									0909	$n$	8

STA-i	LOC.	$\Delta y_i$	LOC.	$M_{wi}$	LOC.	$\bar{\sigma}_{wi}$	LOC.	$T_{wi}$
1	0001	45.0	0051	2.892	0101	8.676	0151	2426.
2	0002	45.0	0052	2.892	0102	8.676	0152	2426.
3	0003	45.0	0053	2.892	0103	8.676	0153	2426.
4	0004	11.0	0054	.4626	0104	1.3878	0154	1004.
5	0005	45.0	0055	2.892	0105	8.676	0155	2426.
6	0006	45.0	0056	2.892	0106	8.676	0156	2426.
7	0007	45.0	0057	2.892	0107	8.676	0157	2426.
8	0008	45.0	0058	2.892	0108	8.676	0158	2426.
9	0009	0	0059	0	0109	0	0159	0
10	0010		0060		0110		0160	
11	0011		0061		0111		0161	
12	0012		0062		0112		0162	
13	0013		0063		0113		0163	
14	0014		0064		0114		0164	
15	0015		0065		0115		0165	
16	0016		0066		0116		0166	
17	0017		0067		0117		0167	
18	0018		0068		0118		0168	
19	0019		0069		0119		0169	
20	0020		0070		0120		0170	

STA-i	LOC.	$y_i$	LOC.	$Z_{b1i}$	LOC.	$\phi_{b1i}$	LOC.	$Z_{b2i}$	LOC.	$\phi_{b2i}$
1	0401	370.0	0201	1.000	0251	.003300	0301	1.000	0351	-.0201
2	0402	325.0	0202	.851	0252		0302	.434	0352	-.0199
3	0403	280.0	0203	.703	0253		0303	-.070	0353	-.0194
4	0404	252.0	0204	.611	0254		0304	-.328	0354	-.0190
5	0405	224.0	0205	.518	0255		0305	-.530	0355	-.0185
6	0406	179.0	0206	.370	0256		0306	-.699	0356	-.0174
7	0407	134.0	0207	.221	0257		0307	-.625	0357	-.0160
8	0408	89.0	0208	.073	0258	.003300	0308	-.273	0358	-.0144
9	0409	0	0209	0	0259	0	0309	0	0359	0
10	0410		0210		0260		0310		0360	
11	0411		0211		0261		0311		0361	
12	0412		0212		0262		0312		0362	
13	0413		0213		0263		0313		0363	
14	0414		0214		0264		0314		0364	
15	0415		0215		0265		0315		0365	
16	0416		0216		0266		0316		0366	
17	0417		0217		0267		0317		0367	
18	0418		0218		0268		0318		0368	
19	0419		0219		0269		0319		0369	
20	0420		0220		0270		0320		0370	



TABLE V

## SYMMETRIC FLUTTER ANALYSIS

Rigid and First Flap Bending Mode

Case 4

Mechanical Inputs

Program No. 1178

100% Fuel - H-21 Range Extension Wing #1

LOC.	ITEM	VALUE	LOC.	ITEM	VALUE	LOC.	ITEM	VALUE	LOC.	ITEM	VALUE
0900	$V/b\omega$	A11	0902	$\omega_{b2}$	25.63	0904	$I_{xx}/2$	404,300.0	0906	$\rho$	$.1147 \times 10^{-6}$
0901	$\omega_{b1}$	1.0	0903	$M_1/2$	14.40	0905	$(\frac{1}{2} + e)$	.300	0907	$b$	67.4
									0908	$s$	61.0
									0909	$n$	8

STA-i	LOC.	$\Delta y_i$	LOC.	$M_{wi}$	LOC.	$\sigma_{wi}$	LOC.	$I_{wi}$
1	0001	45.0	0051	2.892	0101	8.676	0151	2426
2	0002	45.0	0052	2.892	0102	8.676	0152	2426
3	0003	45.0	0053	2.892	0103	8.676	0153	2426
4	0004	11.0	0054	.4626	0104	1.3878	0154	1004
5	0005	45.0	0055	2.892	0105	8.676	0155	2426
6	0006	45.0	0056	2.892	0106	8.676	0156	2426
7	0007	45.0	0057	2.892	0107	8.676	0157	2426
8	0008	45.0	0058	2.892	0108	8.676	0158	2426
9	0009	0	0059	0	0109	0	0159	0
10	0010		0060		0110		0160	
11	0011		0061		0111		0161	
12	0012		0062		0112		0162	
13	0013		0063		0113		0163	
14	0014		0064		0114		0164	
15	0015		0065		0115		0165	
16	0016		0066		0116		0166	
17	0017		0067		0117		0167	
18	0018		0068		0118		0168	
19	0019		0069		0119		0169	
20	0020		0070		0120		0170	

STA-i	LOC.	$\bar{z}_{b1i}$	LOC.	$\phi_{b1i}$	LOC.	$\bar{z}_{b2i}$	LOC.	$\phi_{b2i}$
1	0201	1.000	0251	.0033000	0301	1.000	0351	-.0201
2	0202	.851	0252		0302	.434	0352	-.0199
3	0203	.703	0253		0303	-.070	0353	-.0194
4	0204	.611	0254		0304	-.328	0354	-.0190
5	0205	.518	0255		0305	-.530	0355	-.0185
6	0206	.370	0256		0306	-.699	0356	-.0174
7	0207	.221	0257		0307	-.625	0357	-.0160
8	0208	.073	0258	.0033000	0308	-.273	0358	-.0144
9	0209	0	0259	0	0309	0	0359	0
10	0210		0260		0310		0360	
11	0211		0261		0311		0361	
12	0212		0262		0312		0362	
13	0213		0263		0313		0363	
14	0214		0264		0314		0364	
15	0215		0265		0315		0365	
16	0216		0266		0316		0366	
17	0217		0267		0317		0367	
18	0218		0268		0318		0368	
19	0219		0269		0319		0369	
20	0220		0270		0320		0370	

TABLE VI

TYPICAL OUTPUT SHEET - FLUTTER ANALYSIS  
 ANTISYMMETRIC FLUTTER ANALYSIS  
 RIGID AND FIRST FLAP BENDING MODES

JOB #4485

CASE IAS

Oct. 12, 1960

V/BW  
 8000000 51

A		B		C	
73535170	56	-19454193	53	85616989	53
-23706330	56	-76618636	52	-10208978	53
D		E		F	
-90091250	52	49577181	50	22235164	51
-65250324	53	-22867608	50	-23009971	50
G		H		K	
-13557957	53	-43468827	50	27799010	51
-68238753	53	-17420489	50	-71499957	50
M		N		P	
-36663790	61	59048583	62	-47293843	62
V		ZETA		LAMDA	
19852195	52	55677156	51	15260126	52
84349603	52	20369645	51	84529655	50

V/BW  
 9000000 51

A		B		C	
73011272	56	-24751878	53	10978946	54
-27335358	56	-84664698	52	-13523939	53
D		E		F	
-10451124	53	35802261	50	28520329	51
-75239016	53	-25378434	50	-31256640	50
G		H		K	
-15065998	53	-54792397	50	32852389	51
-78684923	53	-19482675	50	-85332875	50
M		N		P	
-17151336	62	10816808	63	-76407132	62
V		ZETA		LAMDA	
37214423	52	18072757	51	54961385	51
96906073	52	34569478	51	81054705	50

DISTRIBUTION LIST  
WIND TUNNEL TESTS AND FURTHER ANALYSIS OF THE  
FLOATING WING FUEL TANKS FOR HELICOPTER RANGE EXTENSION

Chief  
U. S. Army R&D Liaison Group (9851 DU)  
ATTN: USATRECOM LO  
APO 757  
New York, New York (1)

President  
United States Army Aviation Board  
ATTN: ATBG-DG  
Fort Rucker, Alabama (1)

Chief of Research and Development  
ATTN: Air Mobility Division  
Department of the Army  
Washington 25, D.C. (1)

Chief of Transportation  
ATTN: TCDRD (1)  
ATTN: TCAFO-R (1)  
Department of the Army  
Washington 25, D.C.

Commanding General  
U. S. Army Transportation Materiel Command  
ATTN: TCMAC-APU (1)  
P. O. Box 209, Main Office  
St. Louis 66, Missouri

Commanding Officer  
U. S. Army Transportation Research Command  
ATTN: Executive for Programs (1)  
ATTN: Research Reference Center (4)  
ATTN: Aviation Directorate (4)  
ATTN: Military Liaison & Advisory Office (4)  
ATTN: Deputy Commander for Aviation (1)  
ATTN: Long Range Technical Forecast Office (1)  
Fort Eustis, Virginia

Commanding Officer  
U. S. Army Transportation Research Command Liaison Office  
ATTN: MCLATS (1)  
Wright-Patterson Air Force Base, Ohio

Chief, Bureau of Naval Weapons  
Department of the Navy  
ATTN: RAAE-34 (1)  
Washington 25, D.C.

Headquarters  
U. S. Army Aviation Test Office  
ATTN: FTZAT (1)  
Edwards Air Force Base, Ohio

Commanding Officer and Director  
David Taylor Model Basin  
Aerodynamics Laboratory Library (1)  
Washington 7, D. C.

National Aeronautics and Space Administration  
ATTN: Mr. Bertram A. Mulcahy  
Assistant Director for Technical Information (1)  
1520 H Street, N. W.  
Washington 25, D. C.

National Aviation Facilities Experimental Center  
ATTN: Library (1)  
Atlantic City, New Jersey

Librarian  
Langley Research Center  
National Aeronautics & Space Administration (1)  
Langley Field, Virginia

Ames Research Center  
National Aeronautics and Space Agency  
ATTN: Library (1)  
Moffett Field, California

U. S. Army Standardization Group, U. K.  
Box 65, U. S. Navy 100  
FPO New York, New York (1)

Office of the Senior Standardization Representative  
U. S. Army Standardization Group, Canada  
c/o Director of Equipment Policy (1)  
Canadian Army Headquarters  
Ottawa, Canada

Canadian Army Liaison Officer  
Liaison Group, Room 208  
U. S. Army Transportation School  
Fort Eustis, Virginia (3)

British Joint Services Mission (Army Staff)  
ATTN: Lt. Col. R. J. Wade, RE (3)  
DAQMC (Mov & Tn)  
3100 Massachusetts Avenue, N. W.  
Washington 8, D. C.

Commander Armed Services Technical Information Agency ATTN: TIPCR Arlington Hall Station Arlington 12, Virginia	(10)
Cornell Aeronautical Laboratory, Inc. ATTN: Mr. Richard White 4455 Genesee Street Buffalo 21, New York	(1)
Sikorsky Aircraft Division of United Aircraft Corporation ATTN: John Kabbott Stratford, Connecticut	(1)
Hiller Aircraft Corporation ATTN: Library Palo Alto, California	(1)
Doman Helicopters, Incorporated Danbury Municipal Airport P. O. Box 603 Danbury, Connecticut	(1)
Bell Helicopter Company Division of Bell Aerospace Corporation ATTN: Robert Lynn P. O. Box 482 Fort Worth 1, Texas	(1)
Hughes Tool Company Aircraft Division ATTN: Library Culver City, California	(1)
Kaman Aircraft Corporation ATTN: Library Bloomfield, Connecticut	(1)
Kellett Aircraft Corporation ATTN: Library P. O. Box 35 Willow Grove, Pennsylvania	(1)
McDonnell Aircraft Corporation ATTN: Library St. Louis, Missouri	(1)

Georgia Institute of Technology ATTN: Library Atlanta, Georgia	(1)
Massachusetts Institute of Technology Department of Aeronautics and Astronautics Cambridge, Massachusetts	(1)
Mississippi State College ATTN: Library State College, Mississippi	(1)
University of Wichita ATTN: Library Wichita 14, Kansas	(1)

<p>VERTOL DIVISION, THE BOEING COMPANY, Morton Pennsylvania</p> <p>WIND TUNNEL TESTS AND FURTHER ANALYSIS OF THE FLOATING WING FUEL TANKS FOR HELICOPTER RANGE EXTENSION.</p> <p>Vol. 3-Wing Flutter Analysis, 45° Skewed Hinge by R. Gabel, R. Ricks, V. Capurso. August 1961, 68 p. incl. figs. and app. (TCREC 61-104) Proj. 9X38-09-006 (Contract DA44-177-TC-550)</p> <p>Unclassified Report</p> <p>Anti-symmetric and symmetric flutter investigations are performed on the Range Extension floating wing for various fuel loading conditions and combinations of wing modes. The method employed in this analysis makes use of Theodorsen's oscillating aerodynamic loads for the generalized excitation. Mechanical equations of the system are obtained with Lagrange's method using several combinations of three wing modes, and two rigid fuselage modes as generalized coordinates. Results of the flutter (over)</p> <p>calculations are presented as plots of air-speed against wing modes frequency ratio, from which the flutter speed is determined by the intersection of the actual frequency ratio with the characteristic curve.</p> <p>Results of the analysis indicate that the flutter characteristics of the delta hinge wing arrangement are unacceptable. The investigation shows that for both the 0% and 100% fuel configurations the flutter speeds are below the cruise speed of 80 knots. It is indicated that the low flutter critical speed calculated here is closely associated with the aircraft roll-wing rigid body flap instability which has been determined to be an aircraft flight instability. The wing design is being revised to a straight hinge configuration in which the necessary aerodynamic wing spring is being furnished by a differential flap system. This change, which will eliminate the unusual flap-pitch coupling in the oscillatory airloads, should improve the flutter situation.</p>	<p>UNCLASSIFIED</p> <p>I. Range Extension - Dynamics</p> <p>2. Wing Flutter</p>	<p>VERTOL DIVISION, THE BOEING COMPANY, Morton Pennsylvania</p> <p>WIND TUNNEL TESTS AND FURTHER ANALYSIS OF THE FLOATING WING FUEL TANKS FOR HELICOPTER RANGE EXTENSION.</p> <p>Vol. 3-Wing Flutter Analysis, 45° Skewed Hinge by R. Gabel, R. Ricks, V. Capurso. August 1961, 68 p. incl. figs. and app. (TCREC 61-104) Proj. 9X38-09-006 (Contract DA44-177-TC-550)</p> <p>Unclassified Report</p> <p>Anti-symmetric and symmetric flutter investigations are performed on the Range Extension floating wing for various fuel loading conditions and combinations of wing modes. The method employed in this analysis makes use of Theodorsen's oscillating aerodynamic loads for the generalized excitation. Mechanical equations of the system are obtained with Lagrange's method using several combinations of three wing modes, and two rigid fuselage modes as generalized coordinates. Results of the flutter (over)</p> <p>calculations are presented as plots of air-speed against wing modes frequency ratio, from which the flutter speed is determined by the intersection of the actual frequency ratio with the characteristic curve.</p> <p>Results of the analysis indicate that the flutter characteristics of the delta hinge wing arrangement are unacceptable. The investigation shows that for both the 0% and 100% fuel configurations the flutter speeds are below the cruise speed of 80 knots. It is indicated that the low flutter critical speed calculated here is closely associated with the aircraft roll-wing rigid body flap instability which has been determined to be an aircraft flight instability. The wing design is being revised to a straight hinge configuration in which the necessary aerodynamic wing spring is being furnished by a differential flap system. This change, which will eliminate the unusual flap-pitch coupling in the oscillatory airloads, should improve the flutter situation.</p>	<p>UNCLASSIFIED</p> <p>I. Range Extension - Dynamics</p> <p>2. Wing Flutter</p>	<p>UNCLASSIFIED</p> <p>I. Range Extension - Dynamics</p> <p>2. Wing Flutter</p>	<p>UNCLASSIFIED</p> <p>I. Range Extension - Dynamics</p> <p>2. Wing Flutter</p>
---	---	---	---	---	---

<p>VERTOL DIVISION, THE BOEING COMPANY, Morton Pennsylvania</p> <p>WIND TUNNEL TESTS AND FURTHER ANALYSIS OF THE FLOATING WING FUEL TANKS FOR HELICOPTER RANGE EXTENSION.</p> <p>Vol. 3-Wing Flutter Analysis, 45° Skewed Hinge by R. Gabel, R. Ricks, V. Capurso, August 1961, 68 p. incl. figs. and app. (TCREC 61-104) Proj. 9X38-09-006 (Contract DAAA-177-TG-550)</p> <p>Unclassified Report</p> <p>Anti-symmetric and symmetric flutter investigations are performed on the Range Extension floating wing for various fuel loading conditions and combinations of wing modes. The method employed in this analysis makes use of Theodorsen's oscillating aerodynamic loads for the generalized excitation. Mechanical equations of the system are obtained with Lagrange's method using several combinations of three wing modes, and two rigid fuselage modes as generalized coordinates. Results of the flutter (Over)</p>	<p>UNCLASSIFIED</p> <p>1. Range Extension - Dynamics</p> <p>2. Wing Flutter</p>	<p>VERTOL DIVISION, THE BOEING COMPANY, Morton Pennsylvania</p> <p>WIND TUNNEL TESTS AND FURTHER ANALYSIS OF THE FLOATING WING FUEL TANKS FOR HELICOPTER RANGE EXTENSION.</p> <p>Vol. 3-Wing Flutter Analysis, 45° Skewed Hinge by R. Gabel, R. Ricks, V. Capurso, August 1961, 68 p. incl. figs. and app. (TCREC 61-104) Proj. 9X38-09-006 (Contract DAAA-177-TG-550)</p> <p>Unclassified Report</p> <p>Anti-symmetric and symmetric flutter investigations are performed on the Range Extension floating wing for various fuel loading conditions and combinations of wing modes. The method employed in this analysis makes use of Theodorsen's oscillating aerodynamic loads for the generalized excitation. Mechanical equations of the system are obtained with Lagrange's method using several combinations of three wing modes, and two rigid fuselage modes as generalized coordinates. Results of the flutter (Over)</p>	<p>UNCLASSIFIED</p> <p>1. Range Extension - Dynamics</p> <p>2. Wing Flutter</p>	<p>UNCLASSIFIED</p> <p>1. Range Extension - Dynamics</p> <p>2. Wing Flutter</p>
<p>Calculations are presented as plots of airspeed against wing modes frequency ratio, from which the flutter speed is determined by the intersection of the actual frequency ratio with the characteristic curve.</p> <p>Results of the analysis indicate that the flutter characteristics of the delta hinge wing arrangement are unacceptable. The investigation shows that for both the 0% and 100% fuel configurations the flutter speeds are below the cruise speed of 80 knots. It is indicated that the low flutter critical speed calculated here is closely associated with the aircraft roll-wing rigid body flap instability which has been determined to be an aircraft flight instability. The wing design is being revised to a straight hinge configuration in which the necessary aerodynamic wing spring is being furnished by a differential flap system. This change, which will eliminate the unusual flap-pitch coupling in the oscillatory airloads, should improve the flutter situation.</p>	<p>UNCLASSIFIED</p>	<p>Calculations are presented as plots of airspeed against wing modes frequency ratio, from which the flutter speed is determined by the intersection of the actual frequency ratio with the characteristic curve.</p> <p>Results of the analysis indicate that the flutter characteristics of the delta hinge wing arrangement are unacceptable. The investigation shows that for both the 0% and 100% fuel configurations the flutter speeds are below the cruise speed of 80 knots. It is indicated that the low flutter critical speed calculated here is closely associated with the aircraft roll-wing rigid body flap instability which has been determined to be an aircraft flight instability. The wing design is being revised to a straight hinge configuration in which the necessary aerodynamic wing spring is being furnished by a differential flap system. This change, which will eliminate the unusual flap-pitch coupling in the oscillatory airloads, should improve the flutter situation.</p>	<p>UNCLASSIFIED</p>	<p>UNCLASSIFIED</p>



<p>VERTOL DIVISION, THE BOEING COMPANY, MORTON Pennsylvania</p> <p>WIND TUNNEL TESTS AND FURTHER ANALYSIS OF THE FLOATING WING FUEL TANKS FOR HELICOPTER RANGE EXTENSION.</p> <p>Vol. 3-Wing Flutter Analysis, 45° Skewed Hinge by R. Gabel, R. Ricks, V. Capurso. August 1961, 68 p. incl. figs. and app. (TCREC 61-104) Proj. 9X38-09-006 (Contract DA44-177-TC-550)</p> <p>Unclassified Report</p>	<p>UNCLASSIFIED</p> <p>I. Range Extension - Dynamics</p> <p>2. Wing Flutter</p>	<p>VERTOL DIVISION, THE BOEING COMPANY, MORTON Pennsylvania</p> <p>WIND TUNNEL TESTS AND FURTHER ANALYSIS OF THE FLOATING WING FUEL TANKS FOR HELICOPTER RANGE EXTENSION.</p> <p>Vol. 3-Wing Flutter Analysis, 45° Skewed Hinge by R. Gabel, R. Ricks, V. Capurso. August 1961, 68 p. incl. figs. and app. (TCREC 61-104) Proj. 9X38-09-006 (Contract DA44-177-TC-550)</p> <p>Unclassified Report</p>	<p>UNCLASSIFIED</p> <p>I. Range Extension - Dynamics</p> <p>2. Wing Flutter</p>
<p>Anti-symmetric and symmetric flutter investigations are performed on the Range Extension floating wing for various fuel loading conditions and combinations of wing modes. The method employed in this analysis makes use of Theodorsen's oscillating aerodynamic loads for the generalized excitation. Mechanical equations of the system are obtained with Lagrange's method using several combinations of three wing modes, and two rigid fuselage modes as generalized coordinates. Results of the flutter</p>	<p>I. Gabel, R.</p> <p>II. Ricks, R.</p> <p>III. Capurso, V.</p> <p>UNCLASSIFIED</p>	<p>Anti-symmetric and symmetric flutter investigations are performed on the Range Extension floating wing for various fuel loading conditions and combinations of wing modes. The method employed in this analysis makes use of Theodorsen's oscillating aerodynamic loads for the generalized excitation. Mechanical equations of the system are obtained with Lagrange's method using several combinations of three wing modes, and two rigid fuselage modes as generalized coordinates. Results of the flutter</p>	<p>I. Gabel, R.</p> <p>II. Ricks, R.</p> <p>III. Capurso, V.</p> <p>UNCLASSIFIED</p>
<p>calculations are presented as plots of airspeed against wing modes frequency ratio, from which the flutter speed is determined by the intersection of the actual frequency ratio with the characteristic curve.</p>	<p>UNCLASSIFIED</p>	<p>calculations are presented as plots of airspeed against wing modes frequency ratio, from which the flutter speed is determined by the intersection of the actual frequency ratio with the characteristic curve.</p>	<p>UNCLASSIFIED</p>
<p>Results of the analysis indicate that the flutter characteristics of the delta hinge wing arrangement are unacceptable. The investigation shows that for both the 0% and 100% fuel configurations the flutter speeds are below the cruise speed of 80 knots. It is indicated that the low flutter critical speed calculated here is closely associated with the aircraft roll-wing rigid body flap instability which has been determined to be an aircraft flight instability. The wing design is being revised to a straight hinge configuration in which the necessary aerodynamic wing spring is being furnished by a differential flap system. This change, which will eliminate the unusual flap-pitch coupling in the oscillatory airloads, should improve the flutter situation.</p>	<p>UNCLASSIFIED</p>	<p>Results of the analysis indicate that the flutter characteristics of the delta hinge wing arrangement are unacceptable. The investigation shows that for both the 0% and 100% fuel configurations the flutter speeds are below the cruise speed of 80 knots. It is indicated that the low flutter critical speed calculated here is closely associated with the aircraft roll-wing rigid body flap instability which has been determined to be an aircraft flight instability. The wing design is being revised to a straight hinge configuration in which the necessary aerodynamic wing spring is being furnished by a differential flap system. This change, which will eliminate the unusual flap-pitch coupling in the oscillatory airloads, should improve the flutter situation.</p>	<p>UNCLASSIFIED</p>

<p>VERTOL DIVISION, THE BOEING COMPANY, MORTON Pennsylvania</p> <p>WIND TUNNEL TESTS AND FURTHER ANALYSIS OF THE FLOATING WING FUEL TANKS FOR HELICOPTER RANGE EXTENSION.</p> <p>Vol. 3-Wing Flutter Analysis, 45° Skewed Hinge by R. Gabel, R. Ricks, V. Capurso, August 1961, 68 p. incl. figs. and app. (TCREC 61-104) Proj. 9X38-09-006 (Contract DA44-177-TC-550)</p> <p>Unclassified Report</p> <p>Anti-symmetric and symmetric flutter investigations are performed on the Range Extension floating wing for various fuel loading conditions and combinations of wing modes. The method employed in this analysis makes use of Theodorsen's oscillating aerodynamic loads for the generalized excitation. Mechanical equations of the system are obtained with Lagrange's method using several combinations of three wing modes, and two rigid fuselage modes as generalized coordinates. Results of the flutter</p> <p>calculations are presented as plots of airspeed against wing modes frequency ratio, from which the flutter speed is determined by the intersection of the actual frequency ratio with the characteristic curve.</p> <p>Results of the analysis indicate that the flutter characteristics of the delta hinge wing arrangement are unacceptable. The investigation shows that for both the 0% and 100% fuel configurations the flutter speeds are below the cruise speed of 80 knots. It is indicated that the low flutter critical speed calculated here is closely associated with the aircraft roll-wing rigid body flap instability which has been determined to be an aircraft flight instability. The wing design is being revised to a straight hinge configuration in which the necessary aerodynamic wing spring is being furnished by a differential flap system. This change, which will eliminate the unusual flap-pitch coupling in the oscillatory airloads, should improve the flutter situation.</p>	<p>UNCLASSIFIED</p> <p>1. Range Extension - Dynamics</p> <p>2. Wing Flutter</p> <p>I. Gabel, R.</p> <p>II. Ricks, R.</p> <p>III. Capurso, V.</p> <p>UNCLASSIFIED</p> <p>UNCLASSIFIED</p>	<p>VERTOL DIVISION, THE BOEING COMPANY, MORTON Pennsylvania</p> <p>WIND TUNNEL TESTS AND FURTHER ANALYSIS OF THE FLOATING WING FUEL TANKS FOR HELICOPTER RANGE EXTENSION.</p> <p>Vol. 3-Wing Flutter Analysis, 45° Skewed Hinge by R. Gabel, R. Ricks, V. Capurso, August 1961, 68 p. incl. figs. and app. (TCREC 61-104) Proj. 9X38-09-006 (Contract DA44-177-TC-550)</p> <p>Unclassified Report</p> <p>Anti-symmetric and symmetric flutter investigations are performed on the Range Extension floating wing for various fuel loading conditions and combinations of wing modes. The method employed in this analysis makes use of Theodorsen's oscillating aerodynamic loads for the generalized excitation. Mechanical equations of the system are obtained with Lagrange's method using several combinations of three wing modes, and two rigid fuselage modes as generalized coordinates. Results of the flutter</p> <p>calculations are presented as plots of airspeed against wing modes frequency ratio, from which the flutter speed is determined by the intersection of the actual frequency ratio with the characteristic curve.</p> <p>Results of the analysis indicate that the flutter characteristics of the delta hinge wing arrangement are unacceptable. The investigation shows that for both the 0% and 100% fuel configurations the flutter speeds are below the cruise speed of 80 knots. It is indicated that the low flutter critical speed calculated here is closely associated with the aircraft roll-wing rigid body flap instability which has been determined to be an aircraft flight instability. The wing design is being revised to a straight hinge configuration in which the necessary aerodynamic wing spring is being furnished by a differential flap system. This change, which will eliminate the unusual flap-pitch coupling in the oscillatory airloads, should improve the flutter situation.</p>	<p>UNCLASSIFIED</p> <p>1. Range Extension - Dynamics</p> <p>2. Wing Flutter</p> <p>I. Gabel, R.</p> <p>II. Ricks, R.</p> <p>III. Capurso, V.</p> <p>UNCLASSIFIED</p> <p>UNCLASSIFIED</p>	<p>UNCLASSIFIED</p> <p>1. Range Extension - Dynamics</p> <p>2. Wing Flutter</p> <p>I. Gabel, R.</p> <p>II. Ricks, R.</p> <p>III. Capurso, V.</p> <p>UNCLASSIFIED</p> <p>UNCLASSIFIED</p>
---	--	---	--	--

UNCLASSIFIED

UNCLASSIFIED